MEASUREMENT OF PHYSICAL AND HYDRAULIC PROPERTIES OF ORGANIC SOIL USING COMPUTED TOMOGRAPHIC IMAGERY

by

Kimberly E. Blais
Bachelor of Science, Simon Fraser University, 2003

THESIS SUBMITTED IN PARTIAL FULFILLMENT OF
THE REQUIREMENTS FOR THE DEGREE OF

MASTER OF SCIENCE

In the
Department
of
Geography

SIMON FRASER UNIVERSITY

Fall 2005

APPROVAL

Name:	**Kimberly E. Blais**
Degree:	**Master of Science**
Title of Thesis:	**Measurement of Physical and Hydraulic Properties of Organic Soil Using Computed Tomographic Imagery**
Examining Committee:	
Chair:	**E.J. Hickin**, Professor

Dr. W.L. Quinton, Assistant Professor
Senior Supervisor
Department of Geography, Simon Fraser University

Dr. M.G. Schmidt, Associate Professor
Committee Member
Department of Geography, Simon Fraser University

Dr. R.J. Heck, Assistant Professor, Committee Member
Department of Land Resource Science,
University of Guelph

Dr. J.S. Price, Professor, Committee Member
Department of Geography, University of Waterloo

Dr. D. Stead, Professor, External Examiner
Department of Earth Sciences, Simon Fraser University

Date Approved: September 28, 2005

ABSTRACT

Defining and measuring the physical properties of peat is difficult but essential in order to accurately model the flux and storage of water in peatlands. The goal of this research is to develop a method to measure the physical and hydraulic properties of organic soil using computed tomographic imagery. Specifically, this research seeks to determine if two and three-dimensional images of peat, produced using a MicroCT scanner, can be used to accurately characterize air-filled porosity, active porosity, pore size distribution, pore saturated area and capillary films of porous *Sphagnum* cells at different soil tensions. Unsaturated hydraulic conductivity at similar soil tensions was also determined. Results indicate that the proportion of small air-filled pores in the peat sub-samples increased with increasing depth and unsaturated hydraulic conductivity was greater at deeper depths than shallower depths at equivalent soil tensions, suggesting this method is a potentially valuable tool for measuring peat properties.

Key Words: Peat, organic soil, computed tomography, CT scanning, air-filled porosity

This thesis is dedicated to my sweet and miraculous unborn child.

Oh, how I look forward to the day we finally meet!

ACKNOWLEDGEMENTS

This thesis would not have been possible without the assistance of many people in various capacities throughout my degree. I would like to thank Dr. Richard Heck for advice and guidance and most of all, for allowing me to use the MicroCT on which this thesis was based. I would like to thank Dr. Margaret Schmidt for edits and advice on my thesis and defence presentation. I would like to thank Dr. Jon Price for advice and guidance and Dr. Bill Quinton for his financial support, assistance with the initial research ideas and for giving me the opportunity to go into the field to collect my own soil samples despite my physical limitations.

I would like to acknowledge Dr. Bill Bailey, Chris Bone, Neil Goeller, Dr. Masaki Hayashi and Scott Weston for their help with methodology, data analysis and/or editorial comments to my thesis. Also, thank you to Nicole Wright for assistance and putting up with my ABBA music and "dog opera" in the field as well as use of water level data from Scotty.

I would also like to acknowledge my friends and colleagues: Andrea, Jen, James, Craig, Dan, Gift, Rosemary, Tanya, Cathy, D. James, Don, Jolie, Natalie and Stephanie for all the "good times" and moral support. An extra thank you goes to my hydrology labmates for the crazy antics and serious research that kept me going strong. Thank you also to Dr. Owen Hertzman for his support, encouragement and help to further develop my skills as a teacher and a presenter.

The Geography department staff: Marcia, Hilary, B-Jae, Diane, Ravinder, John and Jasper were always helpful and supportive. I would like to extend a thank you to my external examiner, Dr. Doug Stead for offering valuable insights and recommendations. I would also like to thank him for his assistance above and beyond what was customary as well as the Dean of Grad Studies, Dr. Jon Driver for assistance with my degree completion.

I would like to thank Taskin Shirazi for friendship and invaluable support. Your willingness to help with all aspects of my thesis and beyond was more than I could ever have imagined – the cookies and brownies and entertaining attempts at "pull-ups" were always appreciated.

An extra special thanks must go to Mom, Dad, Rod, Jullie, Brad, Lisa and my nieces and nephews for all the encouragement and utmost faith in my abilities. I love you guys! Lastly, I would like to thank Mark Blais for drawing the exceptional diagrams for my thesis and for putting up with my long work days and nights for the past couple of years. Thanks always for keeping me happy and healthy. I look forward to a new phase of life with you and Baby ♥ Blais.

TABLE OF CONTENTS

LIST OF FIGURES

LIST OF TABLES

CHAPTER 1:
GENERAL INTRODUCTION AND LITERATURE REVIEW

1.1 Introduction

Wetlands occupy 14% of Canada's land surface (NWWG, 1988). The distribution and movement of water; the abundance and diversity of plants, vertebrates, invertebrates and microbes are all ultimately controlled by wetland hydrological processes. Wetlands in the high boreal region of northwestern Canada include bogs, peat plateaus, channel fens and other types of peatlands which collectively occupy 20% of the area's land surface (NWWG, 1988). The quality and quantity of basin runoff is strongly influenced by the presence of wetlands (Price and Waddington, 2000).

Defining the physical and hydraulic properties of organic soils is essential in order to understand and model the flux and storage of water in peatlands. Describing the flow of water and hydraulic properties of soil are key challenges in soil science (Mori et al., 1999). Analysis of organic soils requires special attention to ensure that measured properties are examined as they exist in nature (Boelter, 1976). The incentive for this thesis research was to minimize problems incurred while measuring physical and hydrological properties of organic soil. This was an investigative study to ascertain if images obtained from MicroCT imagery of peat could be used to characterize these properties. MicroCT scanning has the benefit of being able to view the small-scale structure of peat in three dimensions in order to investigate how changes in moisture content affect the soil's ability to store and transmit water. Results obtained from

analysis of organic soil, using this method, can be representative of other northern peatlands as well as other peatlands in Canada. A common technique used for quantifying peat properties is thin section analysis. A major problem with this technique is that thin section production causes peat to change in structure. This is partly because peat is naturally saturated with water which causes the resin, used to impregnate the soil, to harden insufficiently. This results in thin sections that are often warped and filled with bubbles, dust and scratches, thus creating imperfections on the slides and making them difficult to analyse.

This research evaluates the use of computed tomographic imagery or MicroCT technology to define and predict physical and hydraulic properties of organic soil. Air-filled porosity, active porosity, air-filled pore size distribution, pore saturated area and capillary films of porous *Sphagnum* cells at several different soil tensions were evaluated quantitatively and qualitatively using two and three-dimensional images of peat. This thesis research also measured unsaturated hydraulic conductivity, at different soil tensions, so as to provide greater insight into the relationship between soil moisture and hydraulic conductivity.

1.2 Literature Review

1.2.1 Major peatland types of the northern boreal zone

In Canada, peatlands are wetlands that have an accumulation of peat exceeding 40 cm in depth (Price and Waddington, 2000). Peatlands occur most extensively in cool climates where annual moisture inputs exceed evapotranspiration, and where decomposition rates are low (Verry and Boelter, 1978). In the northern boreal zone of

northwestern Canada, precipitation exceeds evapotranspiration by more than 500 mm (Halsey et al., 2000). In this region, common peatland types include bogs, fens, peat plateaus and some types of swamps (NWWG 1998).

1.2.1.1 Bogs

Most bogs are raised and therefore hydrologically-isolated from the surrounding terrain. This makes them ombrotrophic, as they receive nutrients and minerals solely from precipitation (Glaser and Janssens, 1986). In the boreal region of northwestern Canada, however, *Sphagnum*-covered flat bogs predominate. Natural sources of water enter these flat bogs by rainfall and snowmelt (Verry and Boelter, 1978) as well as by runoff from adjacent slopes and ground water. Since flat bogs are located in broad and poorly defined depressions, the water table is generally at or just below the soil surface (NWWG, 1988). Although flat bogs are less hydrologically-isolated than raised bogs and have a slightly higher nutrient content, they are still considered ombrotrophic (NWWG, 1988). Bog vegetation consists mainly of trees such as the *Picea mariana* (Black spruce), ericaceous shrubs such as the *Ledum groenlandicum* (Labrador tea) and wild flowers such as the *Rubus chamaemorus* (Cloudberry). A layer of mosses such as *Sphagnum fuscum* (Rusty peat moss), *Sphagnum fallax* or *Sphagnum angustifolium* (Poor fen moss) (NWWG, 1988) are also present. Flat bogs are generally acidic with pH values ranging between 4.0 and 5.0 (NWWG, 1988) and have relatively low electrical conductivity (Hayashi et al., 2002).

1.2.1.2 Fens

Fens are wetlands with a relatively high nutrient status in comparison to bogs (Verry and Boelter, 1978). They are considered minerotrophic since they receive a higher proportion of inputs from hillslopes and stream channels than from precipitation. As a result, they have relatively high electrical conductivity and neutral pH (Hayashi et al., 2004). Channel fens, particular to this boreal region, have a flat and featureless surface that slopes gently in the direction of drainage (NWWG, 1988). The vegetation is composed of sedges, herbs and shrubs. Moss species, including *Sphagnum fuscum* (Rusty peat moss), *Tomenthypnum nitens* (Golden fuzzy fen moss) and *Pleurozium schreberi* (Feather moss) are also present (NWWG, 1988). Unlike flat bogs, channel fens conduct water primarily in a lateral direction and are typically interconnected, forming a basin drainage network.

1.2.1.3 Peat plateaus

Peat plateaus are transitioned flat bogs arising from the vertical growth of *Sphagnum fuscum* (Rusty peat moss) above the water table (Robinson and Moore, 1999). Peat plateaus are underlain by permafrost which lifts the surface above the surrounding landscape, imposing a barrier to vertical subsurface flow through the channel fens (Hayashi et al., 2004). Peat plateaus are unique in that they are considered peatlands, but unlike flat bogs and channel fens, they are not wetlands, since the water table does not remain within 10 cm of the surface throughout the year, but subsides to depths exceeding 50 cm below the surface (Quinton et al., 2003). Peat plateaus also are able to support species of shrubs, lichens, mosses and trees.

1.2.2 Organic soil

Soils of the Organic order are classified as containing >17% organic carbon or >30% organic matter by weight of which extends from the surface either to a depth of 1.6 m or to a lithic contact (CSSC, 1998). Soils of the Organic Cryosol Great Group Soils predominate throughout the Canadian sub arctic. These soils are defined as having permafrost within one meter of the surface or two meters if strongly cryoturbated (CSSC, 1998). Since organic soils are typically saturated with water for prolonged periods and occur extensively in poorly drained depressions and flat regions of subhumid to perhumid climates (CSSC, 1998), the physiography must be favourable to slow moving water at or near the ground surface.

Organic soils are mainly formed from mosses (such as *Sphagnum* moss), sedges, or other hydrophytic vegetation. The genus *Sphagnum* is a dominant component of peat-forming ecosystems in the northern hemisphere (Halsey et al., 2000). The von Post scale defines the degree of decomposition of peat according to its fibre content, which decreases with increasing decomposition. Organic soil horizons can be classified into three types. Fibric peat has a fibre content > 67%, hemic peat has a fibre content between 33-67% and sapric peat has a fibre content < 33% (Verry and Boelter, 1978). An apparent two layered soil structure can be present in organic soils consisting of an acrotelm and catotelm. Fibric peats typically occur in the upper 30 cm of the soil within the acrotelm layer (Verry and Boelter, 1978). The acrotelm, is the upper layer composed of living, dead and poorly decomposed mosses (Ingram, 1978), where most physical and biological processes occur (Verry and Boelter, 1978). Sapric and hemic peats constitute

the catotelm which is composes the more decomposed (Ingram, 1978), dense, continually saturated, less permeable layer (Ivanov, 1981).

1.2.2.1 Peat formation

Unlike mineral soil, peat is composed entirely of vegetal remains (Brown and Williams, 1972). The sub arctic is characterized by low mean annual air temperatures, low evapotranspiration rates, limited infiltration (Dingman, 1975; Hobbie, 1984) and small soil storage capacities (Brown and Williams, 1972). These conditions enable the accumulation of biomass, including the remains of mosses, sedges, lichens, leaves and needles (NRC, 1995) since plant productivity exceeds decomposition rates. Poor drainage conditions due to frozen, ice-rich ground, leads to the formation of hydric soils that favour the growth of hydrophytic vegetation (NRC, 1995).

1.2.3 Physical and hydraulic properties of peat

To understand and predict the movement of water through peatlands, the physical and hydraulic properties of peatland soils must be known. This requires the use of standard and reliable methods of measurement. Where no such methods exist, new methods must be developed. For each of the critical peat properties listed below, the methods of measurement are described.

1.2.3.1 Bulk Density

Bulk density (D_b) is the mass of dry soil per unit volume of the soil sample (g cm^{-3}), including air space (Brady and Weil, 2002):

$$D_b = \frac{W_d}{V_w} \qquad [1\text{-}1]$$

where W_d is the oven dry weight and V_w is the wet volume of the soil sample (Equation 1-1). Bulk density is useful for estimating the degree of decomposition of organic soil such as peat. In peats, bulk density is usually expressed on a wet-volume basis (Boelter, 1968) because of the reduction in volume with drying. Bulk densities tend to be low for all peats, but are lowest for fibric peats and highest for the more decomposed sapric peats. Boelter (1976) measured bulk density as 0.153 g cm^{-3} in moderately decomposed peat and 0.261 g cm^{-3} in well decomposed peat. Quinton et al. (2000) found that bulk density increased from 40 kg m^{-3} near the surface to 84 kg m^{-3} and 150 kg m^{-3} at deeper depths.

Bulk density is typically determined in the laboratory from the difference in the weight of a sample of known volume before and after drying at 105°C for 1-2 days (Parent and Caron, 1993). Bulk density, D_b, is calculated using Equation 1-1. One difficulty with this method is achieving a precise soil volume. If the volume is not exact, this can overestimate or underestimate the bulk density.

1.2.3.2 Porosity

The total porosity, is the void volume expressed as a percentage of the total soil volume (Hillel, 1998). Total porosity is derived from Equation 1-2

$$n_T = \frac{V_V}{V_T} \qquad [1\text{-}2]$$

where n_T is the total porosity, V_V is the void volume and V_T is the total volume including voids. The total porosity includes pores that are active and inactive in terms of water transmission. Inactive pores include closed and dead-end pores formed by the remains of plant material (Hoag and Price, 1997). In organic soil, the structure and size of particles and inter-particle pores are ultimately controlled by the degree of decomposition whereby both particles and pores decrease in size with increasing decomposition resulting in more dry material per unit volume (Boelter, 1968). Because inactive pores are included in estimates of total porosity, this indicates nothing about the size and shape of soil pores (Hillel, 1998).

Active porosity is the proportion of the total volume that actively transmits water (Hoag and Price, 1997). For organic soil, active porosity can vary with depth from 0.8 near the soil surface to 0.1 in the lower catotelm horizon (Hoag and Price, 1997; Siegel et al., 1995; Romanov, 1968). Hoag and Price (1997) demonstrated that active porosity can be measured through image analysis of thin (~100 μm) sections.

1.2.3.3 Degree of decomposition

The structure and size of particles and inter-particle pores are ultimately controlled by the degree of decomposition whereby both particles and pores decrease in

size with increasing decomposition resulting in more dry material per unit volume (Boelter, 1968). The degree of decomposition is often determined from von Post method which measures the fibre content (CSSC, 1978).

1.2.3.4 Pore size distribution

The flow and storage of water in any pore increases in relation to its size and geometry (Beven and Germann, 1982). For instance, the magnitude of hydrological properties such as hydraulic conductivity, specific yield and bulk density depend on the size, shape and orientation of the soil pores. Consequently, as pore diameter, d decreases, so does the hydraulic conductivity, specific yield and bulk density. Also, as d increases, so does the Reynolds number, N_R. Reynolds number is the ratio of kinetic to viscous energy used to determine hydraulic flow of a system

$$N_R = \frac{\rho v d}{\mu} \qquad [1\text{-}3]$$

where ρ is the density of the fluid, v is the flow velocity and μ is the fluid viscosity (Equation 1-3). As pore diameter decreases N_R is lowered. This then increases viscous dissipation and the likelihood of laminar flow. Smaller diameter pores are indicative of more decomposed and compacted peat, thus reducing water storage capacity, lowering hydraulic conductivity and increasing capillary water retention (Price and Whitehead, 2004). Microscopic analyses, by means of thin sections, have been used to make estimates of pore size distribution.

1.2.3.5 Soil matric potential

Soil matric potential refers to the attractive forces between water and soil particles as characterized by adsorption and capillarity (Brady and Weil, 2002). When soil is unsaturated, the matric potential of the water in the soil is lower than atmospheric pressure. When the pressure is lowered the pressure is considered negative or in a subpressure state. Negative matric potential, soil tension and matric suction are used interchangeably to describe this process. Specifically, they are defined as the negative gauge pressure, relative to the external gas pressure on water content of the soil (Hillel, 1998). Both soil tension and matric suction are used interchangeably throughout this thesis.

One method of attaining particular soil matric potentials is by use of a pressure plate and/or tension table apparatus. This involves using saturated peat samples that are equilibrated in Tempe cells at increasing potentials. A water column is used to control the pressure being exerted. Water can then be extracted from saturated peat at pressures from -10 to -1500 kPa (Joyal et al., 1989). Volumetric moisture content can then be determined gravimetrically for each soil tension by measuring the volumetric moisture content at each tension level. Air trapping can be a problem with the tension plate method and peat shrinkage is often not taken into account (Parent and Caron, 1993).

1.2.3.6 Volumetric moisture content

The porosity of peat is >80% (cm^3 cm^{-3}) so that when saturated contains >80% moisture. The volumetric moisture content is the fraction of moisture per unit volume of soil. One standard method of measuring soil moisture content requires oven drying a known volume of soil to determine the weight difference between a wet state and a dry

state. Volumetric moisture content, θ, is determined using gravimetric wetness and the soil volume measured at saturation using the following expression:

$$\theta = \frac{W_{wet} - W_{dry}}{\rho_w \cdot V_s} \quad [1\text{-}4]$$

where ρ_w, is the density of water, V_s is the sample volume, W_{wet} is the wet weight, and W_{dry} is the oven dry weight (Equation 1-4) (Dingman, 2002).

1.2.3.7 Hydraulic conductivity

Hydraulic conductivity is of fundamental significance to the study of water movement through soils (Rycroft et al., 1975). Variation in physical properties with depth results in depth-variations in peat hydraulic properties (Quinton et al., 2000). "Hydraulic conductivity is defined by Darcy's law, as an empirical relationship connecting the macroscopic velocity of water in a porous medium with gradient of water potential down which the water flows" (Rycroft et al., 1975 p. 553). Hydraulic conductivity, K (Equation 1-5) is measured by the rate at which water passes through soil (LT^{-1}) in response to a potential gradient (Brady and Weil, 2002) and is defined:

$$K = \frac{Cd^2 \times \rho g}{\mu} \quad [1\text{-}5]$$

where: $Cd^2=k$, is the intrinsic permeability; C is a constant of proportionality that reflects the shape and orientation of the soil pores; d is the particle diameter; ρ is the fluid density; μ is the dynamic viscosity of the fluid and g is gravity (Freeze and Cherry, 1979). The hydraulic conductivity of fibric peats is a thousand times higher than that of the deeper sapric peats (Verry and Boelter, 1978) owing to the smaller pore diameter of

the latter. Boelter (1976) found that hydraulic conductivity ranged from 13.90 x 10^{-5} cm sec^{-1} in moderately decomposed peat to 0.45 x 10^{-5} cm sec^{-1} in well decomposed peat. Rycroft et al. (1975) found that hydraulic conductivity ranged from 4.0 x 10^{-2} cm sec^{-1} in undecomposed peat to 1.4 x 10^{-4} cm sec^{-1} in moderately decomposed peat. Therefore, peats at lower depths are more decomposed, retain more water, and drain much more slowly (Verry and Boelter, 1978).

One method of determining hydraulic conductivity in both saturated and unsaturated soil is by use of a permeameter. Using undisturbed core samples, measurements of the hydraulic conductivity can be made using a constant head permeameter. This involves continuously adding water to a reservoir to keep the water level constant where then water drains from the soil by means of an outlet. By determining the hydraulic gradient and the resulting flux of water through a saturated soil column, hydraulic conductivity can then be calculated (Klute and Dirksen, 1986). Because this method maintains a constant head, it is mainly useful for saturated soils. A steady-state head control method is similar to the constant head permeameter but here a constant water flow is maintained in a soil sample at various moisture contents allowing the measurement of hydraulic conductivity of unsaturated soil. The difference is that the soil sample is not completely saturated on a continuous basis. Since a moisture gradient often exists in the soil sample, hydraulic gradient of the sample is measured in order to calculate unsaturated hydraulic conductivity (Klute and Dirksen, 1986).

1.2.4 Microscopic methods of analysis

1.2.4.1 Thin sectioning

Thin section production by polyester resin impregnation provides a means to investigate the spatial arrangement of organic constituents and pores of peat (Fox and Parent, 1993). This method utilizes acetone and polyester resin to impregnate and harden the soil. Once soil cores are extracted, the core is cut in half and the water is removed using acetone replacement by either capillarity exchange or vapour exchange (Fox and Parent, 1993). After the water is removed from the soil core, it is impregnated with a resin solution where it is left to harden. This is done to avoid modifying the soil fabric due to changes in volume. The goal is to have the samples appear clear and isotropic in polarized light and have an acceptable refractive index (Cady et al., 1986) so the soil can be photographed well. Once the sample has hardened, thin sections are cut, cleaned and cemented to a microscope slide with epoxy or balsam. The specimen is ground to a chosen thickness and the slide is cleaned, dried and then covered with a glass slide (Cady et al., 1986). Digital photographs can then be taken of the slides for interpretation using image analysis software such as Sigmascan.

Microscopic analyses of thin sections have been used extensively as a way to directly measure the physical properties of soils and other media. However, this method is difficult to perform using organic soil because the resin takes a long to harden and extensive expertise is required to produce them. Production of thin sections of organic soil can take over a year from when soil samples are collected to when thin sections are ready for analysis. Soil deformation is a possible result of using resin impregnation and thin section analysis. Once extracted from the field, the peat material drains and shrinks

causing variability within its physical composition. When acetone removes the water, the peat shrinks preceding the addition of resin. The peat never fully returns to its natural state before extraction from the field. Royer and Vachaud (1975) showed that *in situ* measurements are better representations of natural states in that laboratory and field measurements can differ slightly. If lab measurements are to be made, this must be done with as little soil disturbance as possible. Schwarzel et al. (2002) found that derivation of pore sizes was flawed due to drainage and shrinkage, especially at high soil water potentials.

When thin sections are cut, they have a tendency to warp and form holes due to insufficient resin hardening. Thin section analysis is destructive, since the soil cannot be used for additional trials or other methods of analysis. During the curing process, the organic material often secretes a waxy film that can cover large areas of the slide. Bubbles, dust and scratches all create imperfections on the slides and cause problems during image interpretation and analysis.

1.2.4.2 Computerized axial tomography

As an alternative to the development of thin sections, computed tomography (MicroCT scanning) offers the prospect of improving measurement of physical and hydrological properties. With the use of a MicroCT scanner, objects can be reconstructed into three-dimensional images. The photons produced by a MicroCT scan interact with the atoms that comprise an object. MicroCT scanning is based on the attenuation of X-rays through materials (Shi et al., 1999); therefore attenuation of an object is the foundation for the images produced by a MicroCT scan. These images appear as raster images and are displayed according to a greyscale which represents variability in density

(Ketcham and Carlson, 2001). Density differences are measured according to the atomic number of an element, which is defined as the number of protons present in an atomic nucleus (Brown et al., 2000). The atomic number therefore defines the chemical elements and density differences present in the scanned object, displayed as a broad greyscale of voxels in the resulting image.

CT imagery has been used widely to characterize pore structure and flow in geological materials (Ketcham and Iturrino, 2005). Ketcham and Iturrino (2005) used a High-resolution X-ray CT (HRXCT) to analyze porosity distribution using a series of felsic volcanic rocks on a scale useful for petrographic observation and analysis. Geotechnical analyses were performed by Shi et al. (1999) using a medical CT scanner to study soil deformation patterns inside soil masses that would otherwise be unobservable.

1.3 Research objectives

The overall goal of this research was to develop a method to analyze and measure the physical and hydraulic properties of organic soil using computed tomographic imagery. To determine if two and three-dimensional images of peat produced using a MicroCT scanner can be used to accurately characterize these properties, the following objectives were addressed:

1) Measure air-filled porosity at four levels of soil tension and for each tension level obtain high-resolution three-dimensional images of seven peat samples,

2) Obtain two-dimensional slices from the three-dimensional images and measure changes in:

(i) pore size distribution at the residual moisture content and

(ii) saturated area at 0.5 m and 5.0 m tensions,

3) Measure unsaturated hydraulic conductivity of seven peat sub-samples,

4) Examine pore structure and microscopic spaces of porous *Sphagnum* cells for different depths, states of decomposition and moisture content.

1.4 Thesis organization

This thesis is divided into several chapters. Chapter 1 consists of an introduction and literature review, Chapter 2 describes the study site and Chapter 3 describes all the methods used for obtaining the results discussed in Chapters 4, 5 and 6. Chapter 4 focuses on the results and discussion for objectives 1 and 2 (i). Chapter 5 describes the results and discussion for objective 3 and Chapter 6 examines the results and discussion for objective 4 and 2 (ii). Chapter 7 summarizes and examines the correlation between the results. Finally, Chapter 8 concludes this thesis research.

CHAPTER 2:
STUDY SITE

2.1 Introduction

Scotty Creek, Northwest Territories was selected as the place of study because it is representative of peatlands in northern boreal and boreal-tundra transition zones which are unique in physical and hydrological properties when compared to other peatlands in Canada. The lack of studies focused on subsurface hydrology in northern Canada stimulated interest for the use of this site for study.

2.2 Location and physiography

Scotty Creek (Figure 2-2) is located 50 km south (121°18′ 11″ W and 61°18′ 44″ N) of the municipality of Fort Simpson, Northwest Territories, Canada (Hayashi et al., 2004) in a Continental High Boreal wetland-dominated region (NWWG, 1988). Fort Simpson is situated at the confluence of two major rivers (Figure 2-1), the Mackenzie and the Liard. This region affects both drainage basins and their tributaries making it an ecologically and hydrologically sensitive region. Scotty Creek lies in the zone of discontinuous permafrost (Figure 2-3) (Hegginbottom and Radburn, 1992). Permafrost is exists below the ground surface and must have remained in a frozen state with a temperature below 0°C for more than two years, regardless of soil texture, water content, or geological character (Whittow, 1984).

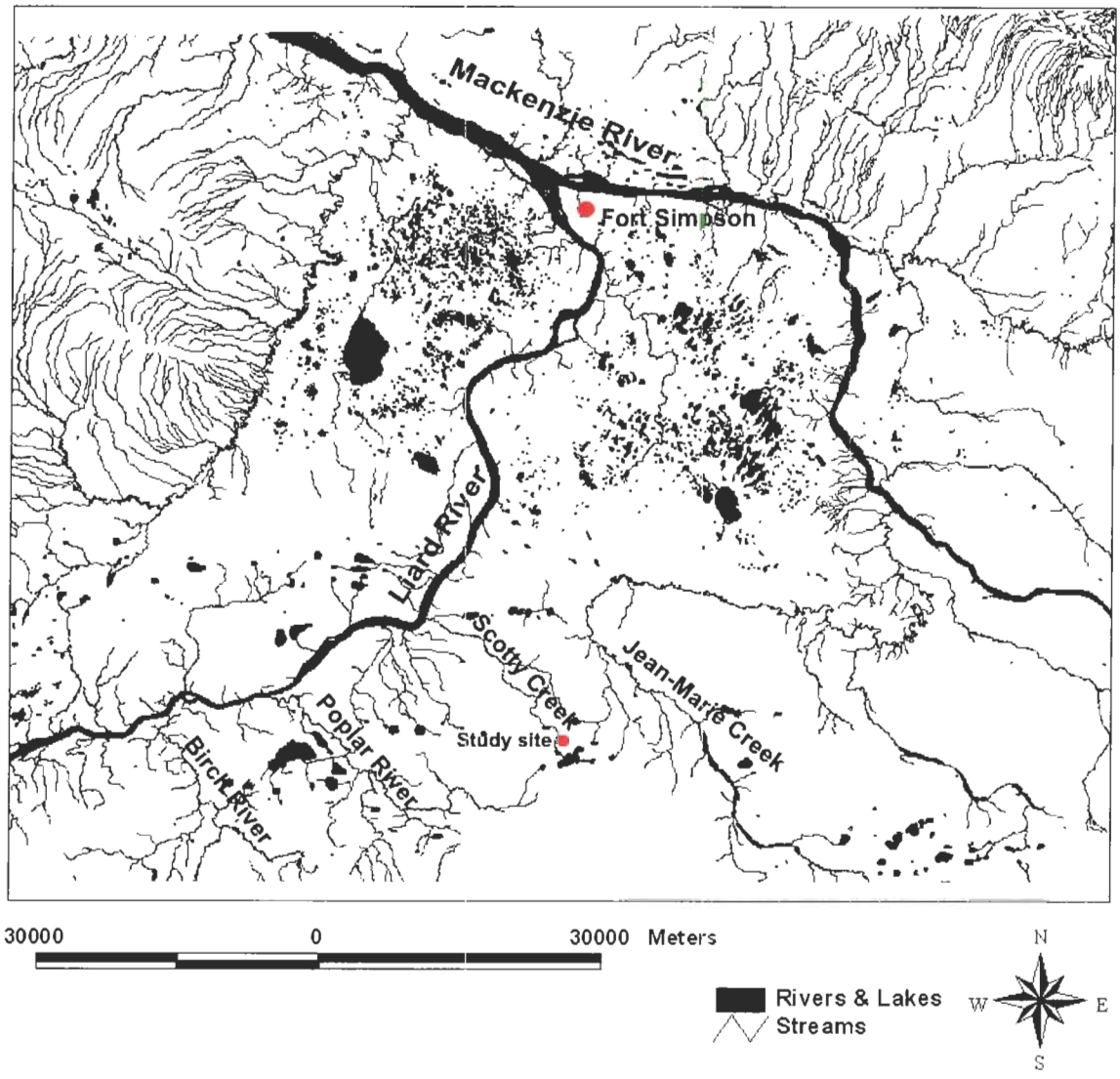

Figure 2-1 Map showing the confluence of the Mackenzie and Liard rivers at Fort Simpson, NT.

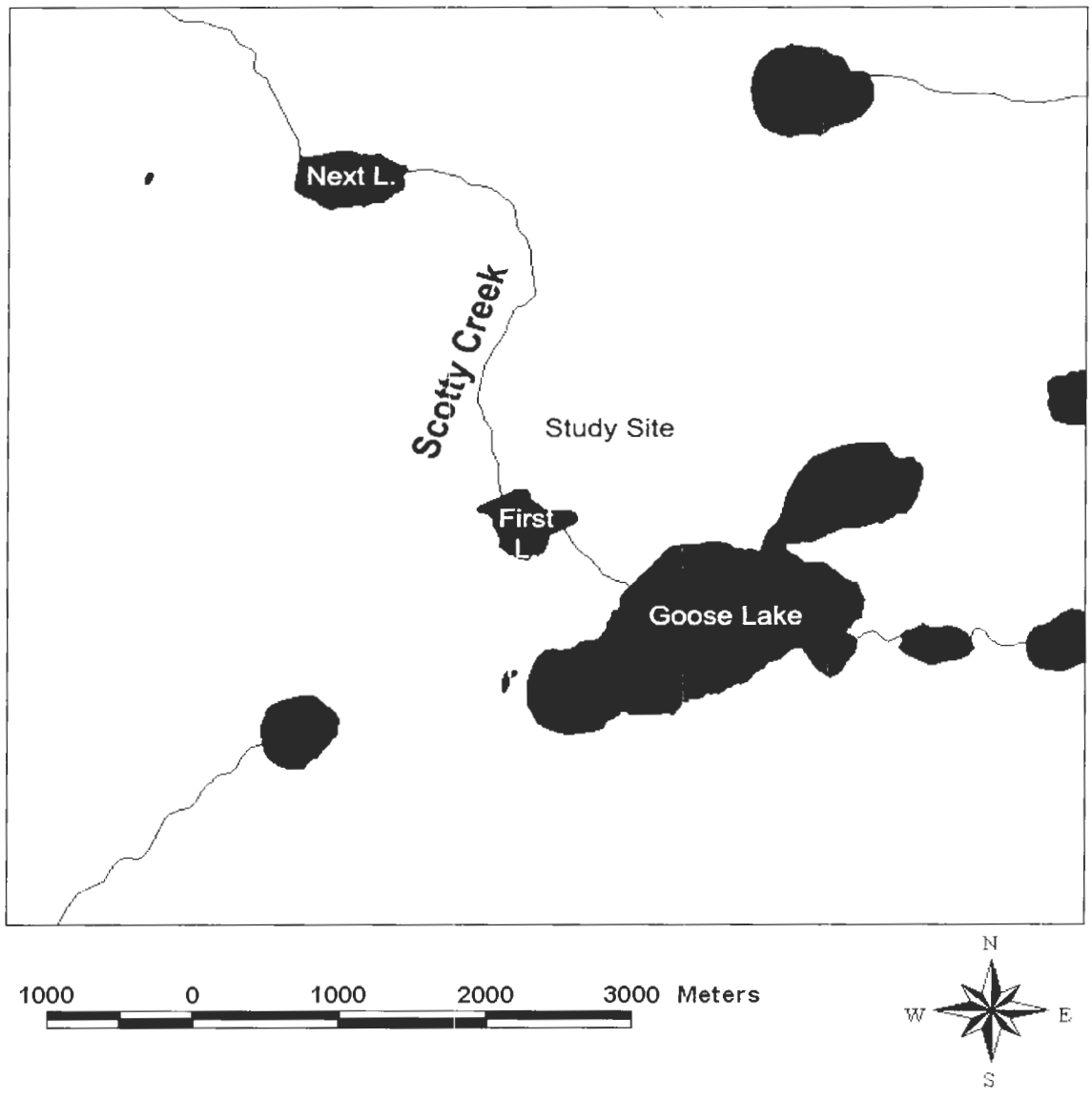

Figure 2-2 Map showing the Scotty Creek study site located at 121°18′ 11″ W and 61°18′ 44″ N.

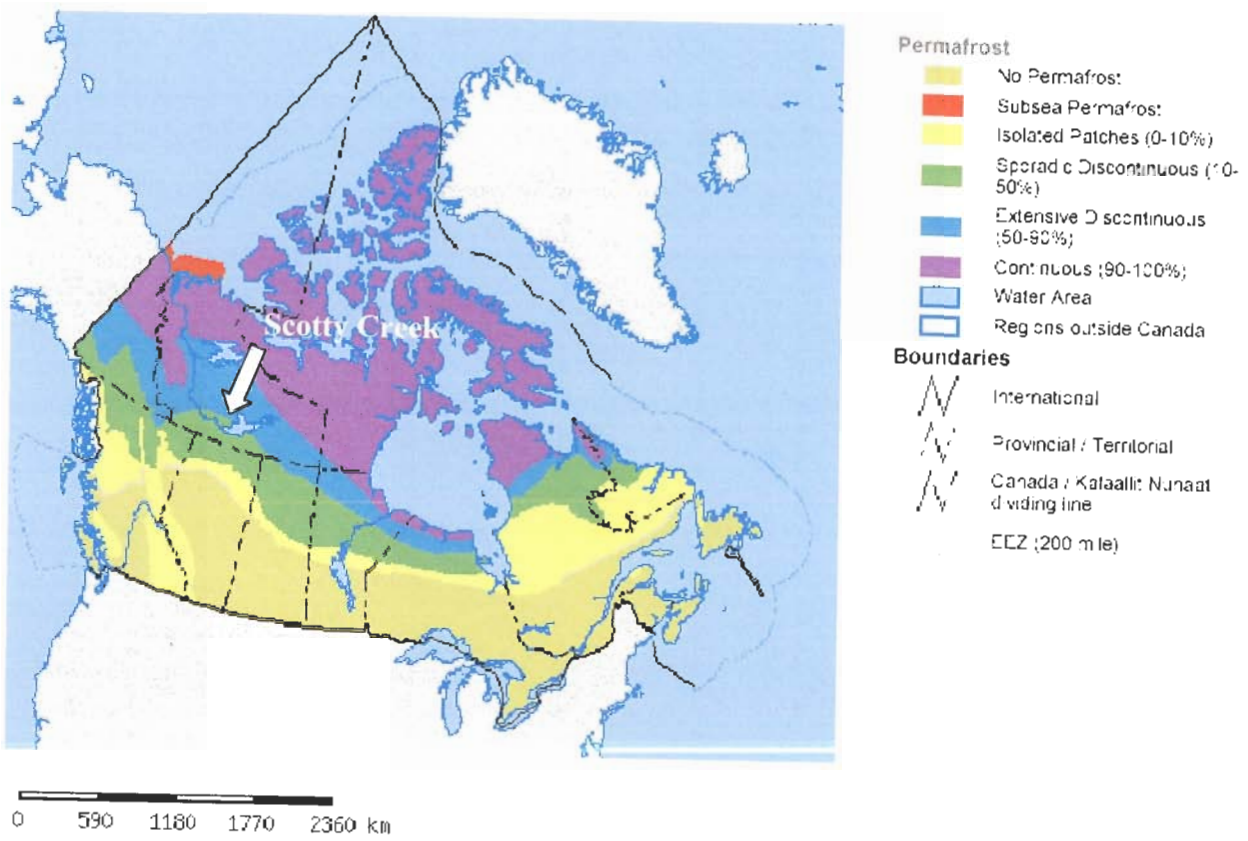

Figure 2-3 **Map showing zones of permafrost and discontinuous permafrost in Canada.**
This map was taken from the Atlas of Canada http://atlas.gc.ca © 2005. Produced under licence from her Majesty the Queen in Right of Canada, with permission of Natural Resources Canada.

Scotty Creek basin has an area of 152 km^2 and is part of the lower Liard River valley. The Liard River flows into the Mackenzie River drainage basin, which spans 1.8 x 10^6 km^2. The Mackenzie River then continues to flow northward and contributes vast amounts of water to the Arctic Ocean (Carmack, 2000). The lower Liard River valley is a peatland-dominated environment (Quinton et al., 2003). Peatlands in this area developed over till, glaciofluvial deposits, lacustrine silt, or bedrock (Robinson and Moore, 1999). The organic soil layer varies from zero to eight meters in depth and is underlain by a thick deposit of silt and clay, having low permeability (Aylesworth and Kettles, 2000). The drainage system at the Scotty Creek study site is composed of poor channel fens, flat bogs and peat plateaus. Peat plateaus are a raised peatland surface and are the only peatland in this study region that have a perennial (permafrost) frost table (Robinson and Moore, 2000). My sampling was focused on bogs and peat plateaus for this thesis research because channel fens are very deep with numerous sedges, mosses and grasses which made sampling very difficult.

2.3 Climate

The Fort Simpson area is characterized by a dry continental climate, with short, dry summers and long cold winters (Quinton et al., 2004). In particular, the climate at Scotty Creek is influenced by the combination of its latitude, continentality (longitude) and local airmasses. Continental arctic airmasses develop between 60° N and 90° N where they become very cold, stable and dry. The average annual maximum temperature recorded in Fort Simpson from 1897-2002 was 1.7 °C. The average annual minimum temperature was -9.4 °C and the average annual mean temperature was -3.8 °C calculated

over the same time period. These annual temperature averages are displayed in Figures 2-4, 2-5 and 2-6. The annual total precipitation was 347.8 mm when averaged from 1897-2002 (Figure 2-7). The spring snowmelt period in Scotty Creek lasts 1.5 – 2 months, usually occurring in mid-April to May and sometimes extending into early June.

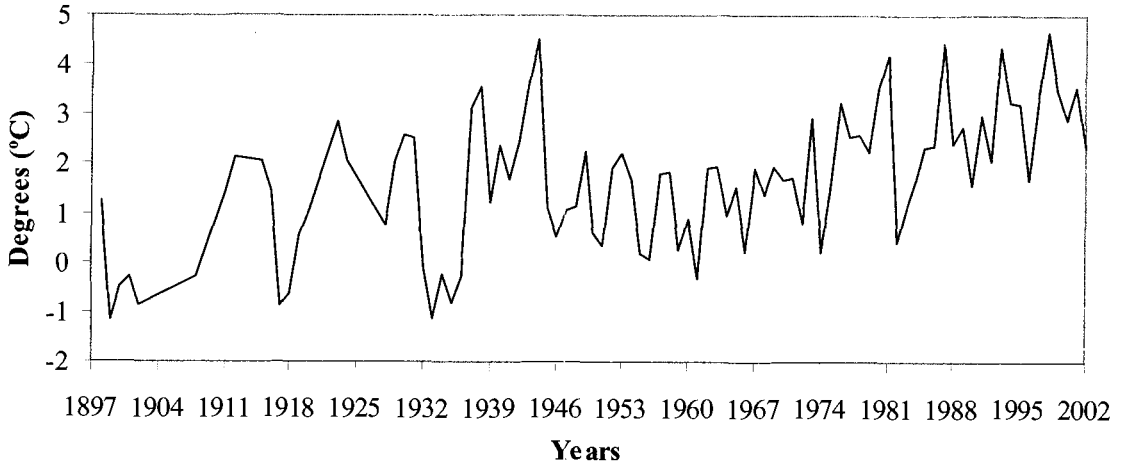

Figure 2-4 Maximum annual temperatures 1897-2002.

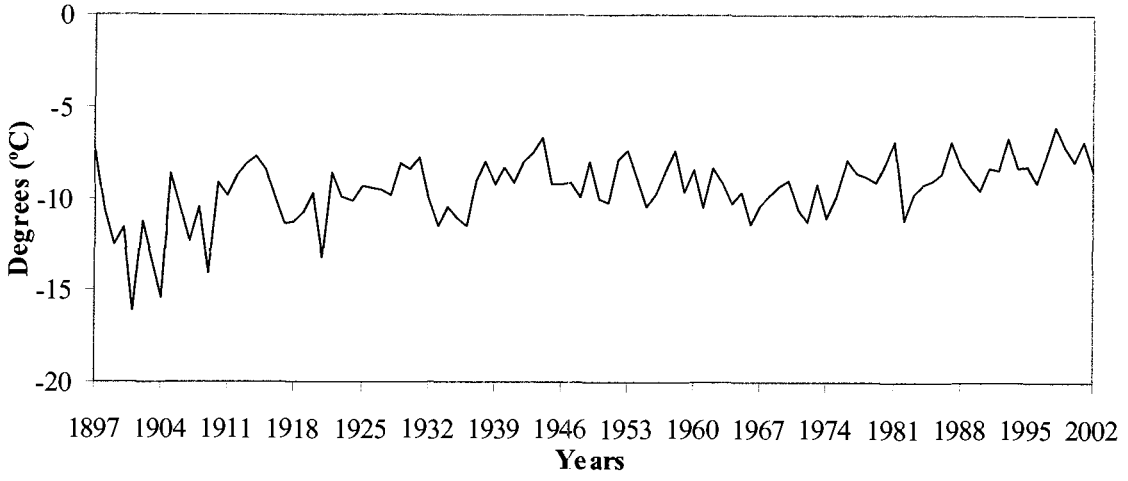

Figure 2-5 Minimum annual temperatures 1897-2002.

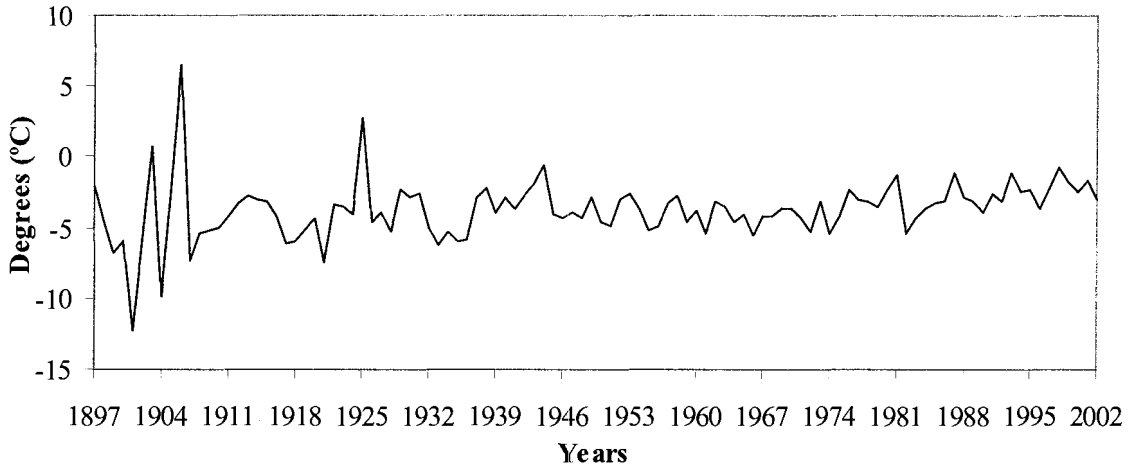

Figure 2-6 Mean annual temperatures 1897-2002 (missing data was interpolated).

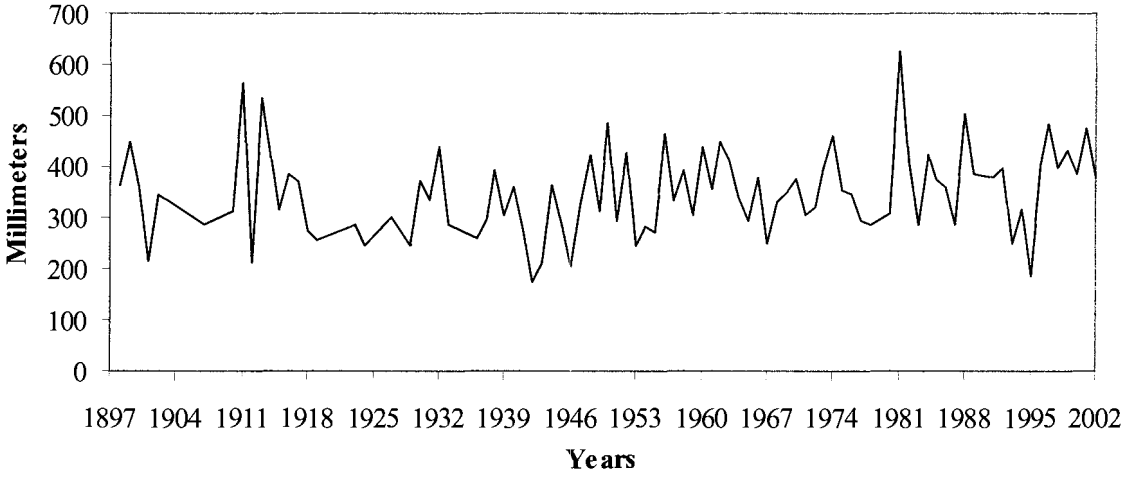

Figure 2-7 Annual total precipitation 1897-2002.

2.4 Vegetation

Peat plateaus are raised above adjacent fens and flat bogs thus support trees and shrubs. Lichens, mosses, liverworts, club mosses, fungi, and wild flowers occur in peat plateaus and flat bogs at this site. The vertical growth of *Sphagnum* mosses creates acidic and nutrient-poor conditions, which limit the diversity of the vegetation that can grow here (van Breemen, 1995; Robinson and Moore, 2000). Appendix A, Tables A-1, A-2, A-3, A-4, and A-5 present lists of vegetation identified at the study site.

CHAPTER 3:
METHODOLOGY

3.1 Introduction

The goal of this research was to explore computed tomographic imagery for use in soil analysis. By means of the MicroCT scanner, three-dimensional images were created for quantitative and qualitative peat analysis. Because there is very little precedent in applying CT scan technology to organic soils, an experimental protocol was adopted whereby a variety of methods were employed in order to overcome challenges in the acquisition, manipulation and interpretation of the three-dimensional imagery.

Developing techniques for insuring proper soil sampling and prevention of consolidation and settlement during sub-sampling and soil transport were some of the challenges faced during this thesis research. Developing expertise for using the MicroCT scanner and its custom software, use of and assemblage of a permeameter and exploring methods and software for thresholding the 2D and 3D images were additional challenges faced. The methodology for this study was characterized into three categories: field, laboratory and analytical methods.

3.2 Field Methods

In June 2004, soil blocks were removed from an undisturbed flat bog and adjacent peat plateau (Figure 3-1(a) and (b)).

Figure 3-1 **(a) Schematic of the peat plateau and flat bog chosen for soil sampling (not to scale) and (b) photo of the flat bog and surrounding peat plateau.**
With extra special thanks to Mark Blais for drawing Figures 3-1 (a), 3-9, 3-15 and 3-16, published by permission.

Peat plateau
Peat bog
0.6 m transitional slope
3.1m radius
Plot #1
Plot #2
Active layer transect

(a)

(b)

On June 3, 2004 a plot was created on the flat bog measuring 1.22 m in length and 1.67 m in width (Figure 3-2) for soil sampling. That size of the plot was marked off so that more undisturbed soil blocks could be removed if problems occurred with sampling. The flat bog itself was approximately 62 m in diameter and had a water table at the soil surface (Figure 3-6). The bog had a slight transitional slope leading to the peat plateau with a height difference of approximately 0.6 meters.

Figure 3-2 Flat bog soil plot. 122 cm in length and 167 cm in width.

The flat bog contained a small number of black spruce trees that varied in height from 0.41 m to 3.00 m. Other vegetation, including bog rosemary shrubs (*Andromeda*

polifolia), acute-leaved mosses (*Sphagnum capillifolium*), Rusty peat moss (*Sphagnum fuscum*), and leatherleaf shrubs (*Chamaedaphne calyculata*), were also identified (Figure 3-3).

Figure 3-3 Photograph of the flat bog used for soil collection, showing typical vegetation and ground cover in the study region.

The peat plateau was dominated by black spruce trees up to 8 m in height, bog cranberry (*Oxycoccus microcarpus*), acute-leaved mosses (*Sphagnum capillifolium*), rusty peat moss (***Sphagnum fuscum***), leatherleaf shrubs (*Chamaedaphne calyculata*), laborador tea shrubs (*Ledum groenlandicum*), capillary thread mosses (*Bryum Capillare*), grey reindeer lichen (*Cladina rangiferina*), green reindeer lichen (*Cladina mitis*), lingonberry (*Vacinium vitis-idaea*) and dwarf bog cranberry (*Andromeda polifolia*) (Figure 3-4).

Figure 3-4 Photograph of the peat plateau used for soil collection, showing typical vegetation and ground cover in the study region.

On June 4, at the peat plateau site, a 0.55 m by 0.62 m plot was prepared in an undisturbed moss covered area (Figure 3-5). That same day, soil blocks were cut and removed from the flat bog and from the peat plateau. The blocks were cut to specific volumes so they to fit in coolers for transport. The flat bog block was 0.36 m x 0.19 m x 0.26 m in size and the peat plateau block was 0.23 m x 0.23 m x 0.23 m in size. The flat bog sample block was completely saturated with water because the water table was at the surface (Figure 3-6); because of this, the volume of the soil block changed once it drained. At the time of sampling, the soil temperature of the flat bog was 12.3°C at the

surface, the soil water temperature was 12.6°C, the air temperature was 18.4°C and the relative humidity was 47.9%. At the surface of the peat plateau the soil temperature was 11.8°C. The depth to the top of the water table was approximately 5 cm and the temperature of the water at this depth was 2.5°C. The air temperature at the time of sampling was 24.1°C and the relative humidity was 35.8%. At the peat plateau plot, the frost table depth was 26 cm. The depth to the frost table was measured by inserting a graduated steel rod into the soil plot to the top of the frozen saturated layer (Figure 3-7). Sampling depth was limited by the frost table height in this case. There was also a layer of water sitting on the frost table which caused the soil block to drain once it was removed from the ground.

Figure 3-5 Photograph showing the plot created in the peat plateau.

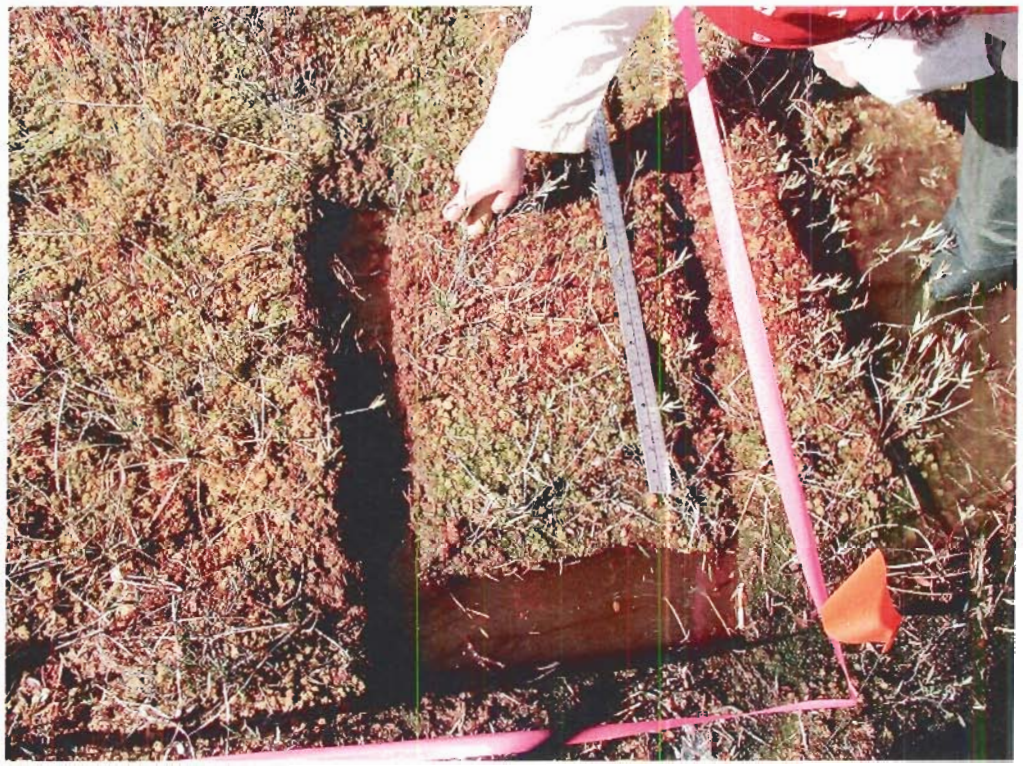

Figure 3-6 Picture showing the removal of the soil block and the height of the water table in the flat bog.

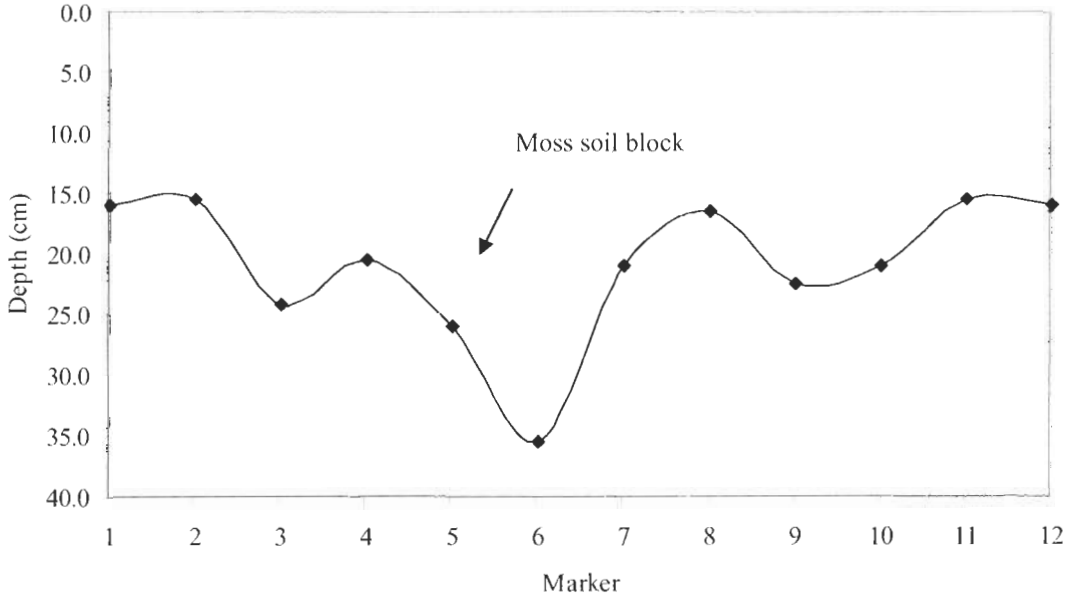

Figure 3-7 Peat plateau, active layer survey at time of sampling. The peat block was taken from marker 5.
Each marker was 1 m apart. Line connecting discrete data points was smoothed using MS Excel.

3.3 Laboratory Methods

3.3.1 Soil sub-sampling

The soil blocks were transported from Scotty Creek to Simon Fraser University where they were measured for changes in volume due to consolidation and water drainage. Peat is very compressible and deformable and can adapt to changes in moisture content through its ability to expand and contract (Ingram, 1983) because of its high porosity. When the water table falls, the effective stress is transferred from the overlying peat onto the peat matrix resulting in settlement (Price, 2003). Ivanov (1981) demonstrated that a compression curve formed a relation between external compression, moisture capacity and total porosity of peat. Price and Schlotzhauer (1999) further identified the importance of including compression in determining water balances. Price (2003) discussed the role of peat deformation on methane flux, water retention, hydraulic conductivity and specific yield.

The results of the changes in size are displayed in Table 3-1 and 3-2. The sub-sample depths measured in the laboratory are the depths used to label samples and datasets throughout this thesis.

Table 3-1 Flat bog sub-sampling depths. The soil depths *in situ* and the depths sub-sampled in the lab, varied due to drainage and compaction of the soil.

In situ (cm)	Lab (cm)
3.86	3
12.86	10
25.71	20
32.14	25

Table 3-2 Peat plateau sub-sampling depths. The soil depths *in situ* and the depths sub-sampled in the lab, varied due to drainage and compaction of the soil.

In situ (cm)	Lab (cm)
3.14	3
10.45	10
18.82	18

The blocks were sub-sampled once they were moderately frozen. They were frozen to a point where the soil no longer fell apart when handled and to a point where it was still possible to cut into it. The soil was cut to size by trimming and shaping the peat around the sub-sample edges with shears and scissors, in stages, to prevent the soil from displacing and compacting (Figure 3-8).

Figure 3-8 Trimming and shaping a sample of flat bog soil.

Numerous sub-samples were shaped and placed into sealed vials for storage. The flat bog block was sampled at 3 cm, 10 cm, 20 cm and 25 cm depths and the peat plateau block was sampled at 3 cm, 10 cm and 18 cm depths (Figure 3-9) so as to obtain equally spaced specimens that represented different stages of decomposition. The sub-samples were frozen in the sealed vials and transported in a cooler by myself to the Department of Land Resource Science at the University of Guelph for CT imaging. The sub-samples were supported by bubble wrap and ice-packs, to minimize movement and hence, disturbance to the sub-samples.

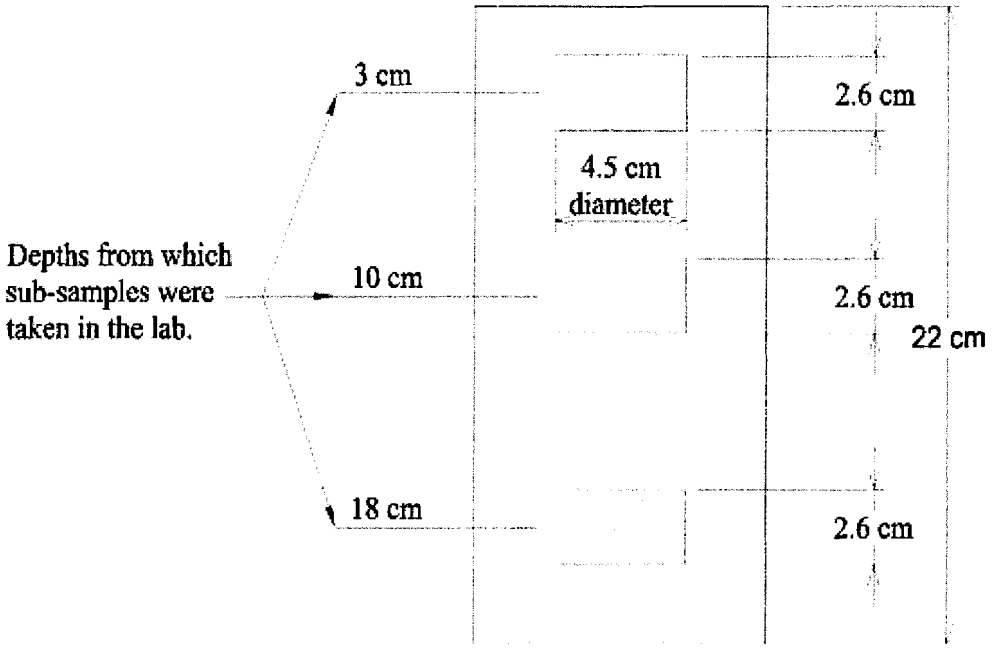

Figure 3-9 Schematic of sub-sampling the peat plateau soil block.

3.3.2 Pressure plate extraction

Water in unsaturated soil is held under cohesive strength arising from negative pore water pressure and surface tension effects occurring at the interface of the pore water, pore air, and pore particles (Lu and Likos, 2004) where capillarity and adsorption produce a negative matric potential or matric suction head (Hillel, 1998). Pressure head is a physical mechanism of water retention in the form of a concave meniscus extending between soil particles (Freeze and Cherry, 1979).

In total seven sub-samples (3 from the peat plateau and 4 from the flat bog) 4.5 cm in diameter and 2.6 cm in height, with a volume of 20.77 cm^3 were placed in PVC tubes. A mesh cloth was attached to allow water to escape while keeping the soil in place (Figure 3-10).

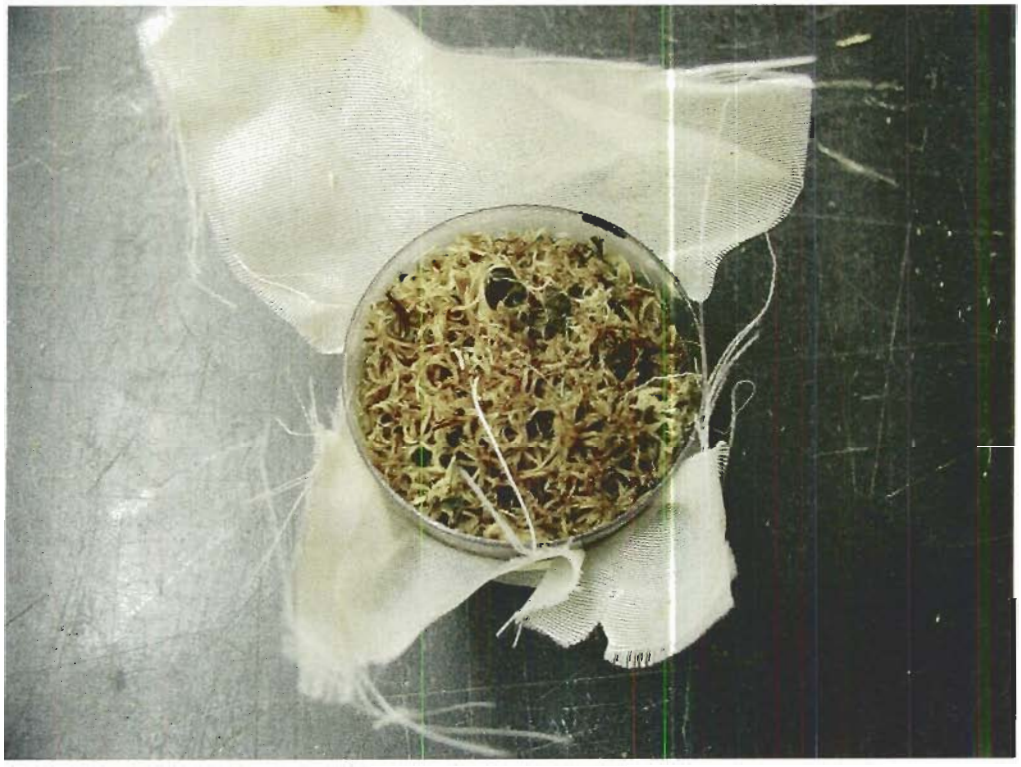

Figure 3-10 Sub-sample in PVC tube with mesh attached for water release.

Each sub-sample was saturated and weighed (Denver Instrument Company TR4102 Max: 4100 g) then placed in a MS-8-130 High-Resolution MicroCT Scanner (Figure 3-13). Afterwards, the sub-samples were sent to the Laboratory Services Division at the University of Guelph where laboratory technicians performed the suction tests. For each sub-sample the procedure was repeated for three additional volumetric moisture contents, corresponding to 0.02 m, 0.51 m and 5.01 m of matric suction or tension head. These tensions were chosen since they represented significant points or changes in moisture on the moisture characteristic curve (Figure 4-1). The sub-samples were brought to these tension levels using a five bar pressure plate CAT #1600 (Figure 3-11).

Figure 3-11 Pressure plate used for matric suction tests.

3.3.3 MicroCT scanning

After a short training session, the workings of the MicroCT became familiar enough to start scanning the soil on my own. All seven sub-samples were individually placed in the MicroCT scanner for imaging (Figure 3-12) after each level of tension was reached. The MicroCT scanner source yielded a 130 kVp monochromatic x-ray beam, at a voltage of 80 kV, with a 100 mA current, at a 0.045086 mm resolution. The three-dimensional images were reconstructed from 720 views taken at half angle increments over 360°. Two frames were taken per view with an exposure of 1700 ms. The detector was a high resolution digital x-ray camera detector system. The focal spot to the soil position was 270 mm, the focal spot to detector position was 354.35 mm and the detector spacing was 0.0295857988 m. A 2 x 2 pixel binning was used to create 875 x 1750 pixels on the 110 x 55 mm detector imaging area.

Figure 3-12 MS-8-130 High-Resolution MicroCT Scanner.

Pixel binning helped maintain a manageable file size for analysis. Additionally lucite filtration (0.076 m depth and 0.07 m height) functioned as a bath to compensate for systematic differences in the thickness of the sample cylinder (Figure 3-13).

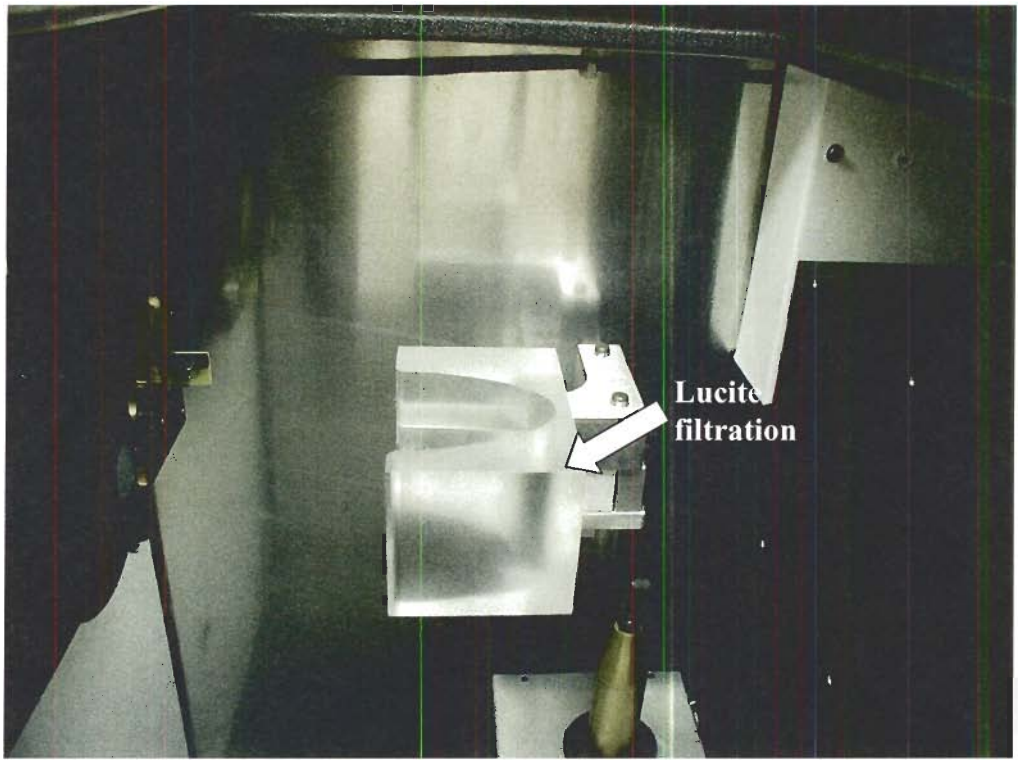

Figure 3-13 A photograph showing the inside of the MicroCT scanner with the lucite filtration in place.

After the scanning was completed, the soil sub-samples were dried in a soil oven at 105°C for 24 hours. The sub-samples were then weighed and for each tension level and sub-sample depth, volumetric moisture content was determined gravimetrically using Equation 1-4 and bulk density was determined using Equation 1-1.

3.3.4 Permeameter

Laboratory measurements of hydraulic conductivity permit the hydraulic gradient and overall pressure to be controlled (Rycroft et al., 1975). In this study, a steady-state head control permeameter was assembled by myself, at Simon Fraser University, to measure unsaturated hydraulic conductivity of the peat sub-samples for both terrain types at a range of soil tensions. Construction of the permeameter was based on the design of Klute and Dirksen (1986) and Booltink et al. (1991). Horizontal sub-samples were cut from the each of the soil blocks (Figure 3-14) (3 from the peat plateau and 4 from the flat bog) and placed in a PVC tube so that lateral unsaturated hydraulic conductivity could be measured. Each sub-sample was cut to a height of 10.0 cm and a diameter of 5.15 cm.

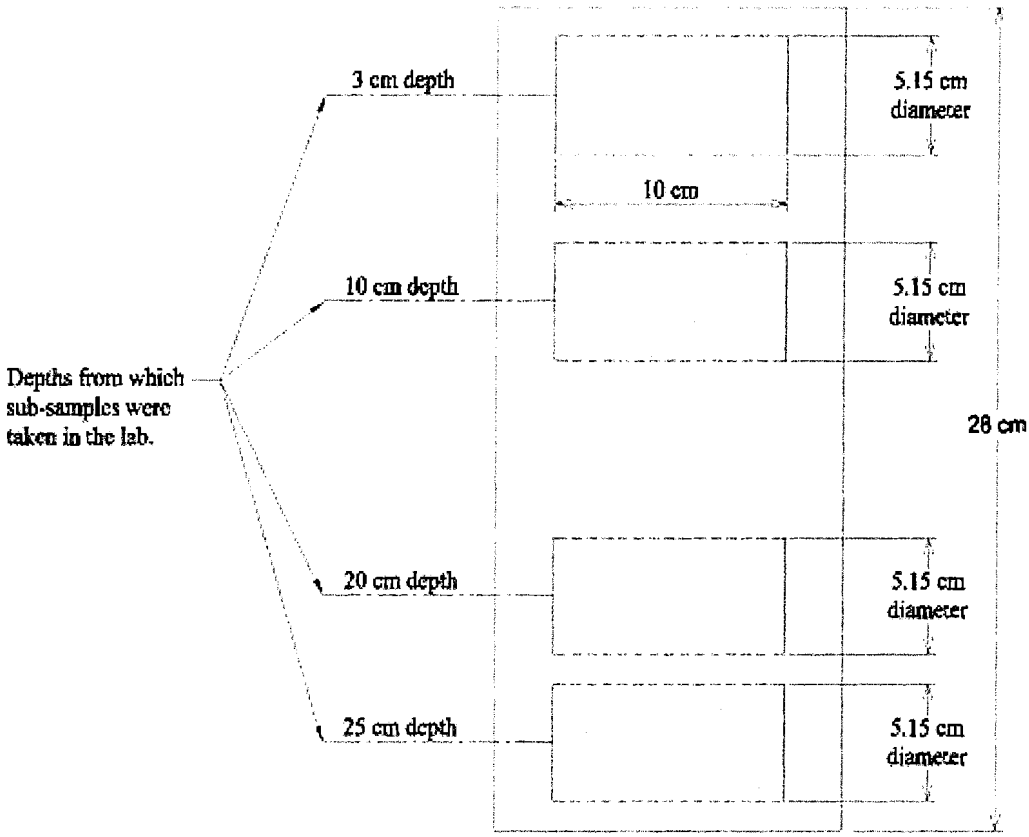

Figure 3-14 Schematic of sub-sampling the flat bog soil block.

A 4.5 cm diameter steel tube was used to provide a suction crust infiltrometer (Booltink et al., 1991). A mixture of one part cement to nine parts sand was mixed and placed at one end of the tube which was held together with cheesecloth and left to harden (Figure 3-15). The hydraulic conductivity of the crust was 1.0×10^{-6} m sec^{-1}. A second crust was made of two parts cement and eight parts sand that had a measured hydraulic conductivity of 3.8×10^{-7} m sec^{-1}. The purpose of the crusts was to ensure a steady flux of water into the underlying sub-samples (Booltink et al., 1991).

The soil sub-samples were held in a PVC tube cut to a length of 13.4 cm and a diameter of 5.15 cm. A mesh (cheesecloth) was used to hold the soil in place in the PVC

tube (Figure 3-15) and to maintain continuous contact between the soil and the sand column. Two holes (0.6 cm diameter) were made in the PVC tube to allow porous cup tensiometers to penetrate the soil at two points. The porous cups were soaked in de-aired water overnight and then were attached to tubing. De-aired water was placed in the tubes and the tubes were attached to the apparatus to implement a negative pressure head at each point. This tubing was used to measure hydraulic gradient by means of the negative pressure head determined from these two points – one near the top and one near the bottom of the soil volume.

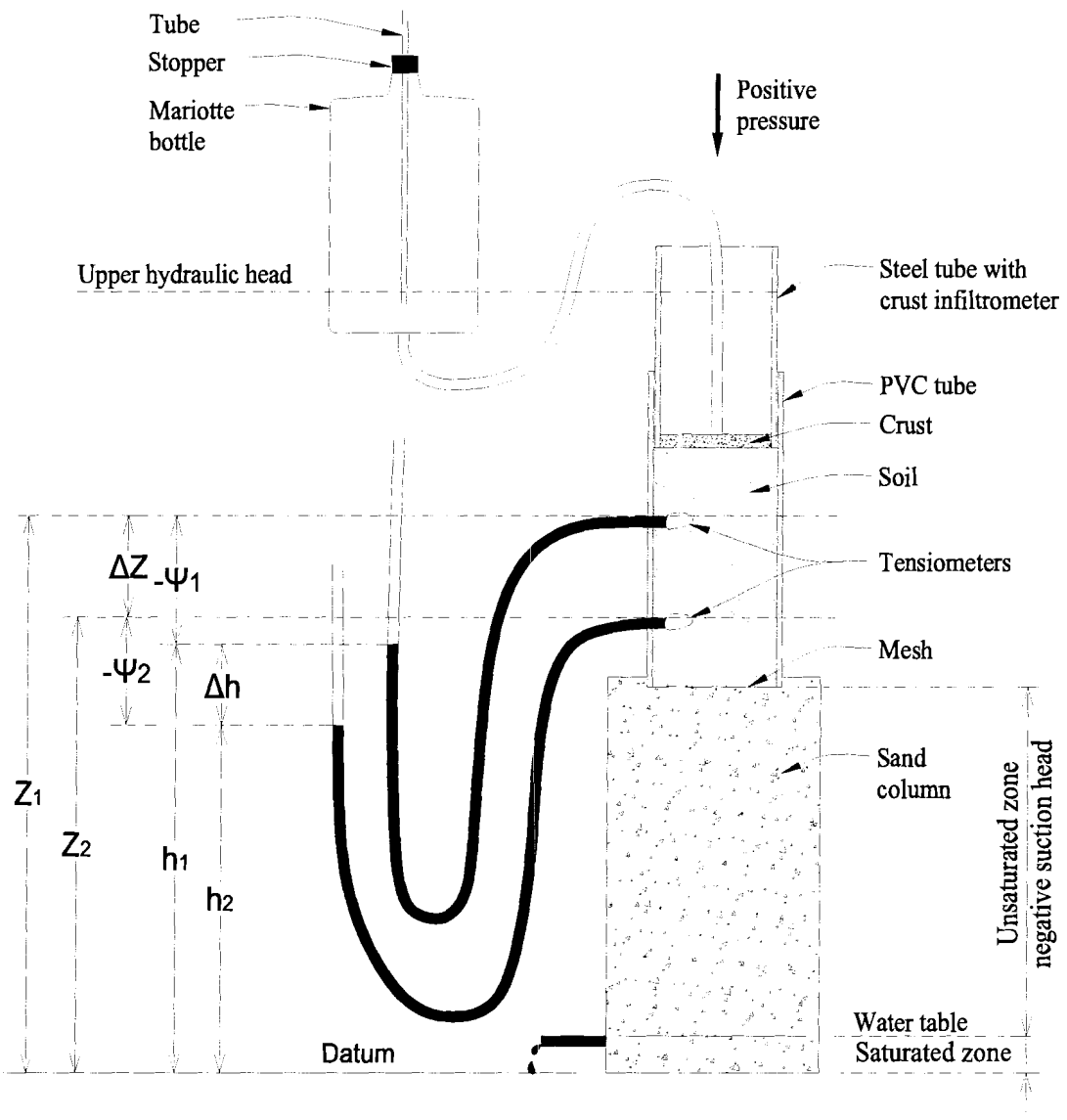

Figure 3-15 Schematic of the permeameter used to determine unsaturated hydraulic conductivity of the peat plateau and flat bog sub-samples.

A gradient of head was produced using a sand column placed below the peat sub-sample to create a unit-gradient flow (Booltink et al., 1991). A Mariotte bottle was used to control the water supply and hydraulic head to the upper end of the system (Klute and Dirksen, 1986). The positive pressure head from the Mariotte bottle was controlled by its height in relation to the steel tube (and crust infiltrometer) (Klute and Dirksen, 1986). A hole was made in the bottom of the bottle to allow tubing to be attached to it. This tubing

provided a connection for water to the steel tube and hence the sub-sample. A stopper with a tube for airflow was placed on the Mariotte bottle to allow water to drain from the bottle at a constant rate (Figure 3-15). The rate of water flow through the unsaturated peat was measured as a volume per minute ($cm^3\ min^{-1}$).

Unsaturated hydraulic conductivity was calculated from Darcy's law (Equation 3-2).

$$K = \frac{q \times \Delta z}{\Delta h} \qquad [3\text{-}2]$$

where elevation head, Δz, was calculated using Equation 3-3 as the difference between z_1 and z_2 or the elevation of each porous cup.

$$\Delta z = z_1 - z_2 \qquad [3\text{-}3]$$

The hydraulic head (Δh) was calculated using Equation 3-4

$$\begin{aligned} h_1 &= z_1 + (-\Psi_1) \\ h_2 &= z_2 + (-\Psi_2) \end{aligned} \qquad [3\text{-}4]$$

where $-\psi$ is the negative pressure head, otherwise described as soil tension, and z is the elevation head. The hydraulic head was then calculated from the difference between h_1 and h_2 (Equation 3-5).

$$\Delta h = h_1 - h_2 \qquad [3\text{-}5]$$

The flow rate (q) was calculated from the measured flow rate (volume time^{-1}) and the cross-sectional area of the soil sub-sample (Equation 3-6).

$$q = \frac{volume}{time} \times \frac{1}{area} \qquad [3\text{-}6]$$

In order to determine the volumetric moisture content of each sub-sample, each sub-sample was weighed after each new matric suction application. The sub-samples were oven dried to determine the dry weight of each. Volumetric moisture content was then determined for each tension level using Equation 1-4. The data was fitted to soil moisture characteristic curves (Figure 5-3 and 5-4) with the addition of values from Figure 4-1. The soil moisture characteristic curve was then plotted adjacent to a hydraulic conductivity curve, which relates hydraulic conductivity to matric suction, K (ψ) (Mualem, 1976). The unsaturated hydraulic conductivity and matric suction values were fitted to the Mualem (1976) equation (Equation 3-7)

$$\frac{K(\psi)}{K_s} = \frac{\left\{1 - (\propto |\psi|)^{n-1}\left[1 + (\propto |\psi|)^n\right]^{-m}\right\}^2}{\left[1 + (\propto |\psi|)^n\right]^{m/2}} \qquad [3\text{-}7]$$

where K_s is the saturated conductivity, ψ is the matric suction and m and n are fitting parameters where $m = 1\text{-}1/n$ (Hillel, 1998). The values used for saturated hydraulic conductivity in the graphs, were obtained from Quinton et al. (2000).

3.4 Analytical Methods

3.4.1 MicroCT scanner - three-dimensional imagery

A MicroCT scanner was used to create three-dimensional imagery of seven sub-samples at four levels of soil tension. This procedure allows the internal structure of the soil to be reconstructed from the multiple projections of the soil (Curry et al., 1990). In this case, projections are produced from scanned thin cross-sections of each sub-sample from the transmitted photons being measured by the radiation sensitive detector. The detector accumulates all the energy of the transmitted photons and provides the numerical data to be used in reconstructing an image (Curry et al., 1990). The quality of the images is related to the number of projections applied to reconstruct the image. The reconstruction of thin cross-sections of each sub-sample produces voxels, or three-dimensional pixels. Each voxel is assigned a number proportional to the degree that voxel attenuated the x-ray beam (Curry et al., 1990). The attenuation coefficient (μ) is used to quantify the soil as it is attenuated. Attenuation values are based on the atomic number and density of an object. The value of the linear attenuation coefficient is determined using the equation for monochromatic radiation, Beer's law (Equation 3-8)

$$N = N_0 e^{-\mu x} \qquad [3\text{-}8]$$

where N is the number of photons transmitted, N_0 is the initial number of photons, e is the natural logarithm, μ is the linear attenuation coefficient and x is the absorber thickness (air, soil/water) (Curry et al., 1990).

Calculations were made by MicroCT reconstruction software (EVS Beam) based on the linear attenuation coefficient of each voxel in the image matrix. A CT number was

assigned to each voxel allowing the computer to produce an image based on a 16-bit (signed data) greyscale. CT numbers are therefore proportional to the linear attenuation coefficient of each voxel in the image (Curry et al., 1990). A CT number or Hounsfield unit (H) is determined by relating the linear absorption of each voxel to the linear attenuation coefficient for water (Equation 3-9) (Curry et al., 1990)

$$CT_{number} = K\frac{\mu_p - \mu_w}{\mu_w} \qquad [3\text{-}9]$$

where K is the magnification constant, μ_p is the linear attenuation coefficient for each pixel and μ_w is the linear coefficient for water.

Thousands of CT numbers were produced to represent the variation in density throughout the soil. Values of air were found to be the lowest because the density of air is 1.29 kg m^{-3}, or 1/800th the density of water. CT numbers of approximately -1000 for air and 0 for water were distinguishable in the images.

3.4.1.1 Measuring air-filled porosity

The peat sub-samples contained organic matter (no mineral soil), water and air. Because air was the easiest to discern in the images and because water and organic compounds were not discernable from each other, organic material and water were considered together and air was distinguished alone.

Due to the large size of the files generated by the MicroCT scanner during image reconstruction, the software split the three-dimensional images into numerous smaller-sized files. Additional custom MicroCT software was then used to concatenate these smaller files back into one complete soil volume. These images often consisted of files

greater than 800 MB. Because Microsoft Windows cannot presently handle image files that are 800 MB or larger (without crashing), the volumes had to be cropped into smaller images, by removing the PVC tube and edges of the sub-samples. Images were all cropped into the same-sized elliptical cylinders (30.478 x 30.455 x 21.124 mm (x,y,z)) to ensure a direct comparison. Frequency distributions were derived using the voxel values produced by each soil sub-sample (Appendix B). The histograms changed from negative skewness at saturation to positive skewness at 5.0 m matric suction - demonstrating that the pores were gradually filled with air as matric suction increased. The histograms represent both unimodal and bimodal distributions, depending on the tension applied and the depth of the sub-sample. In both the peat plateau and flat bog sub-samples, the shallower depth sub-samples (3 cm and 10 cm) have bimodal distributions at 0.02 m matric suction (Figures C-1, C-2, C-4 and C-5 in Appendix B). The deeper depth sub-samples are limited to unimodal distributions at all levels of tension (Figures C-3, C-6 and C-7 in Appendix B).

From visual examination of the images and the frequency distributions, there is no clear threshold between soil/water and air. A region of uncertainty around the soil edges (Figure 3-16) represented a zone of transition (mixed voxels) between soil/water and air.

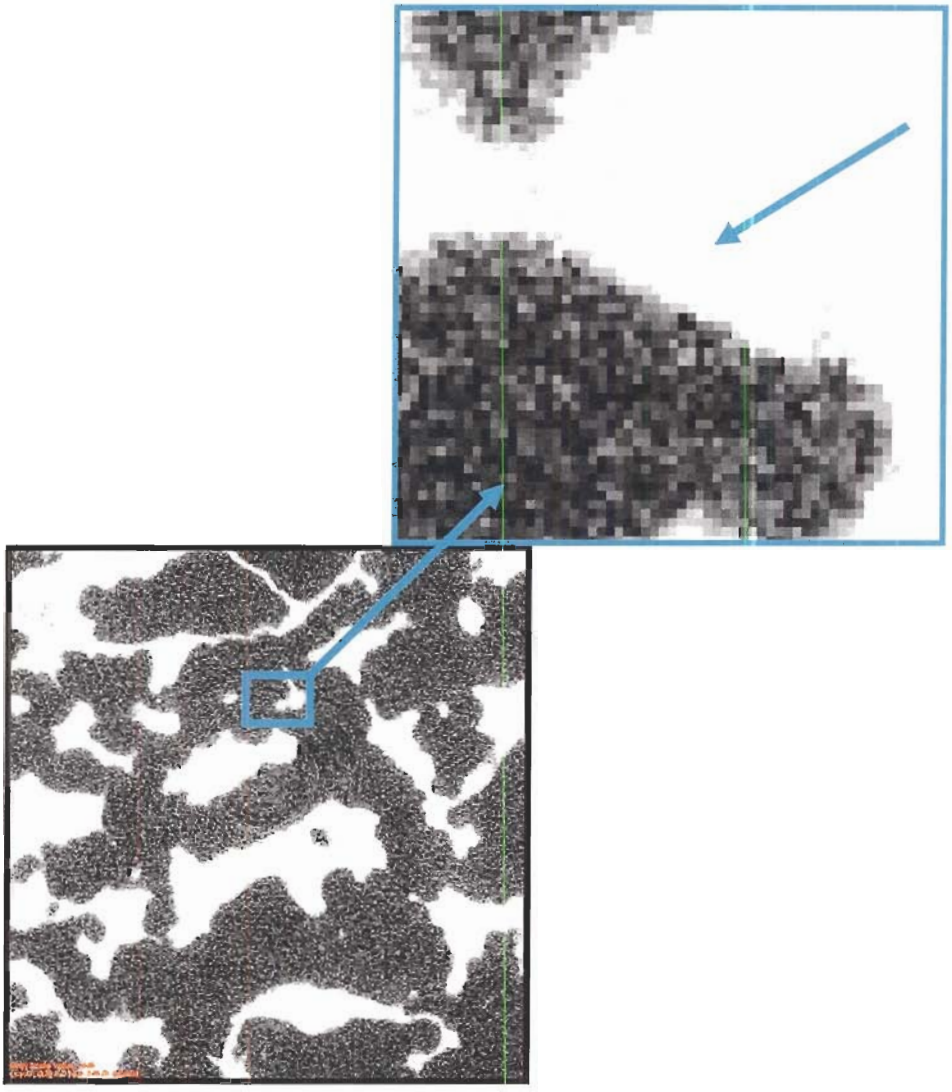

Figure 3-16 An example of the uncertain boundary that exists in all the images. The dark area represents the air content and the white area represents the soil/water content of the soil.

3.4.2 Fuzzy set theory

In order to make accurate measurements of air-filled porosity for each sample at each level of tension, a new approach was needed to deal with fuzzy boundaries or regions of uncertainty. Fuzzy set theory was applied to the sub-samples. Fuzzy sets violate the boolean algebra law of excluded middle and the law of contradiction by allocating an object membership in more than one set to a varying degree (Robinson,

2003). An open form linear membership function was used for defining these uncertain boundaries (Figure 3-17). Open form membership functions are regarded as non-decreasing with values between zero and one only within a bounded interval or an interval that includes its endpoints (Bohlin et al., 2000; Robinson, 2003).

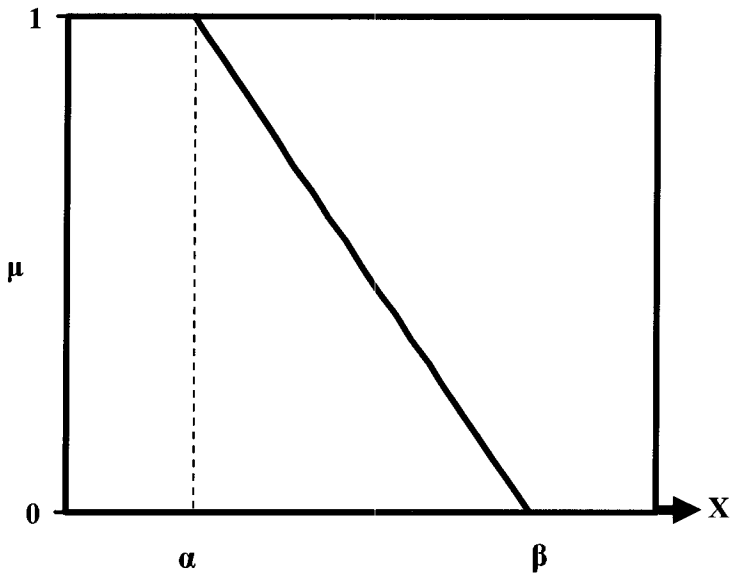

Figure 3-17 Linear membership function, modified from Robinson et al. (2003).

Mixed voxels are voxels that do not completely belong to one set or another, but are part of one set or another to a varying degree (Figure 3-18). This suggests that the voxels comprising the inter-modal zone in Figure 3-18 are those occurring at or near the walls of the soil pores. Fuzzy set theory was applied to this region in order to clarify the boundary within the inter-modal zone

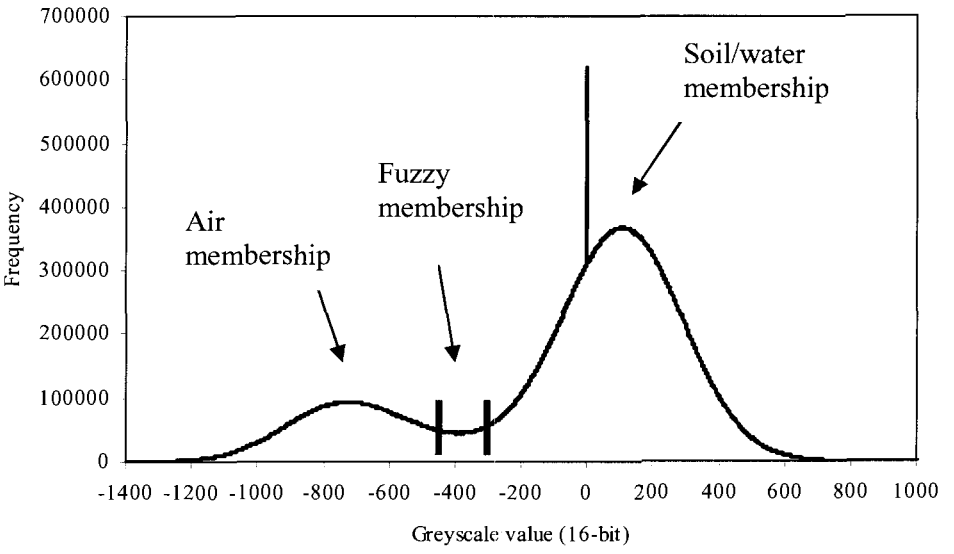

Figure 3-18 An example of the certain and uncertain regions. Members of both air and soil/water are certain regions and the fuzzy region is the uncertain region.

A region of fuzzy values was chosen by visually studying the histograms created by each frequency distribution of voxel values (Figure 3-18) and by examining the images individually to determine which voxels were not clearly part of one set or another (Figure 3-16). A linear membership function (Equation 3-10) was applied to these fuzzy values. The membership function acted as a 'grade of membership' as part of a scale that varied continuously between zero and one (Bourrough and McDonnell, 1998)

$$\mu = \begin{cases} \dfrac{(\beta - x)}{(\beta - \alpha)} for \alpha \le x \le \beta \\ 0 \end{cases} \qquad [3\text{-}10]$$

where one represented full membership: 1 for $x < \alpha$ and zero represented non-membership: 0 for $x > \beta$ (Figure 3-17). Once the fuzzy region was determined, the slope of the line was used to assign a range of values to that fuzzy transition zone.

The voxel values were weighted to a fuzzy set based on this linear membership function and the frequency of the voxel value in the image. The number of voxels that belonged to each fuzzy set was therefore established so that the amount of air that was in the soil sub-samples could then be calculated. This procedure was repeated for all seven sub-samples at all four soil tensions.

As a means of deciding if this method was useful for determining air-filled porosity, two other methods were used for comparison and evaluation (Figure 3-19). The 'autothreshold' function in Microview (custom MicroCT software) uses the frequency distribution of voxel values in the images to determine the threshold between two entities (Appendix B). Using the peat plateau sub-sample images, this function was used to obtain an autothreshold value. This threshold value was then used to calculate the air-filled porosity for each peat plateau image. The same images were then thresholded visually using each corresponding frequency histogram. From the mid-point of the intermodal zone, a value was chosen as the cut-off between soil/water and air. This decision was based on the location of the intermodal region in the histogram. Air-filled porosity was calculated by assigning those voxels to one entity or another. A comparison was made between all three methods (Figure 3-19). Out of the three methods, both the autothresholding and visual thresholding methods underestimated and overestimated air-filled porosity by a large degree in comparison to the fuzzy membership. For example at 18 cm depth and at lowest volumetric moisture content (Figure 3-19 (c)),

autothresholding estimated the air-filled porosity as 74% and visual thresholding estimated it to be 92%. Alternatively, fuzzy sets estimated the air-filled porosity as 81%. Autothresholding estimated 74% for all depths at that volumetric moisture content, indicating that this method lacks the ability to detect changes in air content. With the visual thresholding, the air-filled porosity actually increased at this tension level, with depth. This produced an overestimation in air-filled porosity since it is more likely that air-filled porosity would be higher at shallower depths (Figure 3-19). Both autothresholding and visual thresholding ran into difficulties especially when the distribution of voxels was unimodal instead of bimodal. Autothresholding had difficulty detecting changes in air content at high and low volumetric moisture contents and at deeper depths where the distribution was primarily unimodal. Similar problems with visual thresholding occurred. It was difficult to determine the inter-modal region (where it did not exist) when limited to a unimodal distribution. Based on this comparison of methods, fuzzy membership was deemed to be the most consistent method for determining three-dimensional air-filled porosity.

a. 3 cm depth

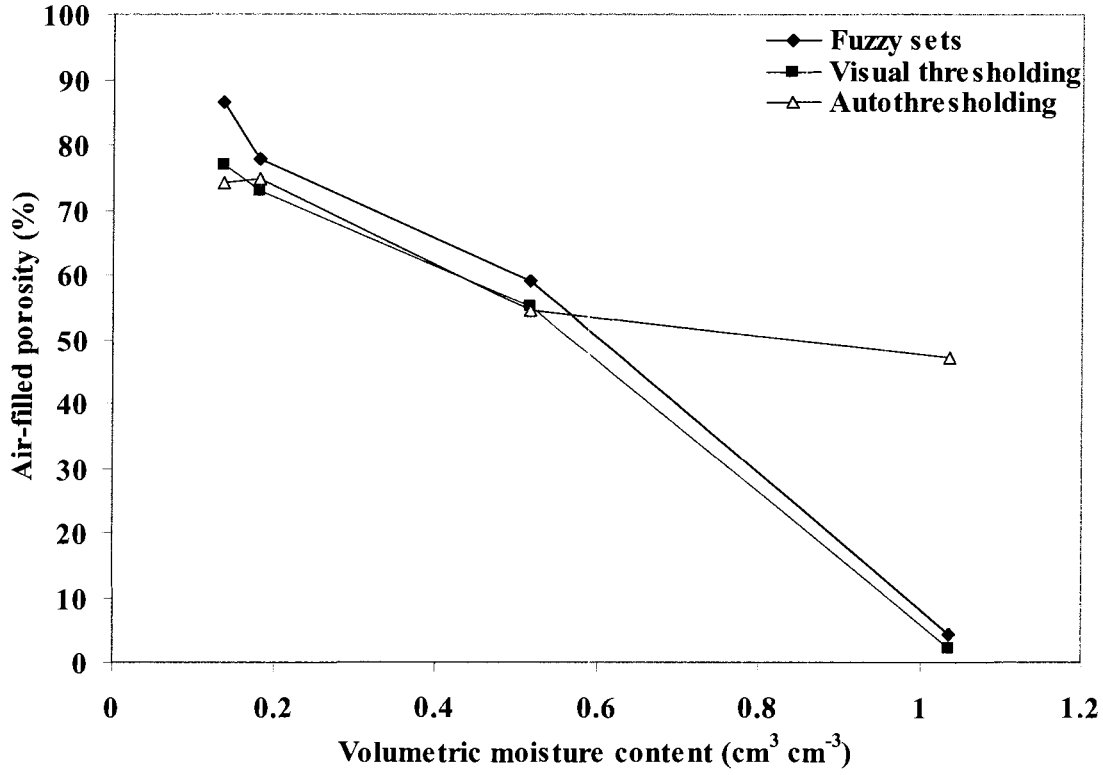

b. 10 cm depth

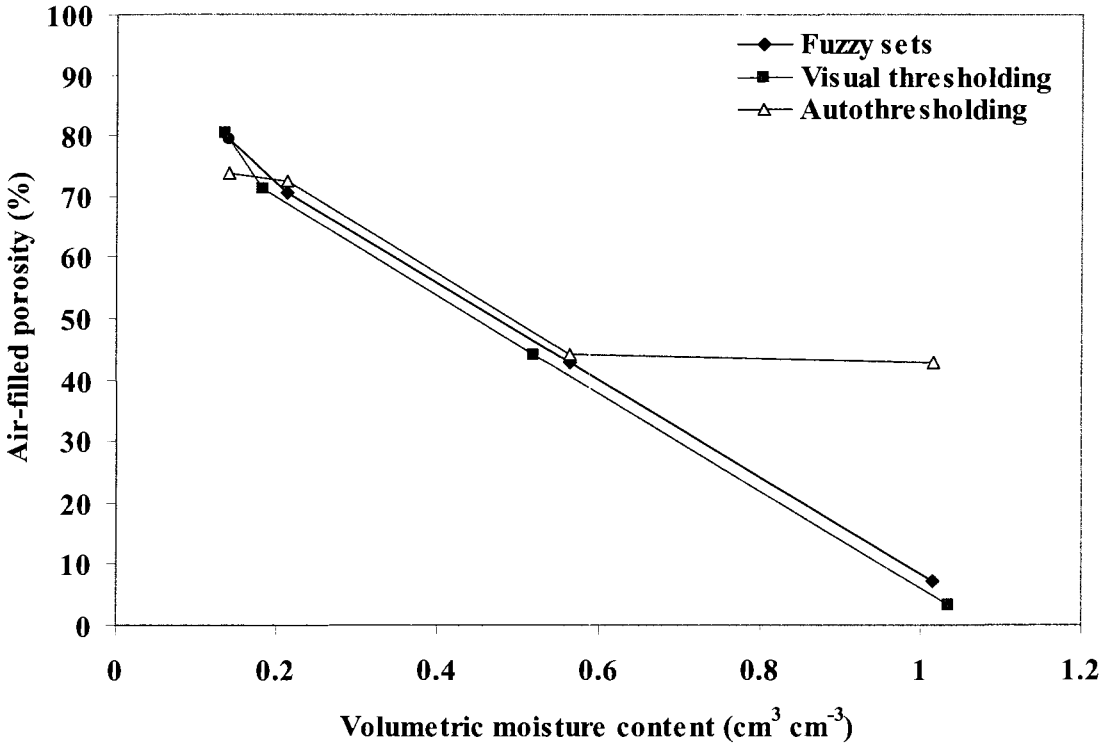

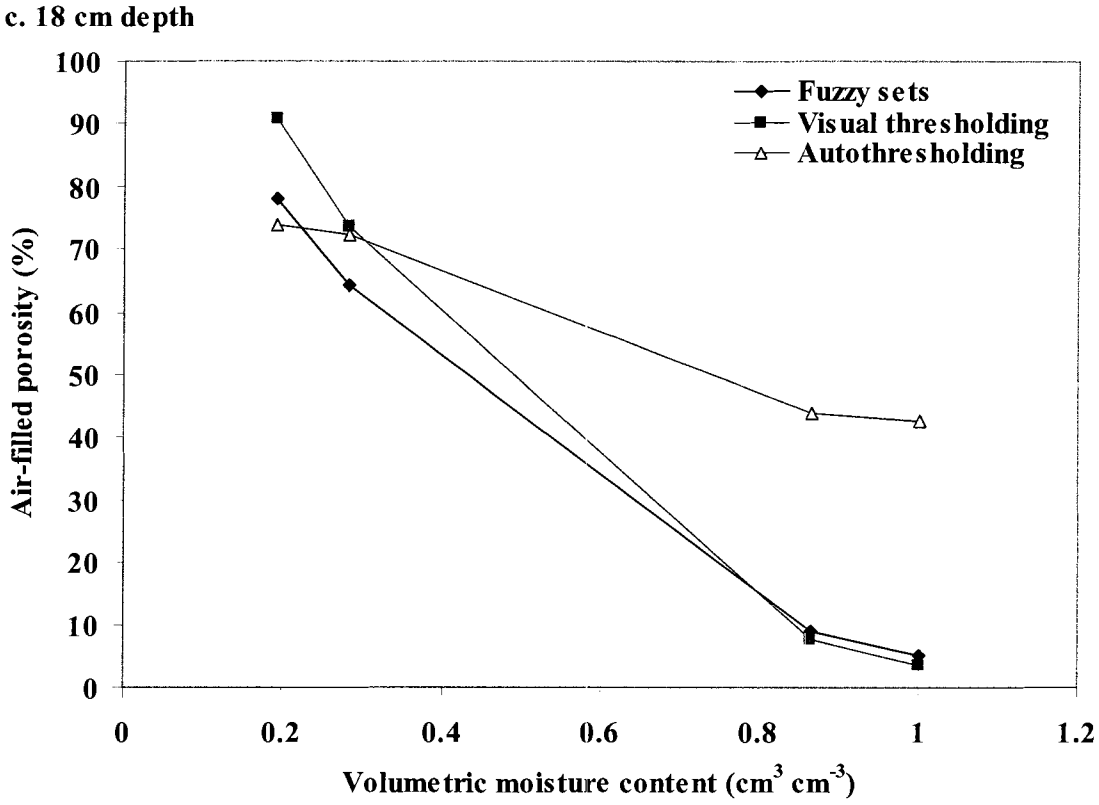

Figure 3-19 A comparison of three methods of thresholding the three-dimensional images: Fuzzy sets, visual thresholding and autothresholding.
This was done for the peat plateau at 3 depths (a) 3 cm depth (b) 10 cm depth (c) 18 cm depth.

3.4.3 MicroCT scanner - two-dimensional imagery

As mentioned previously, three-dimensional imagery of seven peat sub-samples were produced using a MicroCT scanner. MicroCT images are referred to as slices, as they are consistent with what would be observed if the soil sub-samples were sliced open along the scan plane (Ketcham and Iturrino, 2005).

Two-dimensional slices (30.52 mm x 22.70 mm) were extracted from these three-dimensional soil volumes and were used to measure a number of pore properties. Pore

size distribution of pore area, pore diameter and pore hydraulic radius (presented as cumulative frequencies) were determined using these two-dimensional images.

The peat blocks were initially sampled horizontally as depicted in Figure 3-9 and scanned by the MicroCT scanner with the same orientation. Because of this, the soil volumes were positioned horizontally. In order to view the soil volumes from a lateral perspective, the images were re-positioned using Microview custom software. Two-dimensional slices were exported from the three-dimensional soil volumes, each having a thickness of 45 microns. Ten slices, equally spaced throughout the 30.45 mm x 30.52 mm x 22.70 mm (x,y,z) soil sub-sample, were extracted. This was done to account for variability that may exist throughout the sub-samples. Pore area, pore diameter and pore hydraulic radius were measured using the slices at the highest tension level, 5 m, for all sub-samples.

3.4.3.1 Supervised classification

Classification is a form of quantitative analysis used to determine accurate estimates of pixels of interest (Richards and Jia, 1999). The images had a 45 micron resolution and were defined according to a 16-bit greyscale. At this resolution, detecting the edges of pores was a difficult task. Computer classification has the ability to identify pixels based on their numerical properties (Richards and Jia, 1999), such as a greyscale, and output them as a new image. The purpose for classifying the images was to automatically categorize pixels into specific classes or themes, therefore defining the uncertain boundary between variables (air and soil/water) in the two-dimensional images (Figures 3-16 and 3-18). Classification is a method in which all the pixels in an image

that have equivalent spectral signatures are recognized. In this case, the air-filled pores and soil/water were identified as separate classes.

Supervised classification organizes variables by pattern recognition - based on the user's knowledge of the image variables. Supervised classification was performed on each slice individually using remote sensing software (ER Mapper). Specific regions were manually delineated as either air or soil/water using vector polygons. By drawing vector training regions and saving them with the raster region dataset, regions of interest were identified and numerical values at each point were assigned to a class. From this, the remote sensing software processed the images into two classes, black and white in order to improve differentiation between air and soil/water.

3.4.3.2 Cellular automata

After supervised classification had been completed, the two-dimensional slices, had a resolution of 45 microns. The binary images contained a small number of single, unattached pixels. Some of these single pixels were not consistent with greyscale values that were likely to represent air and soil/water. The majority of the greyscale values were in the greyscale range for soil/water and air but a small number of pixels had extremely high or low values. This method was therefore used to remove any pixels in the images that did not belong to either air or soil/water.

Used in spatial analysis, cellular automata is a procedure, which behaves in accordance with local pixel relationships. A cellular automaton (Idrisi Kilimanjaro) was used to reclassify the images to remove all single 45 micron pixels. With this method, all pixels in the images are designated as cells. A cellular automaton starts with a

configuration of cells where each cell occupies a space as part of a two-dimensional array or a matrix of cells arranged in the form of a square grid (Itami, 1994). Characteristics of cellular automata are defined according to: 1) the spatial arrangement of the cells; 2) how those cells evolve; 3) that each cell takes on a predetermined set of possible values; 4) each cell evolves the same way; and 5) the rules for the evolution of a cell depend on the local neighbourhood cells around it (Wolfram, 1984). Each cell is in a neighbourhood defined by the set of cells nearest to it geometrically (Couclelis, 1985).

An algorithm was applied to each square grid of cells thereby summing the values of the neighbouring cells and applying a deterministic rule (where no randomness is involved in the development of future states of the system) based on that current cell's value and the neighbourhood sum (Itami, 1994). Having applied an algorithm recursively to each cell in the square grid (a value is generated by repeating a particular mathematical operation), this reclassifies the image. The images were reclassified by filtering the image, using a 3 x 3 grid, to remove all single 45-micron pixels, unless they were attached to another pixel. Those pixels with pixel neighbours attached to it on the top, bottom, right and left remained in the image. The pixels that had diagonal or no neighbours were reclassified as soil/water or visa versa.

A number of iterations were run to make sure this process was conducted completely. Seven iterations were sufficient enough to remove all the single pixels. This process resulted in images that only had pores 90 microns or larger in diameter.

3.4.3.2.1 Two-dimensional pore area, diameter and hydraulic radius

Pore area and pore perimeter was measured directly with Sigmascan, image analysis software. Pore diameter was calculated using pore area. Diameter, d, was calculated using Equation 3-11

$$d = 2\sqrt{\frac{A}{\pi}} \qquad [3\text{-}11]$$

where A is the area of the pores. Pore hydraulic radius was calculated using Equation 3-12

$$H = \frac{2A}{P} \qquad [3\text{-}12]$$

where hydraulic radius, H, is a length parameter used to describe the area, A, of the pore and the length of its wetted perimeter, P.

3.4.4 Three-dimensional isosurfaces

The soil volumes were cropped from their original sizes of 4.5 cm in diameter and 2.6 cm in height (20.77 cm^3 volume) to 30.45 x 30.52 x 22.70 mm (x,y,z) cubic volumes. Isosurfaces were created from the peat plateau and flat bog sub-samples (Figures 4-15, 4-16, 4-17, 4-18, 4-19, 4-20 and 4-21). In all images, black space represents the air content of the soil and the black/grey represents the soil and water content.

3.4.5 Two-dimensional pore-saturated area measured at two levels of moisture

Measurements were made of specific pores at two levels of matric suction (0.5 m and 5.0 m) using the same two-dimensional slices in the sub-sample volumes. Pore saturated area was measured at the deepest depths for both the peat plateau (18 cm) and flat bog (25 cm) sub-samples. The same individual pores were identified in each image by magnifying a smaller region of pores (Figure 3-20, 3-21 and Figure 3-22, 3-23). Pore area, pore diameter and pore hydraulic radius were measured and calculated using Sigmascan, image analysis software.

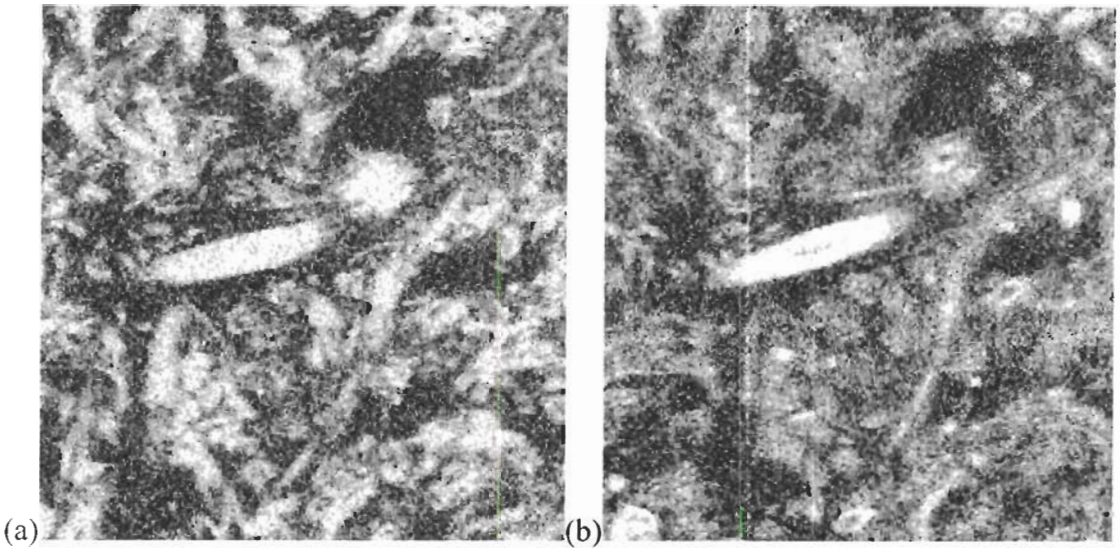

Figure 3-20 Two-dimensional slices (11.75 mm x 13.68 mm) taken from the centre of a three-dimensional volume of peat plateau sub-sample at 18 cm depth, at different soil tensions. Black area represents air content and white represents the soil/water. (a) 0.5 m matric suction (b) 5.0 m matric suction.

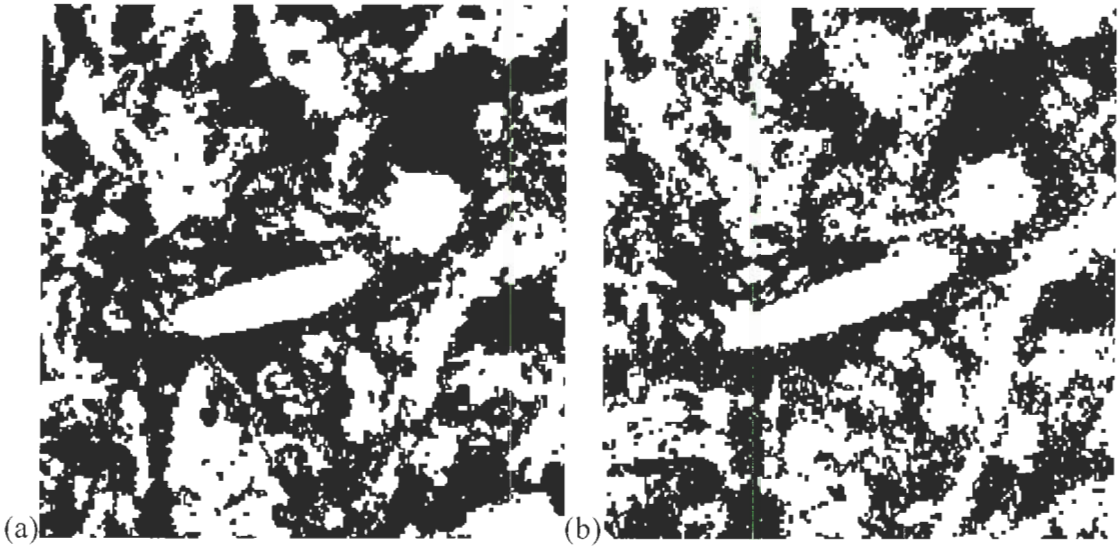

Figure 3-21 Two-dimensional slices taken from the centre of a three-dimensional volume of a peat plateau sub-sample at 18 cm depth, at different soil tensions.
The slices have been converted to binary images using supervised classification and cellular automata. Black area represents air content and white represents the soil/water. (a) 0.5 m matric suction (b) 5.0 m matric suction.

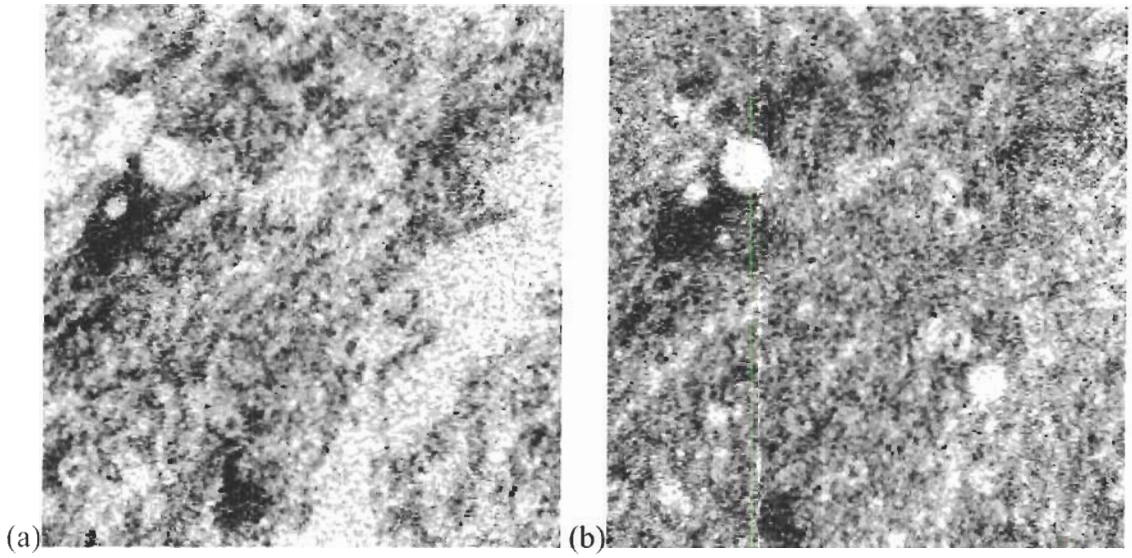

Figure 3-22 Two-dimensional slices (10.62 mm x 11.16 mm) taken from the centre of a three-dimensional volume of a flat bog sub-sample at 25 cm depth, at different soil tensions. Black area represents air content and white represents the soil/water. (a) 0.5 m matric suction (b) 5.0 m matric suction.

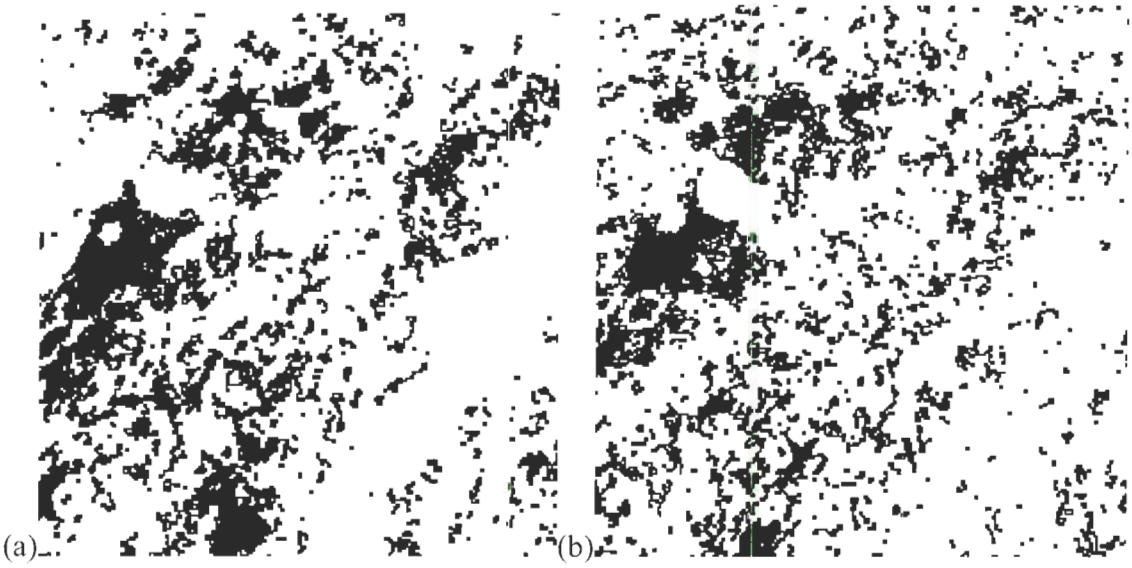

Figure 3-23 Two-dimensional slices taken from the centre of a three-dimensional volume of a flat bog sub-sample at 25 cm depth, at different soil tensions.
The slices have been converted to binary images using supervised classification and cellular automata. Black area represents air content and white represents the soil/water. (a) 0.5 m matric suction (b) 5.0 m matric suction.

3.4.6 Comparison of MicroCT 2D images and electron microscope images

Sphagnum leaves are formed from the association of two cell types, hyaline (H) and chlorophyllose (Cl) (Figure 3-24). They form a sinuous parallelogram network of narrow chlorophyllose cells that border the much larger and porous hyaline cells (Kremer et al., 2004). Hyaline cells are perforated with large pores (Figure 3-25), are specialised for water retention, and are dead and empty when they are functionally mature (Kremer et al., 2004). In order to determine if the hyaline cells can be resolved from the MicroCT images, images produced by electron microscopes were used as a comparison and as a reference (Figure 3-24 and 3-25). Two-dimensional slices were extracted from the three-dimensional flat bog volumes in order to compare variations in cell structure with depth, decomposition and moisture content at a 20 micron resolution. These were CT scanned in August 2003 (Figure 3-26). These sub-samples were different than those CT scanned in August 2004, but were extracted from the same study site.

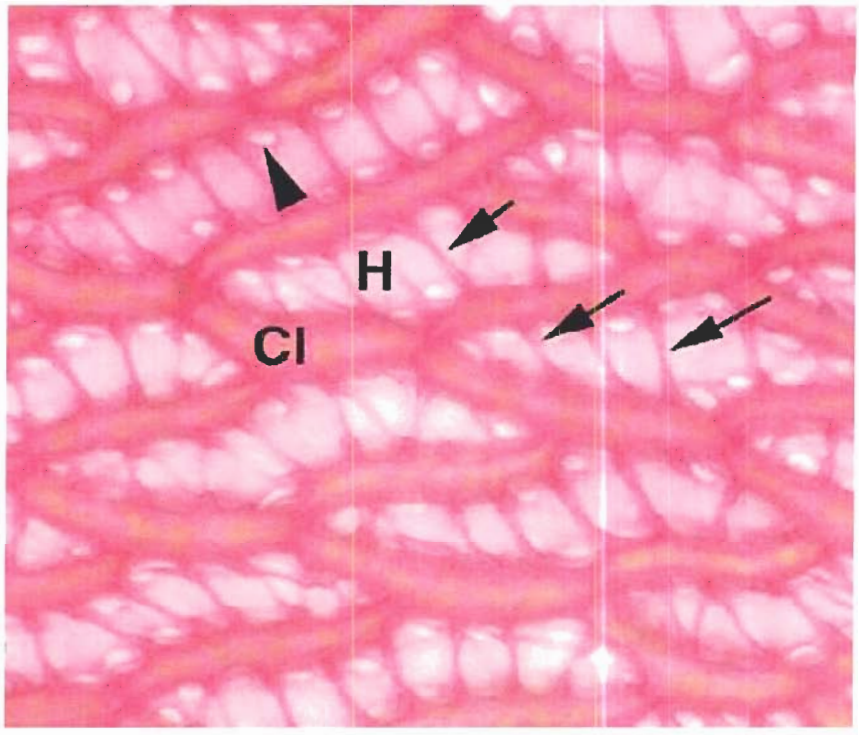

Figure 3-24 Sphagnum hyaline cells (H) with secondary wall thickenings (arrow) and pores (arrowhead) and chlorophyllous cells (Cl) of a mature Sphagnum leaf stained with ruthenium red
Source: Kremer et al. 2004, reprinted by permission.

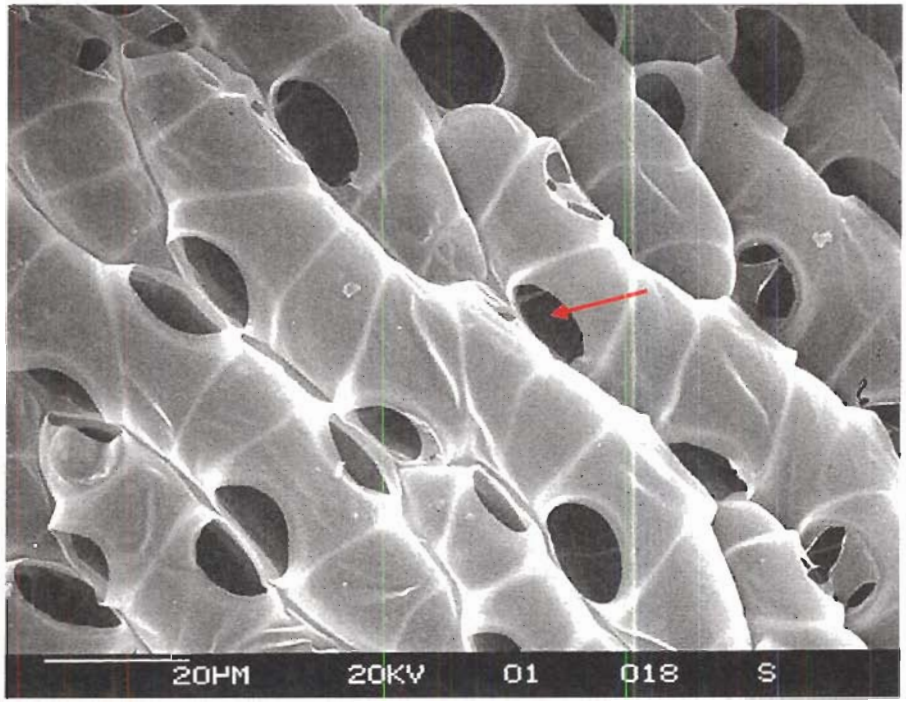

Figure 3-25 A 20 µm electron microscopic image of Sphagnum rubellum. Shows a magnified view of the hyaline cells, its cell wall thickenings, and its pores (red arrow).
Source: Ellis, 2001, reprinted by permission.

The images produced from the sub-samples, did not have any soil tension applied so they were scanned in the MicroCT scanner at an unknown moisture content. In comparison, the images CT scanned in August 2004, had tensions applied to them to represent different stages of volumetric soil moisture. An evaluation of these images was done to identify the response of the hyaline cells to changes in moisture in the flat bog. The peat plateau sub-samples were not used in this study since it was more difficult to see the porous *Sphagnum* cells in the MicroCT scanned images.

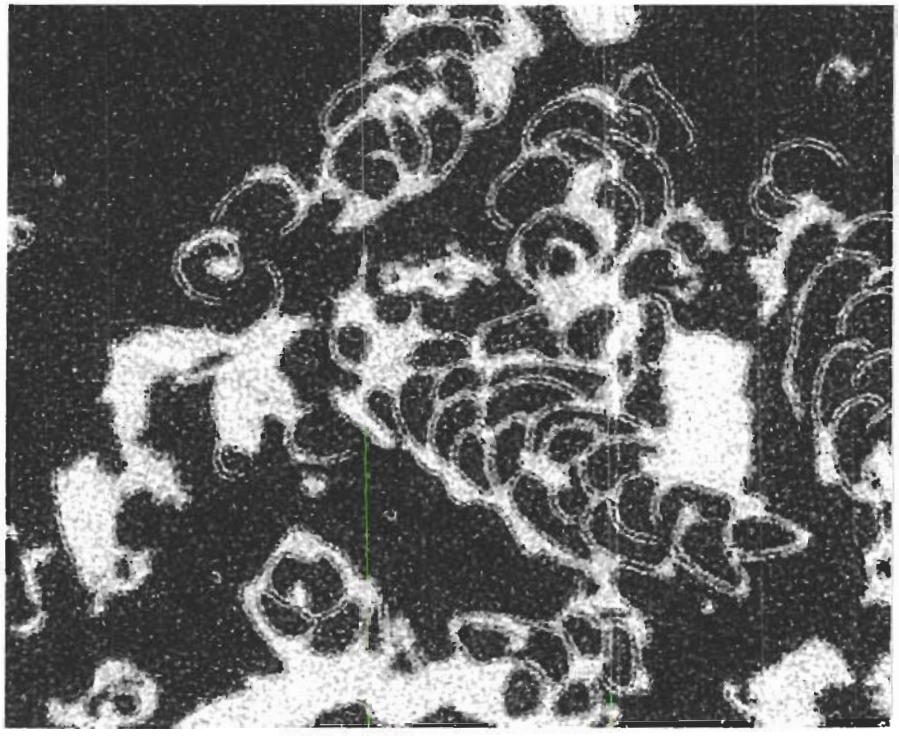

Figure 3-26 MicroCT image (looking from the top) of a flat bog sample at a 20 micron resolution and 16.88 mm x 13.74 mm in size.
The image shows a magnified view of the Sphagnum stems containing hyaline and chlorophyllose cells. Black space represents air and white/grey space represents soil and water.

3.5 Summary

Table 3-3 is an overall summary of the methods described in Chapter 3.

Table 3-3 Methods summary

Type of samples/images	MicroCT scanning	Type of analysis	Size of samples/images	Resolution	Analytical Method(s)
Peat sub-samples	yes		4.5 cm diameter x 2.6 cm height	45 microns	
3D image	yes	Air-filled porosity	Elliptical cylinders 30.478 mm x 30.455 mm x 21.124 mm	45 microns	Fuzzy set theory
2D image	yes	Pore size distribution	30.52 mm x 22.70 mm	45 microns	Supervised classification/cellular automata
2D image	yes	Pore saturated area	11.75 mm x 13.68 mm	45 microns	Supervised classification/cellular automata
2D image	yes	Peat structure	15.5 mm x 19.96 mm	20 microns	Comparison of MicroCT 2D images and electron microscope images
2D image	yes	Peat structure	30.61 mm x 30.50 mm	45 microns	Comparison of variability in cell structure with depth, decomposition and moisture content
Peat sub-samples	no	Unsaturated hydraulic conductivity	5.15 cm diameter x 10.0 cm height		Hydraulic conductivity - tension association

CHAPTER 4:
PHYSICAL PROPERTIES OF PEAT

4.1 Soil moisture – tension association

The results from the laboratory drainage tests are displayed in a soil moisture characteristic curve (Figure 4-1). This was done to evaluate how moisture retention changes with increasing depth. The soil moisture characteristic curve (Figure 4-1) only reflects desorption of the sub-samples since they were MicroCT scanned at progressively drier states.

The soil moisture characteristic curve (Figure 4-1) was compiled using the four levels of matric suction and the van Genuchten equation (Equation 3-1)

$$\theta(h) = \frac{(\theta_s - \theta_r)}{\left(1 + (\alpha h)^n\right)^m} \qquad [3\text{-}1]$$

where θ is the volumetric moisture content, θ_s is the saturated moisture content, θ_r is the residual moisture content, α, h and n are fitting parameters and $m = 1\text{-}1/n$, which is related to the symmetry of the curve (van Genuchten, 1980).

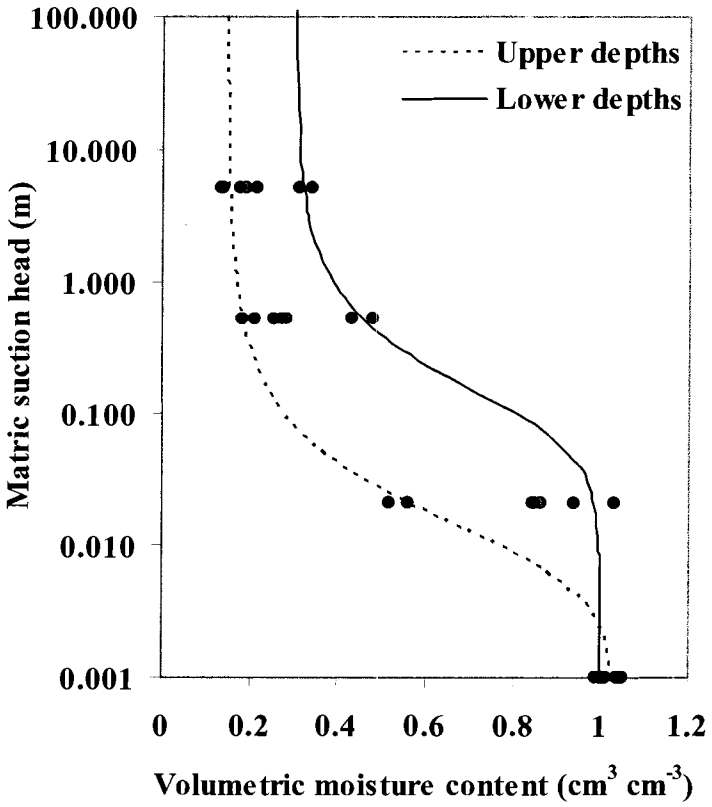

Figure 4-1 Soil moisture characteristic curve.
Note: There is an underestimation of soil volume. because of peat swelling after saturation.

The soil moisture characteristic curve (Figure 4-1) exhibits a decrease in volumetric moisture from saturation to residual moisture content (5.0 matric suction). Residual moisture content refers to the residual wetness that remains in small intra-aggregate pores at high soil tensions (Hillel, 1998). All peat sub-samples experienced a loss in volumetric moisture content with an increase in tension from saturation to 0.02 m. In the peat plateau, the 3cm sub-sample lost 55% of its moisture and the 10 cm sub-sample lost 36% of its moisture (Tables C-1 and C-2 in Appendix C). The lower depth sub-sample (18 cm) lost 13% of its volumetric moisture content (Table C-3 in Appendix

C). In the flat bog, the 3 cm sub-sample lost up to 15% of its moisture and the 10 cm sub-samples lost 11% of its moisture content (Tables C-4 and C-5 in Appendix C). In the lower depth sub-samples (20 cm) however, there was only a moisture loss of 10%. At 25 cm, moisture was primarily retained as there was only a 2% loss of moisture (Tables C-6 and C-7 in Appendix C).

The largest reduction in soil moisture content was during the next increment of matric suction - from 0.02 m to 0.5 m tensions. There was a moisture loss of 82% at 3 cm depth to a 72% loss at 18 cm depth in the peat plateau samples (Tables C-1, C-2 and C-3 in Appendix C). The same increase in tension resulted in a 73% loss at 3 cm to a 54% loss at 25 cm depth in the flat bog sub-samples (Tables C-4, C-5, C-6 and C-7 in Appendix C).

With the increase in matric suction to 5.0 m, additional water loss was relatively minute. Approximately 13% of moisture was retained in the 3 cm and 10 cm sub-samples and 20% of moisture was retained in the 18 cm peat sample at this tension level. The flat bog sub-samples retained slightly more moisture with 19-22% moisture retention at 3 cm and 10 cm and 30-33% at 20 cm and 25 cm depths.

It is possible that the largest pores allowed for the initial loss of moisture at 0.02 m and 0.5 m tension and that only the small pores, cells and interparticle spaces retained moisture at higher levels of tension. The largest number of pores drained at 0.5 m tension, which is consistent with Boelter (1968) who states that a large proportion of the soil moisture is lost before 0.5 m tension has been reached. The capacity for peat to retain water at this level of tension is low – especially in upper soil layers. This is because peat that is less decomposed (as it is in shallow soil layers), has a high number of large pores

and high air-filled porosity as a result. Boelter (1968) also contends that the largest pores can therefore yield as much as 80% of their water content to drainage at low suctions. More decomposed peat, found in lower profile layers, contain finer pores and therefore can retain water in them at higher tensions. Water contents are therefore much higher in more decomposed peat than in less decomposed peat (Boelter, 1968).

The soil moisture characteristic curve shows that from 0.5 m to 5.0 m matric suctions, there is a stronger potential for the peat to hold water in the deeper, more decomposed sub-samples. The upper level of the soil moisture characteristic curve (5.0 m matric suction) (Figure 4-1) shows that the moisture content of the sub-samples is not expected to vary appreciably with a further increase in tension. The pores that have been drained to this point would be the most active in transmitting water when the soil is in a saturated state.

4.2 Air-filled porosity

There was a general increase in air-filled porosity, in all the samples, as the volumetric moisture content decreased (Figure 4-2 and 4-3). At 5.0 m tension, the highest air-filled porosities were found in sub-samples near the top of the profile (3 cm) with maximum values of 86.5% for the peat plateau and 89.5% for the flat bog (Figure 4-2 and 4-3). In comparison, at 18 cm depth, the air-filled porosity is 77.9% for this level of tension on the peat plateau (Table C-1, C-2 and C-3 in Appendix C). In the flat bog, the air-filled porosity was 51.6% at 25 cm depth (Table C-4, C-5, C-6 and C-7 in Appendix C). Results therefore show a general decrease in air-filled porosity with depth at the same tension in both the peat plateau and flat bog sub-samples. This is consistent with the findings of Boelter (1969) contends that bulk density, hydraulic conductivity and pore

size distribution vary with soil depth, since lower profile layers are more decomposed, contain smaller fragments of organic material and are more consolidated than upper layers. This decreases air-filled pore space. A linear association is evident in both Figures 4-2 and 4-3 which indicates that when the pores are not filled with water, they are filled with air. This implies that the air-filled porosity results are inversely related to of the soil moisture – tension results discussed previously.

a. 3 cm depth

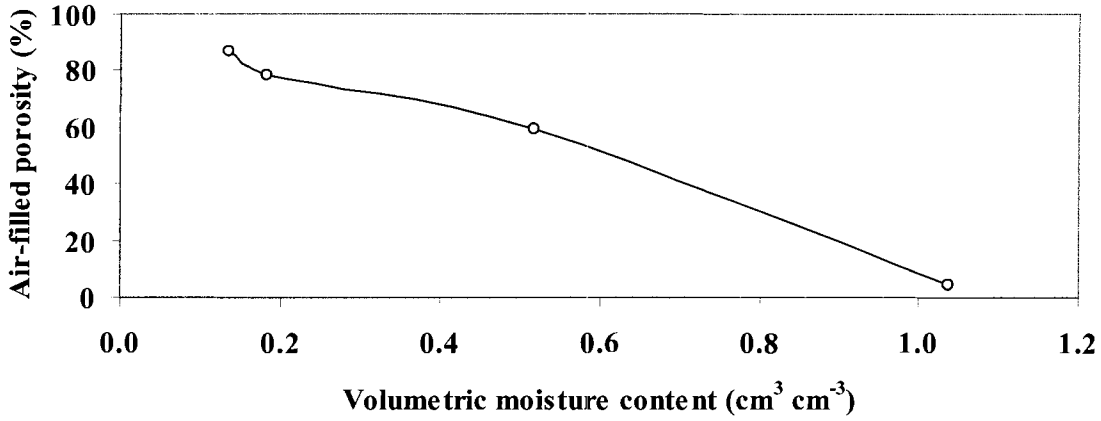

b. 10 cm depth

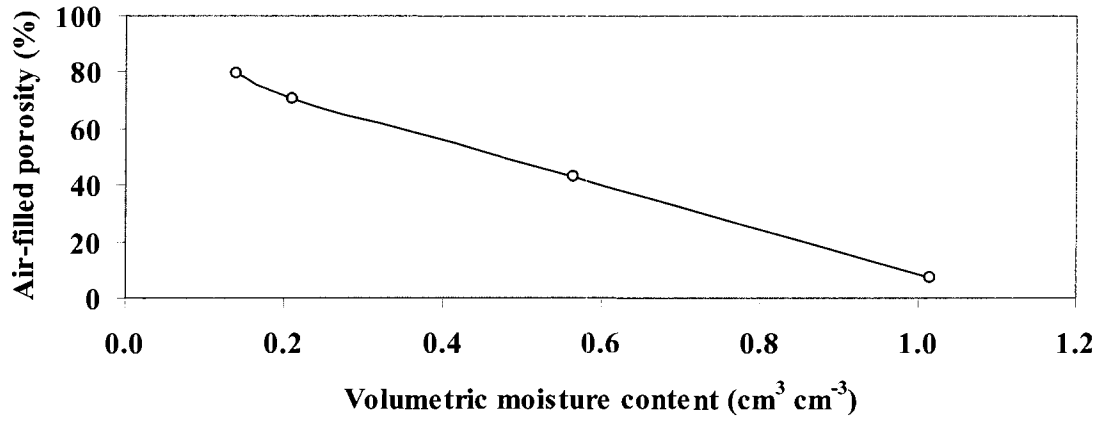

c. 18 cm depth

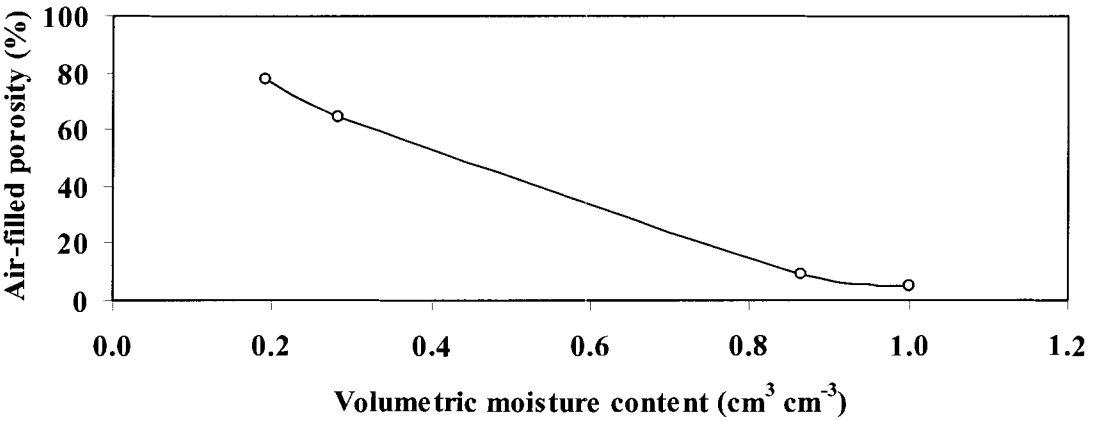

Figure 4-2 Air-filled porosity(%) – peat plateau 3cm to 18 cm depth. (a) 3 cm depth (b) 10 cm depth (c) 18 cm depth.
Note: There is an underestimation of soil volume. because of peat swelling after saturation.

a. 3 cm depth

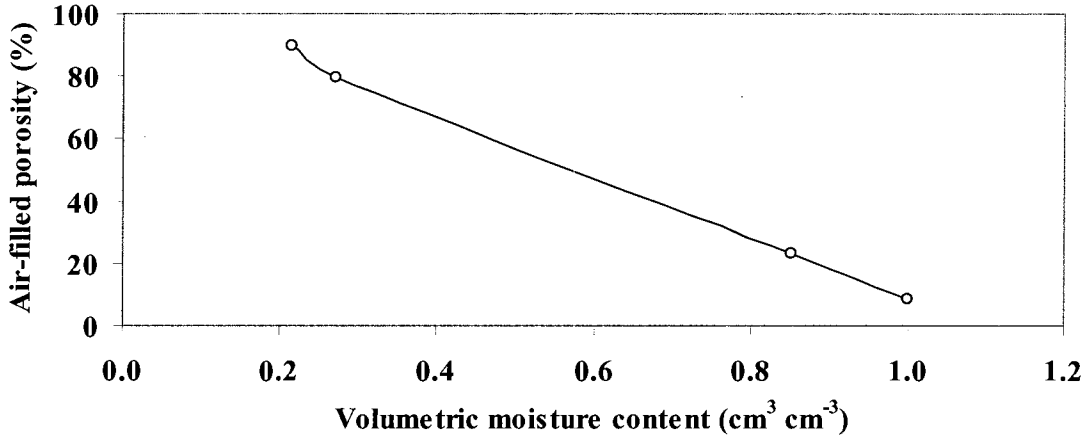

b. 10 cm depth

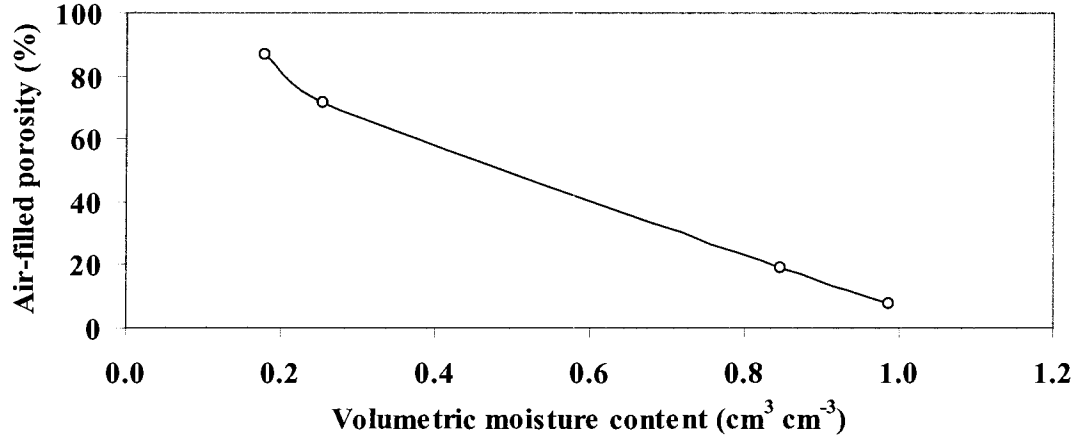

c. 20 cm depth

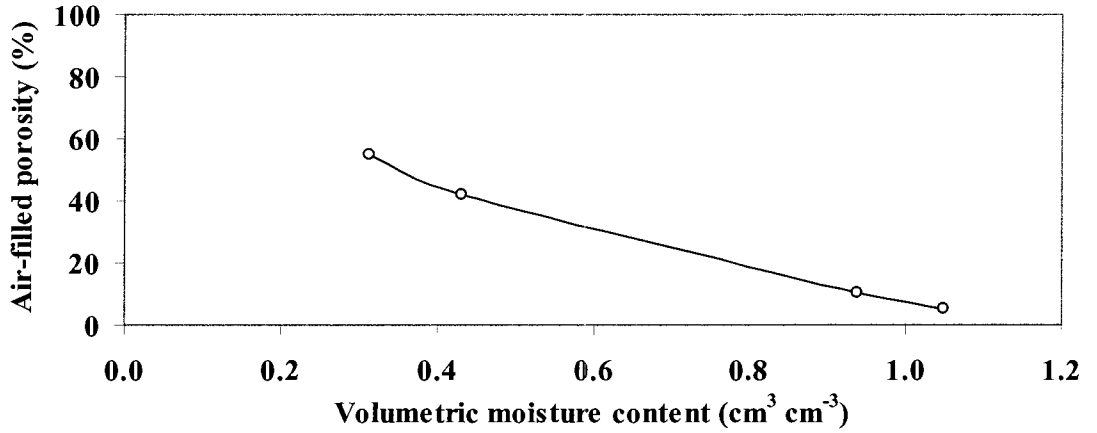

d. 25 cm depth

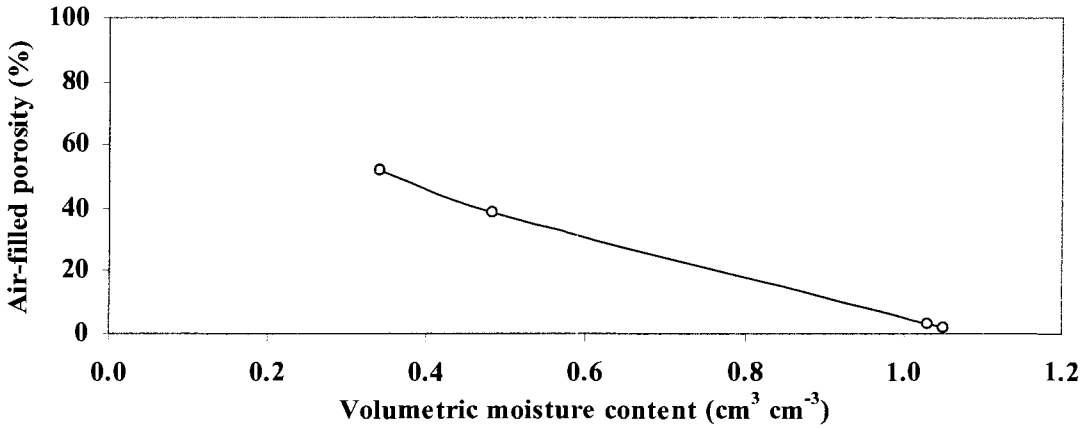

Figure 4-3 Air-filled porosity (%) – flat bog 3 cm to 25 cm depth. (a) 3 cm depth (b) 10 cm depth (c) 20 cm depth (d) 25 cm depth.
Note: There is an underestimation of soil volume. because of peat swelling after saturation.

Peat is a biological source of atmospheric methane (Price and Waddington, 2000) since it produces biogenic gases as a by-product of decomposition. Once the peat is warmed, this rate of decomposition increases and there is a corresponding increase in the rate of biogenic gas production. When the sub-samples were removed from the field to the laboratory, the increase in temperature effectively increased the production of biogenic gas in the sub-samples upon saturation. This along with the fact that air occupies space in soil in the form of discontinuous bubbles, even at saturation; this prevented the saturated sub-samples from being completely free of air (Hillel, 1998). Biogenic air bubbles were therefore measured, and found to occupy between 2 and 8% of the saturated sub-sample volumes (Appendix C). As noted in the figure captions (Figures 4-2, 4-3), an underestimation of the soil volumes was made. The soil was shaped to fit inside the PVC tubes where the volume was measured based on the volume of the tube. Since the peat was shaped prior to saturation, when saturated, the soil sub-samples

swelled slightly. This slight change in soil volume effected the overall volumetric moisture content calculations by a small percentage, producing volumetric moisture contents greater than 100% at saturation, in most of the sub-samples. As well, once each soil tension was reached, the soil volume changed slightly with drying. Obtaining a consistent volume was therefore difficult to achieve. Measurement of soil air content, according to an underestimate of soil volume, implies a percentage of inaccuracy in the results. This problem should be addressed further when applying this method to future research.

4.3 Active porosity

The air-filled porosity measured at residual moisture content (5.0 m matric suction) is the active porosity of the soil. Hoag and Price (1997) define active porosity as the porosity or percentage of pores that actively transmits water through the soil. Any residual moisture retained in the soil is no longer transmitted through the soil because all that remain are closed and dead-end pores formed by partially intact or intact plant cells (Hayward and Clymo, 1982).

Since the largest pores are the first to lose water when drained, they are the most connective pores and therefore most likely to contribute to fluid flow at or near saturation. According to Poiseuille's Law, as matric suction increases, the first pores to drain and fill with air are the pores which are the largest and most conductive to flow (Hillel, 1998). The air-filled porosity measured at residual moisture content contains the percentage of pores that contribute to the active transmission of subsurface flow at saturation and is here forward referred to as the active porosity.

Active porosity was measured by Quinton et al. (2000) using thin section analysis of peat extracted from the Canadian Arctic tundra. Using photographs of thin sections, the percentage of void space was determined. The porosity of peat particles was considered inactive and was not considered in the porosity estimates. Quinton et al. (2000) measured the active porosity to be 80-84% at 3 cm, and 63-50% at 29 cm depth. Hoag and Price (1997) estimated active porosity using thin sections produced from peat cores taken from an undisturbed Newfoundland blanket bog. A point-count method was used to tally the actively flowing pores but to exclude the closed pores and plant material (Hoag and Price, 1997). Active porosity was reported as nearly 60% at the surface and 12% at 60 cm depth.

In the present study, the active porosity varied from 86.5% at 3 cm depth to 77.9% at 18 cm depth in the peat plateau sub-samples and varied from 89.5% at 3 cm depth to 51.7% at 25 cm depth in the flat bog sub-samples (Appendix C). These results provide similar approximations to both the Hoag and Price (1997) and Quinton et al. (2000) studies, and are fairly consistent with estimates made by Quinton et al. (2000). This increases the confidence in the estimates made in this study.

4.4 The acrotelm-catotelm boundary

The bog samples showed a large decrease in air-filled porosity between the upper and lower layers - specifically between 10 cm and 20 cm depths (Figure 4-2), indicating that a transition occurred within this depth range. Flat bogs often have two major hydrological layers (Figure 4-3). As mentioned in Chapter 1, the upper, acrotelm layer, is composed of living and poorly decomposed plant debris, has an effective exchange of moisture with the surface and subsurface, frequent water level fluctuations and a high

hydraulic conductivity (Ivanov, 1981). The lower, catotelm layer, contains decomposed plant debris, has a slower exchange of water, a constant water level, and a very low hydraulic conductivity (Ivanov, 1981). The acrotelm thickness is defined by the distance the water table drops during the summer and the catotelm is defined as the area permanently saturated year round (Ivanov, 1981).

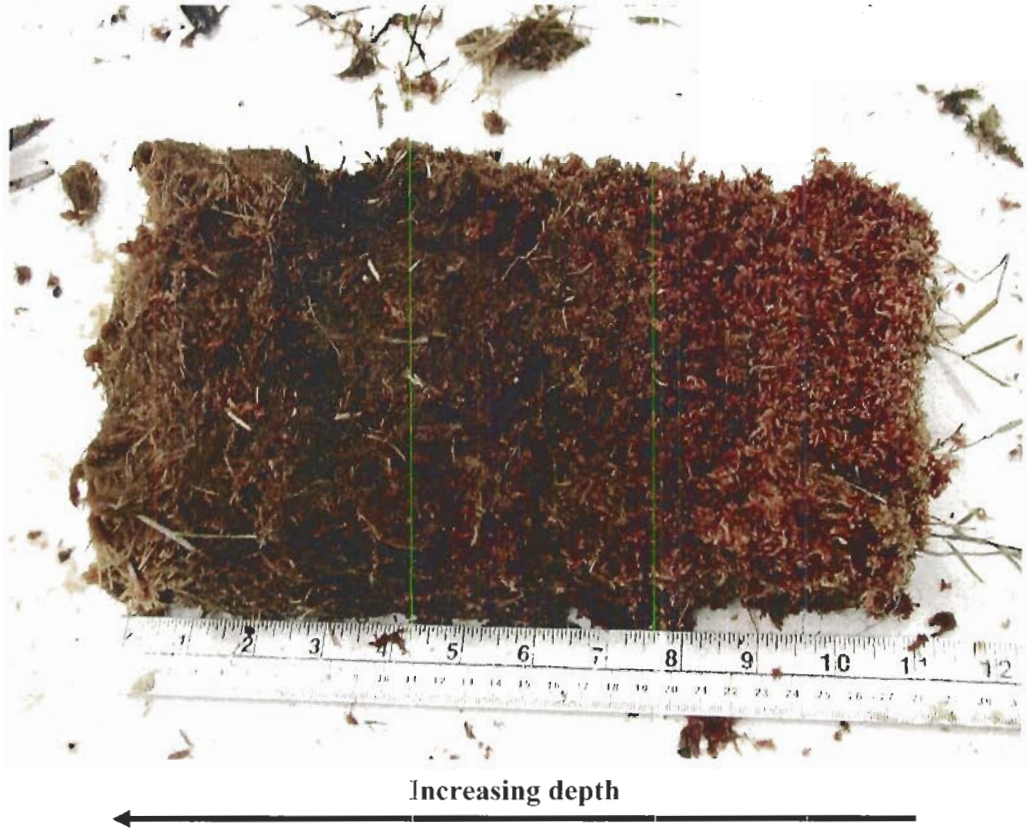

Figure 4-4 Photograph – peat removed from the flat bog shows two major hydrological layers - indicated by the change in hue with depth.

In the present study, it is shown that the flat bog at shallow depths has an active porosity of 87% to 90%, decreasing to 52% to 55% at deeper depths (Figure 4-2 and 4-3). This indicates a sharp change in soil physical properties with depth. Peat removed from the flat bog shows two major hydrological layers - indicated by the change in hue with

depth (Figure 4-4). The acrotelm-catotelm transition is also characterized by an abrupt change in bulk density (Charman, 2002). The peat plateau samples exhibit a gradual change in bulk density indicating that an acrotelm-catotelm transition does not exist (Figure 4-5). In the flat bog, the bulk density shows a rapid change with depth (Figure 4-6), indicating that it varied greatly from shallower to deeper layers. It ranged from an average of 0.030 g cm^{-3} between 0 cm and 12.9 cm depths to an average of 0.054 g cm^{-3} between 27.7 cm to 32.1 cm depths (Figure 4-6).

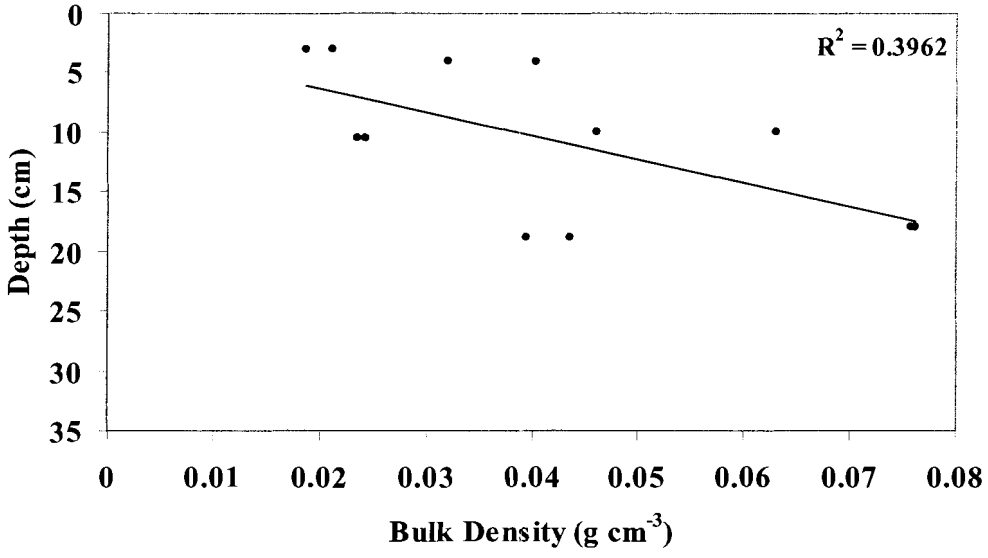

Figure 4-5 Bulk density of peat plateau soil sub-samples.

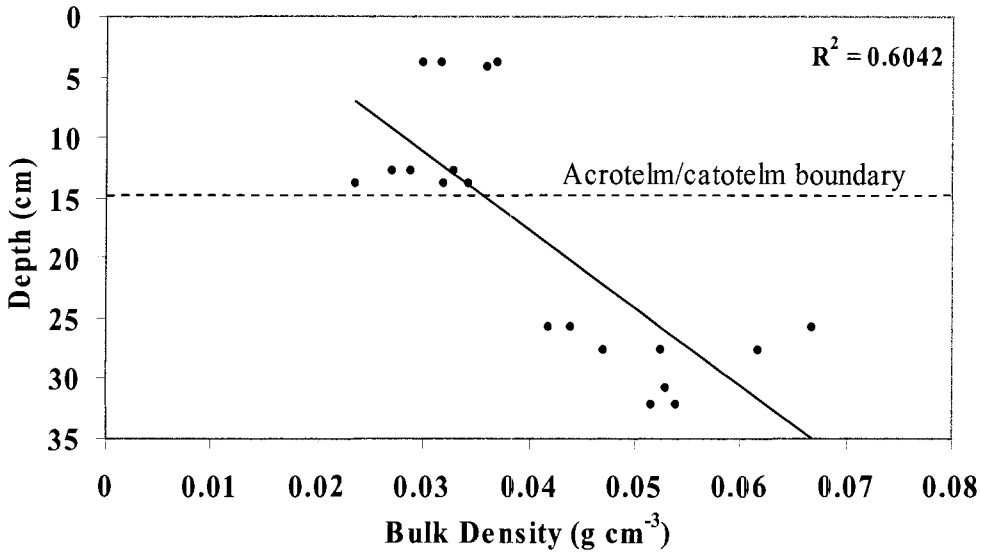

Figure 4-6 Bulk density of flat bog soil sub-samples.

The deepest depth to which the water level drops in an annual cycle is indicative of a defined boundary (Charman, 2002). Water level data taken throughout the melt season illustrates that the water table descended from above the ground surface to approximately 30 cm below the ground surface in the peat plateau (Figure 4-7). The water table in the flat bog descended from above the ground surface to nearly 15 cm below the ground surface (Figure 4-8). This agrees with the results of air-filled porosity and bulk density in the flat bog. Together, these results indicate that an acrotelm/catotelm boundary likely occurs in the flat bog between depths of 13 and 17 cm depths (Figure 4-3 and Figure 4-6). Results also indicate that an acrotelm/catotelm boundary was not detectable in the peat plateau because the available sub-samples did not go beyond 18 cm depth for measurements of air-filled porosity and bulk density, where sub-samples would be required beyond 30 cm depth. This was not possible since a frost table limited the sampling depth in the peat plateau.

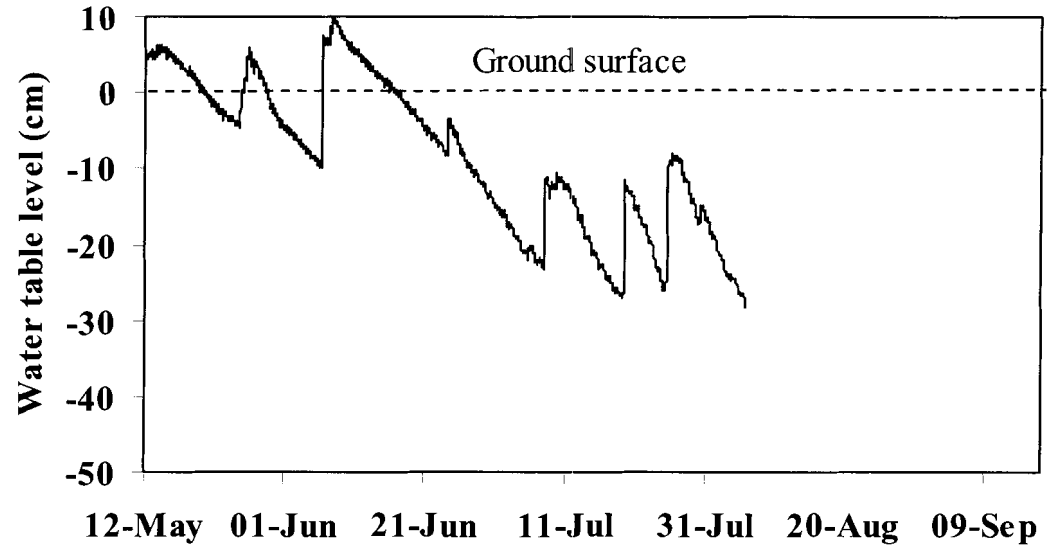

Figure 4-7 Peat Plateau water level measurements from May 12 to August 5, 2004 at Scotty Creek. Source: Wright, 2004, unpublished data, published by permission.

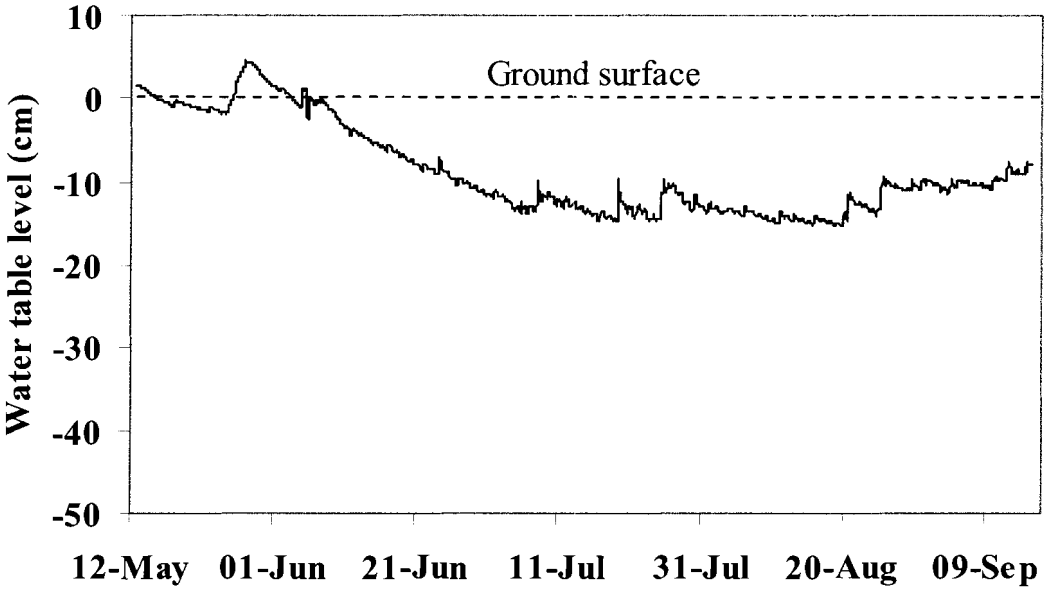

Figure 4-8 Flat bog water level measurements from May 12 to September 16, 2004 at Scotty Creek. Source: Wright, 2004, unpublished data, published by permission.

4.5 Two dimensional pore size distribution

4.5.1 Pore area

Pore area, at residual moisture content (5.0 m tension), was calculated by summing the number of pixels in each pore using the classified binary images and image analysis software (Sigmascan). The cumulative percentage of total pore area for each depth is shown in Figure 4-9. The relative proportion of pores in the sub-samples increased with increased depth (Table 4-1). This was limited to a 90 micron diameter, or the smallest detectable size. At 3 cm depth, 7% of pores were 166 mm^2 or less in size and at 10 cm depth, 10% of pores were 166 mm^2 or less in size. Alternatively, 100% of pores were 166 mm^2 or less in the 18 cm sub-sample. The majority of pores that contributed to the total pore area of the sub-samples at 3 cm and 10 cm depths were 374 mm^2 or greater in area, indicating that larger pores dominated the air-filled space at these depths. However, in the deepest sub-sample (18 cm), smaller pores (166 mm^2 or less) contributed to the majority of air-filled space in the sub-sample.

Pore area was measured at residual moisture content (5.0 m tension) for the 3 cm, 10 cm, 20 cm and 25 cm depth flat bog sub-samples. The cumulative percentage of total pore area for each depth is shown in Figure 4-10. Similar to the peat plateau sub-samples, there was an increase in the relative proportion of pores with increased depth (Table 4-1). The 3 cm sub-sample had the largest range of pore sizes, ranging from 435 mm^2 or less in size. The 25 cm sub-sample had the smallest range of pore sizes, where all pores were less than or equal to 56 mm^2. Pores 56 mm^2 or less in size contributed 70%, 52% and 23% to the total pore area at depths of 20 cm, 10 cm and 3 cm respectively.

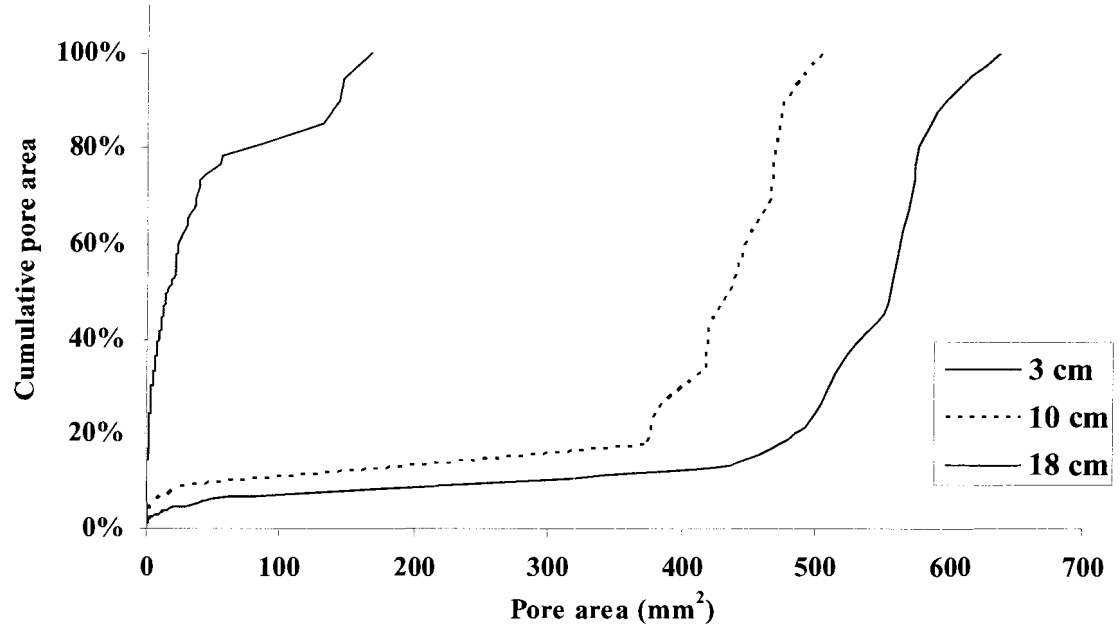

Figure 4-9 Pore area of peat plateau sub-samples measured at 5.0 m matric suction. From bottom to top: 3 cm, 10 cm and 18 cm depths.

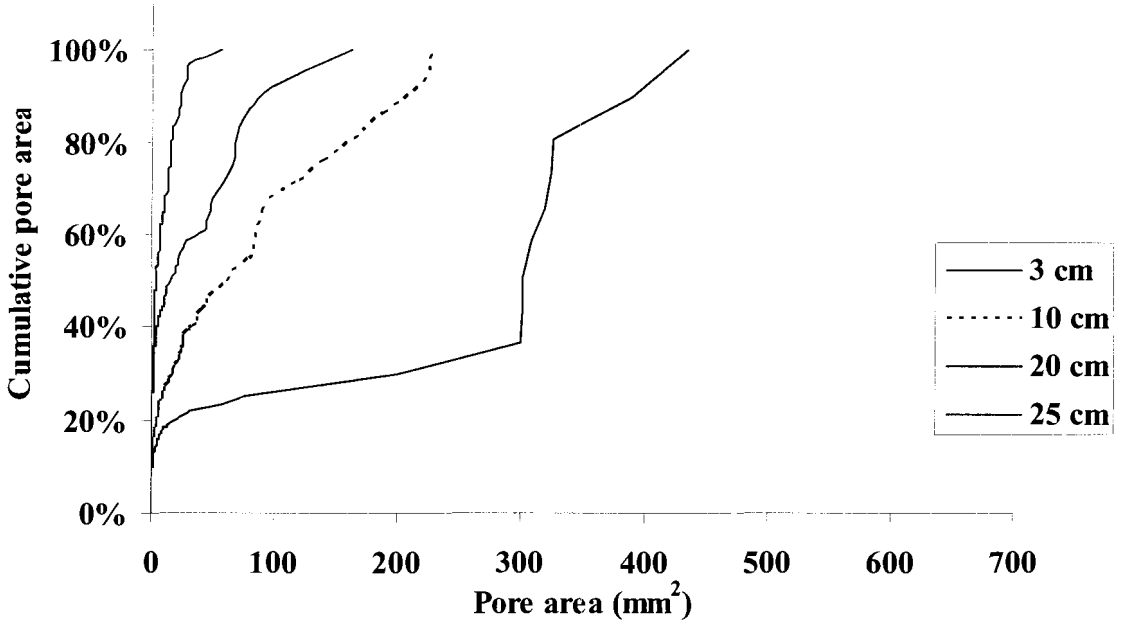

Figure 4-10 Pore area of flat bog sub-samples measured at 5.0 m matric suction. From bottom to top: 3 cm, 10 cm, 20 cm and 25 cm depths.

Table 4-1 Number of pores measured at each depth.

	Depth (cm)	Number of pores measured
Peat Plateau:		
	3	2241
	10	3411
	18	10903
Flat Bog:		
	3	7872
	10	11301
	20	11802
	25	15081

4.5.2 Pore diameter

The pore diameter results denote similarities to that of the pore area in that the number of pores with small diameters increased with increased soil depth (Table 4-1). Results of the peat plateau sub-samples showed (Figure 4-11) that at 18 cm depth, 93% of pores were 5 mm or less in diameter. At 10 cm depth, only 74% of pores were 5 mm or less in diameter and at 3 cm, 60% of pores were 5 mm or less in diameter. The peat plateau sub-samples were visually very porous. The 3 cm sub-sample was the most porous of all the sub-samples which resulted in it having the largest range of pore diameters (0.10 mm to 28.5 mm). By comparison, the 10 cm sub-sample also had a large range of pore diameters, but not to the same extent as at the 3 cm depth, with pores that ranged from 0.10 mm to 25.4 mm in diameter. The 18 cm sub-sample had the smallest range of pore diameters, with pores ranging from 0.10 mm to 14.6 mm in diameter.

Pore diameter was also measured from the flat bog sub-samples (Figure 4-12). Similar to the peat plateau sub-samples, the proportion of small pore diameters increased with increasing depth (Table 4-1). Results show that at 25 cm depth, 98% of pores were

5 mm or less in diameter and at 20 cm depth, 95% of pores were 5 mm or less in diameter. At 10 cm depth, 89.3% of pores were 5 mm or less in diameter, similar to 3 cm depth where 88.8% of pores were 5 mm or less in diameter. At 3 cm depth, pores ranged from 0.10 mm to 23.5 mm in diameter.

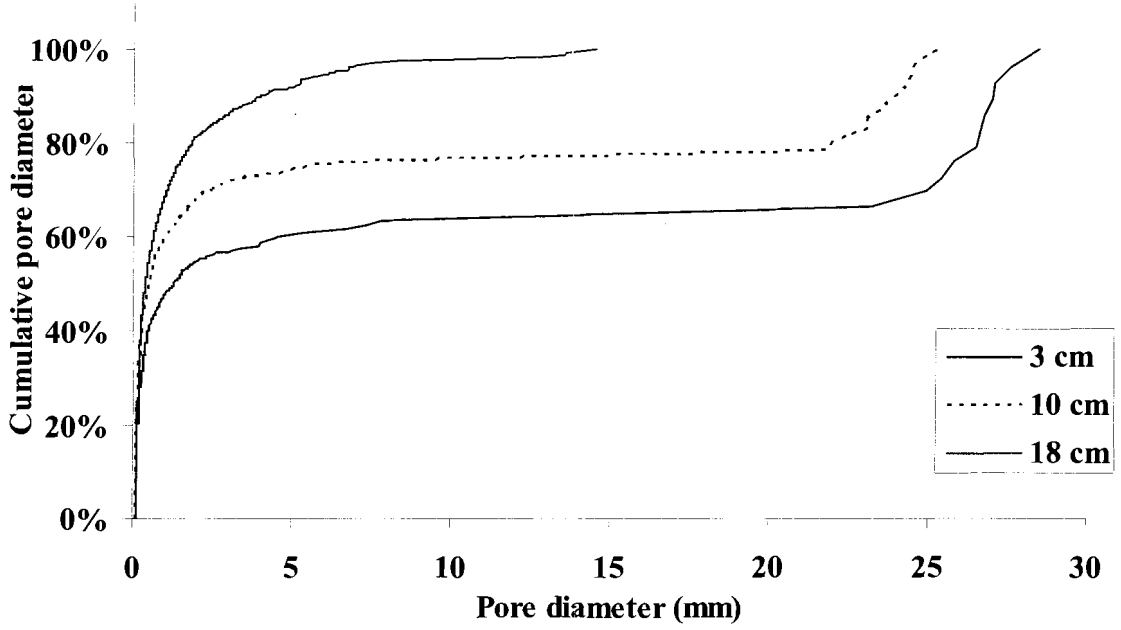

Figure 4-11 Pore diameter of peat plateau sub-samples measured at 5.0 m matric suction.

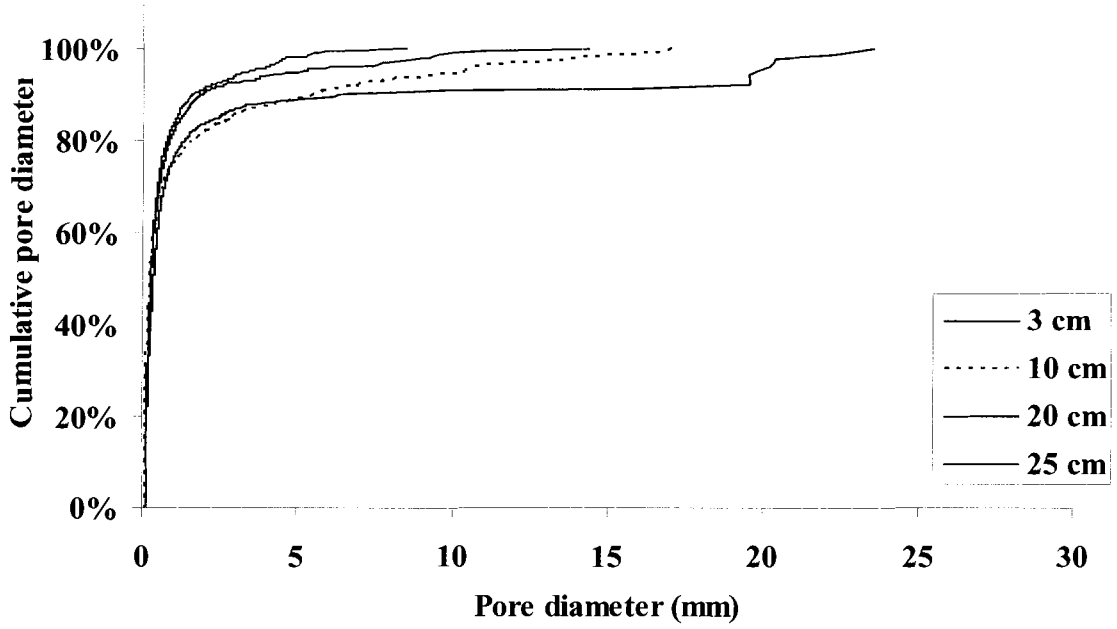

Figure 4-12 Pore diameter of flat bog sub-samples measured at 5.0 m matric suction.

The number of pores detected at deeper depths was significantly larger likely because the sub-samples are in later stages of decomposition and more consolidated than upper depths. This is related to the higher bulk density values found at lower soil depths (Figures 4-5 and 4-6). Greater bulk density after drainage and settlement of the peat is related to a loss of macropores and a concurrent increase in micropores (Silinis and Rothwell, 1998). This result has implications for the viscosity of the water in the peat sub-samples. As discussed in Chapter 1, the Reynolds number is inversely related to viscosity (Equation 1-3). As the diameter of pores decrease with depth ,as described in Figure 4-11 and Figure 4-12, Reynolds number is lowered and resistance to flow and the likelihood of laminar flow both increase.

4.5.3 Pore hydraulic radius

In the peat plateau sub-samples, hydraulic radii increased with increased soil depth (Figure 4-13) (Table 4-1). At 18 cm depth, 82% of pores were 0.1 mm or less. At 10 cm depth, 75% of pores and at 3 cm depth, 72% of pores had hydraulic radii that were 0.1 mm or less. Pores that had hydraulic radii that were 0.2 mm or smaller in size, accounted for 90% of pores at 3 cm depth, 95% of pores at 10 cm depth and 98% of pores at 18 cm depth. This indicated that the majority of pores were 0.2 mm or less at all depths in the peat plateau sub-samples.

In the flat bog sub-samples, generally, the hydraulic radii increased with increased soil depth (Figure 4-14) (Table 4-1). The cumulative summary showed that at 3 cm depth, 70% of pores had hydraulic radii of 0.1 mm or less and at 10 cm depth, this increased to 88%. At 20 cm depth, 81% of pores and at 25 cm depth, 89% of pores had hydraulic radii of 0.1 mm or less. There was a general increase in the number of pores this size, from 3 cm to 25 cm depths. It showed that out of those hydraulic radii that were 0.1 mm or less, 10 cm had a greater number of detectable pores than 20 cm depth. This inconsistency changed as larger hydraulic radii pore were detected. At a hydraulic radius of 0.2 mm or less, 97.9% of pores at 3 cm depth, 98.6% of pores at 10 cm depth, 99.2% of pores at 20 cm depth and 100% of pores at 25 cm depth had hydraulic radii in this category. Overall, there was an increase in the size and number of pores with small and large hydraulic radii with depth.

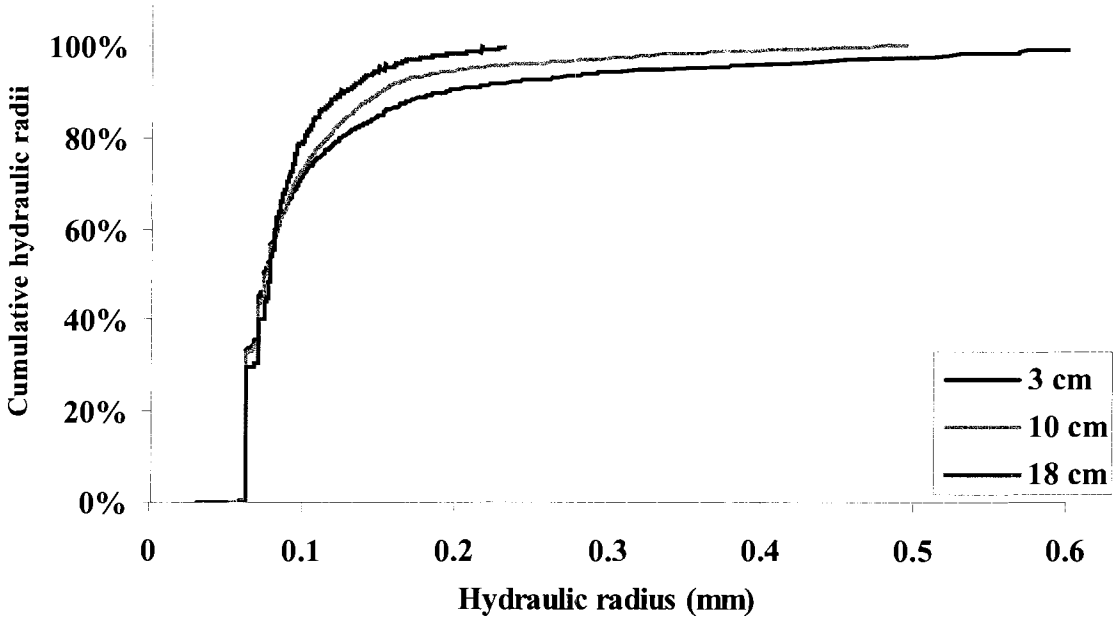

Figure 4-13 Hydraulic radius of peat plateau sub-samples measured at 5.0 m matric suction.

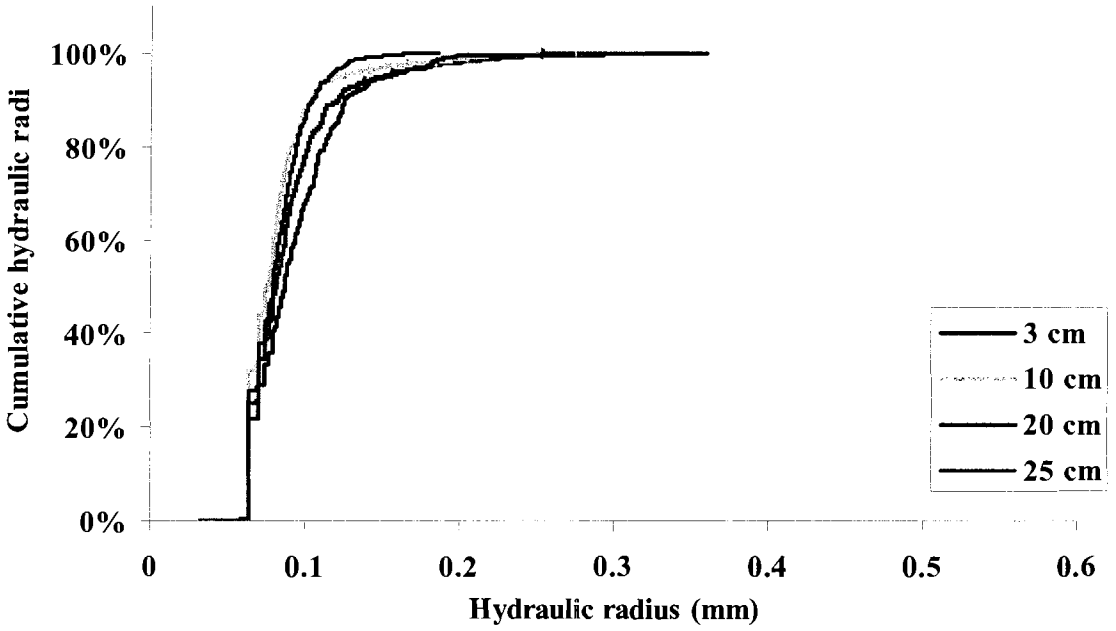

Figure 4-14 Hydraulic radius of flat bog sub-samples measured at 5.0 m matric suction.

4.6 Three-dimensional isosurfaces

4.6.1 Peat plateau isosurfaces

Three-dimensional isosurfaces of peat plateau soil at 3 cm, 10 cm and 18 cm depths are displayed in Figures 4-15, 4-16, & 4-17. In the images, black represents air space and the grey represents the soil and water content. The soil volumes are (x,y,z) 31.19 mm, 31.19 mm, 23.00 mm in size. Each image represents a specific matric suction head, (a) 0.001 m (saturated) (b) 0.02 m (c) 0.5 m and (d) 5.0 m. An increase in air space is evident as soil tension increases. This is also indicated by the increase in air-filled porosity at higher tension levels (Figure 4-2).

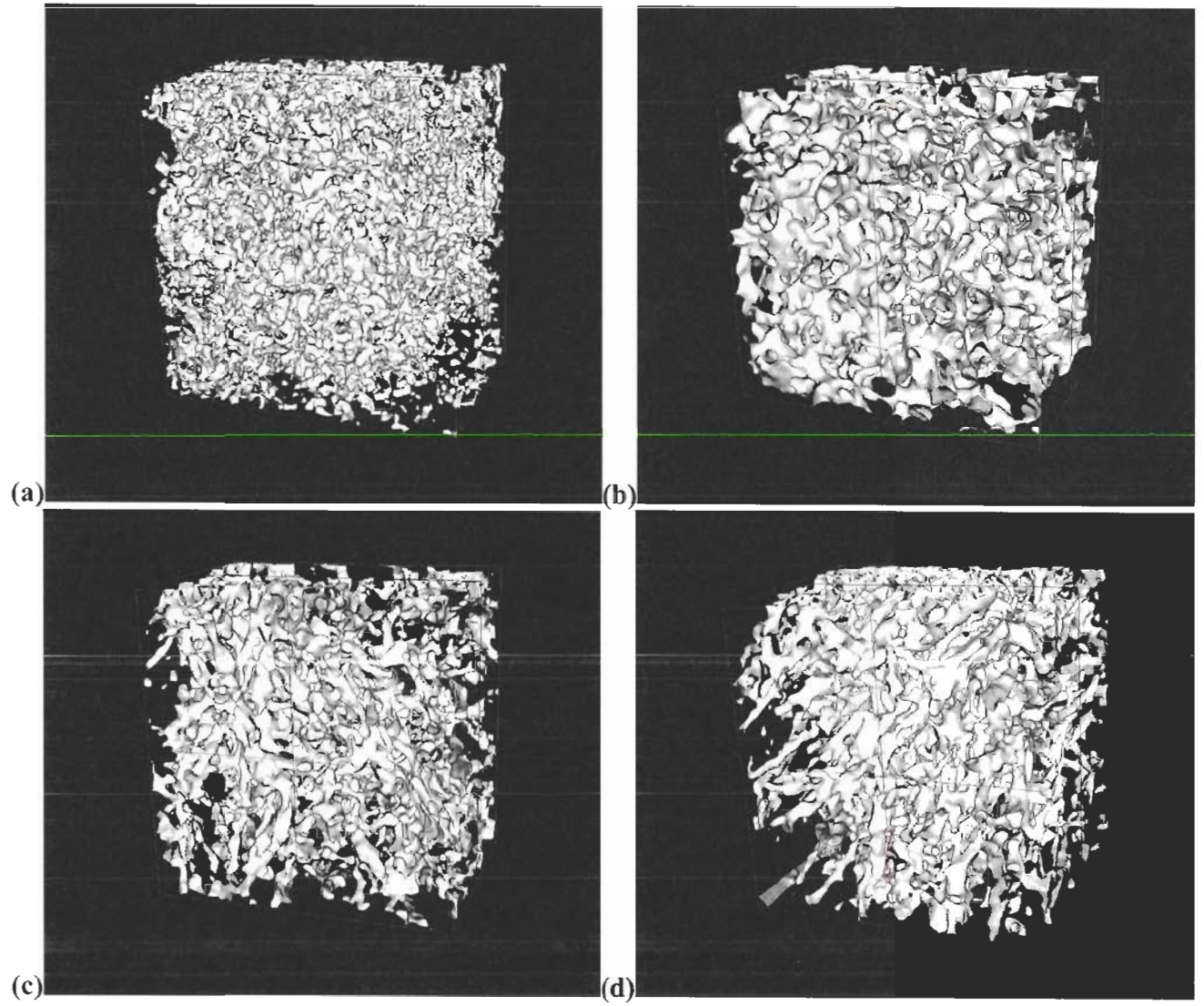

Figure 4-15 Three-dimensional isosurfaces of peat plateau soil volumes at 3 cm depth.

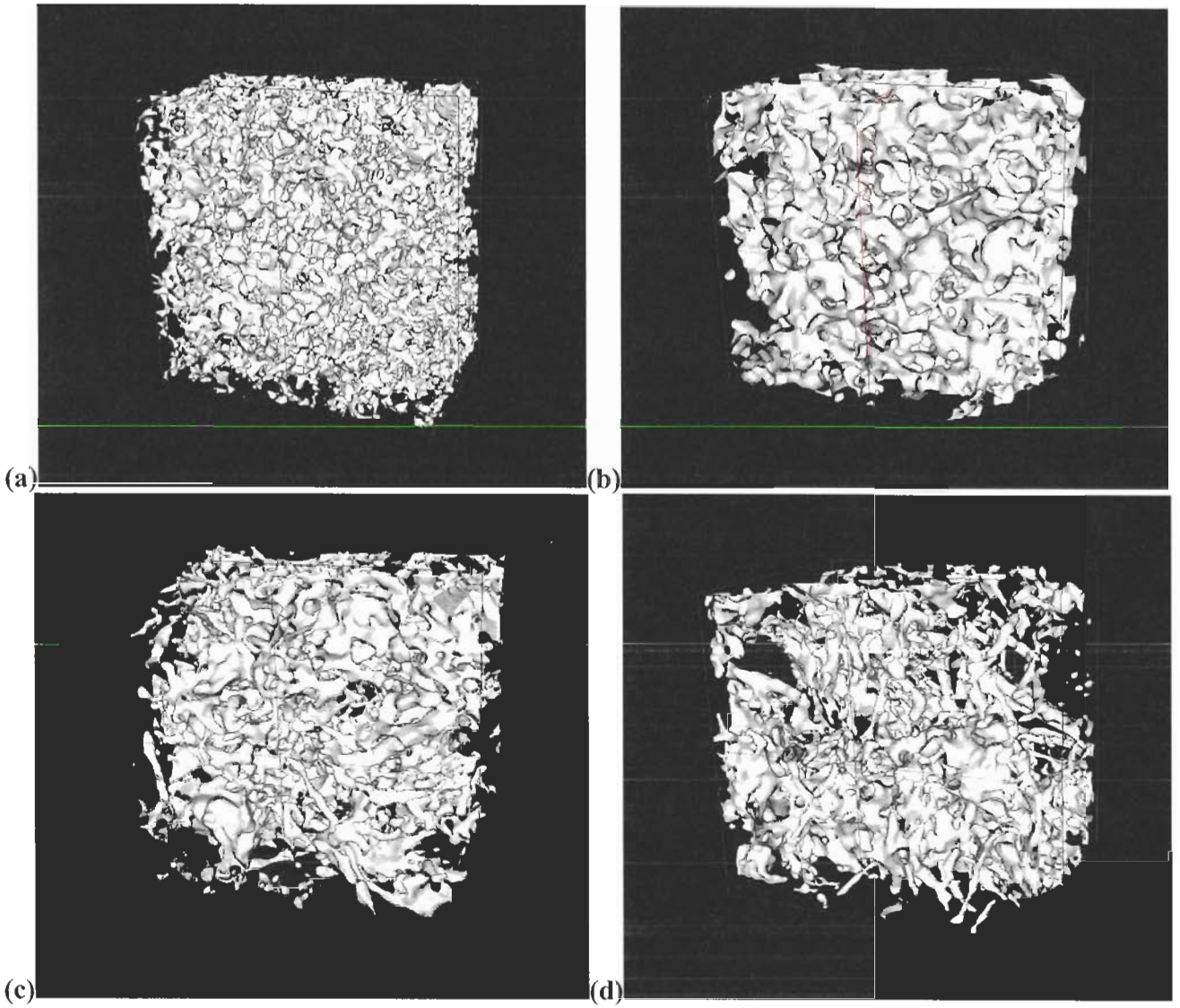

Figure 4-16 Three-dimensional isosurfaces of peat plateau soil volumes at 10 cm depth.

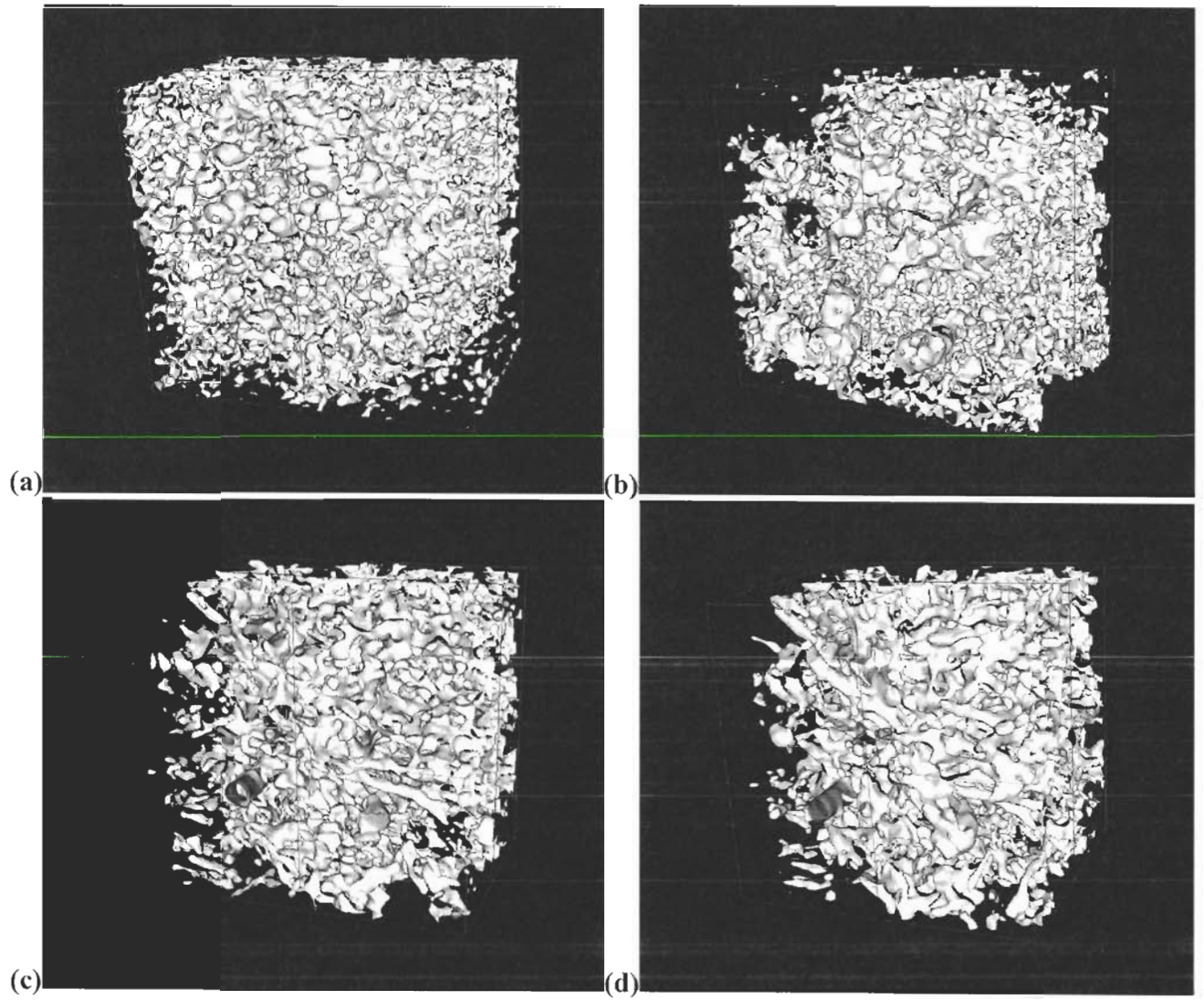

Figure 4-17 Three-dimensional isosurfaces of peat plateau soil volumes at 18 cm depth.

4.6.2 Flat bog isosurfaces

Three-dimensional isosurfaces of flat bog soil at 3 cm, 10 cm, 20 cm and 25 cm depths are displayed in Figures 4-18, 4-19, 4-20 and 4-21. In the images, black represents air space and the grey represents the soil and water content. The soil volumes are (x,y,z) 30.45 mm, 30.52 mm, 22.70 mm in size. Each image represents a specific matric suction head, (a) 0.001 m (saturated) (b) 0.02 m (c) 0.5 m and (d) 5.0 m. As in the peat plateau, at saturation, the soil and water comprise the majority of the volume but as the tension increases, the soil/water volume decreases and air space increases (Figure 4-3).

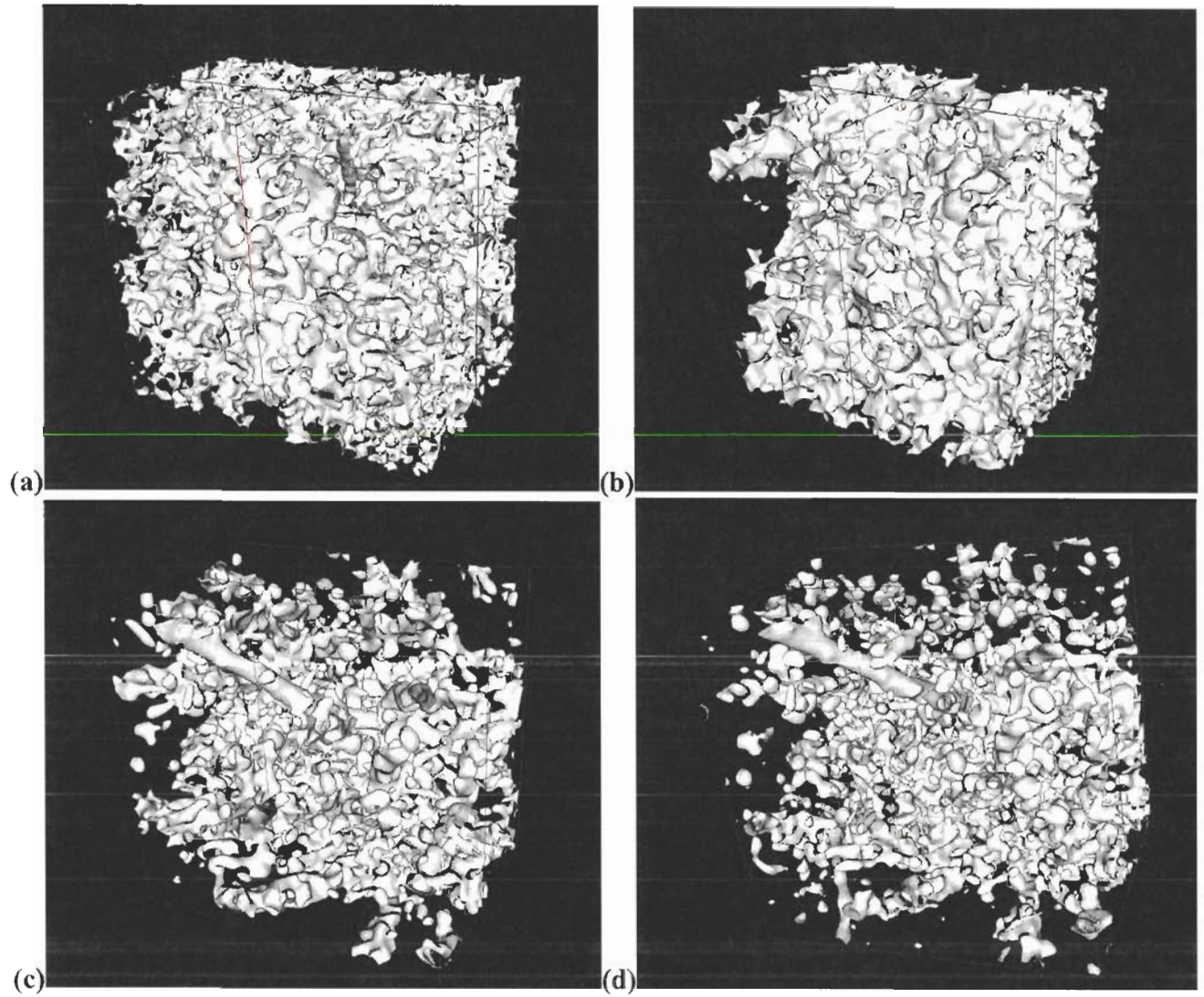

Figure 4-18 Three-dimensional isosurfaces of flat bog soil volumes at 3 cm depth.

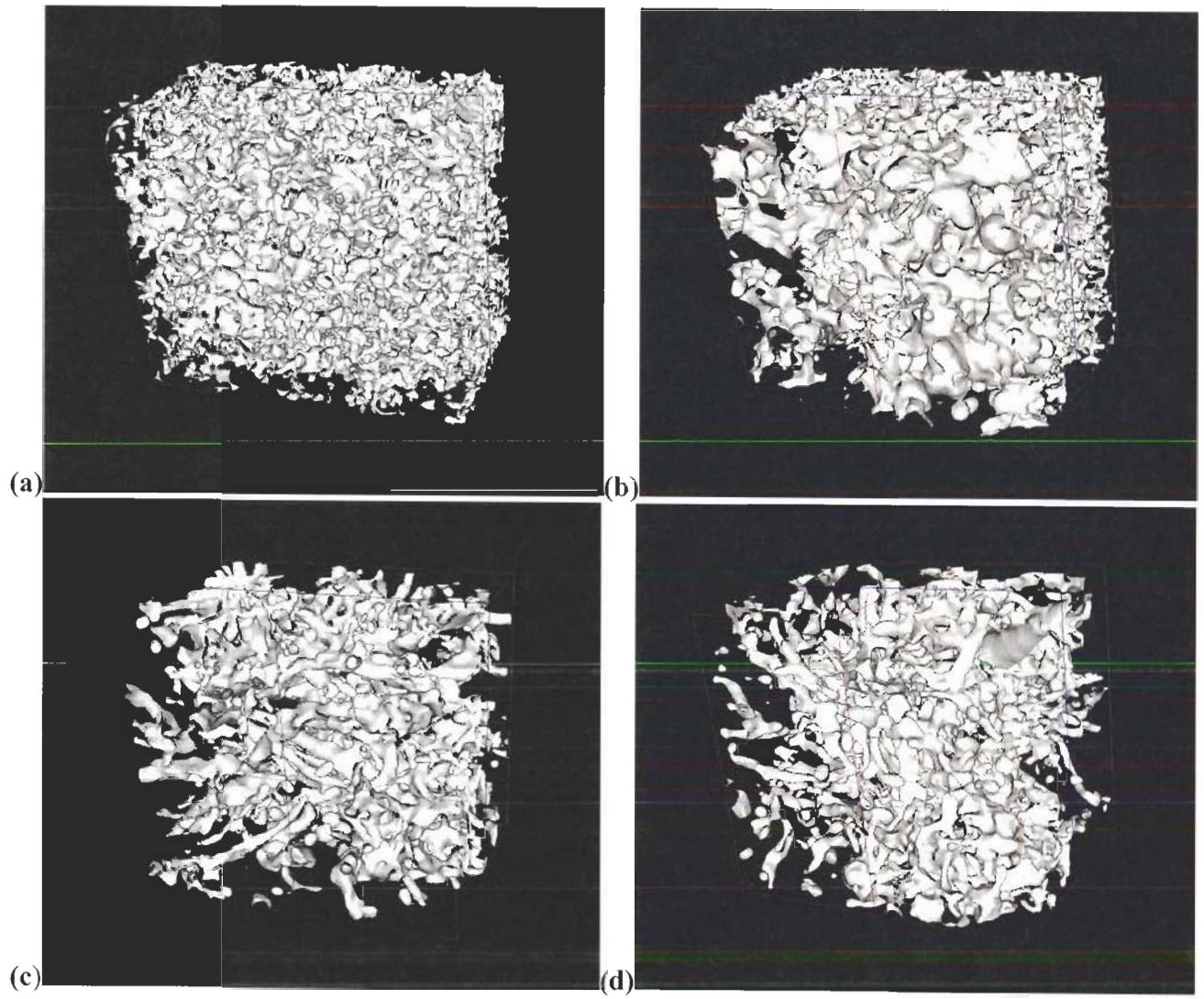

Figure 4-19 Three-dimensional isosurfaces of flat bog soil volumes at 10 cm depth.

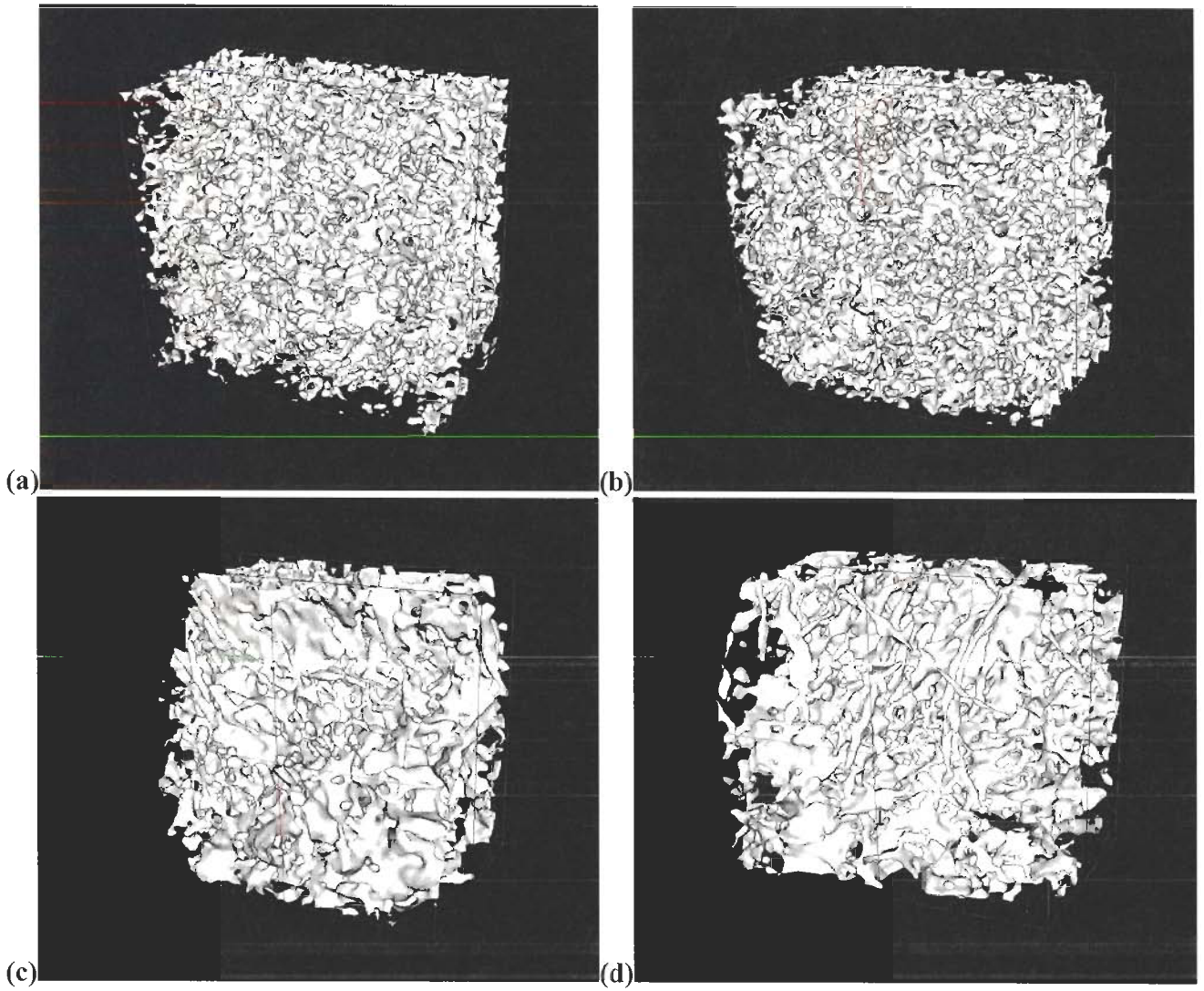

Figure 4-20 Three-dimensional isosurfaces of flat bog soil volumes at 20 cm depth.

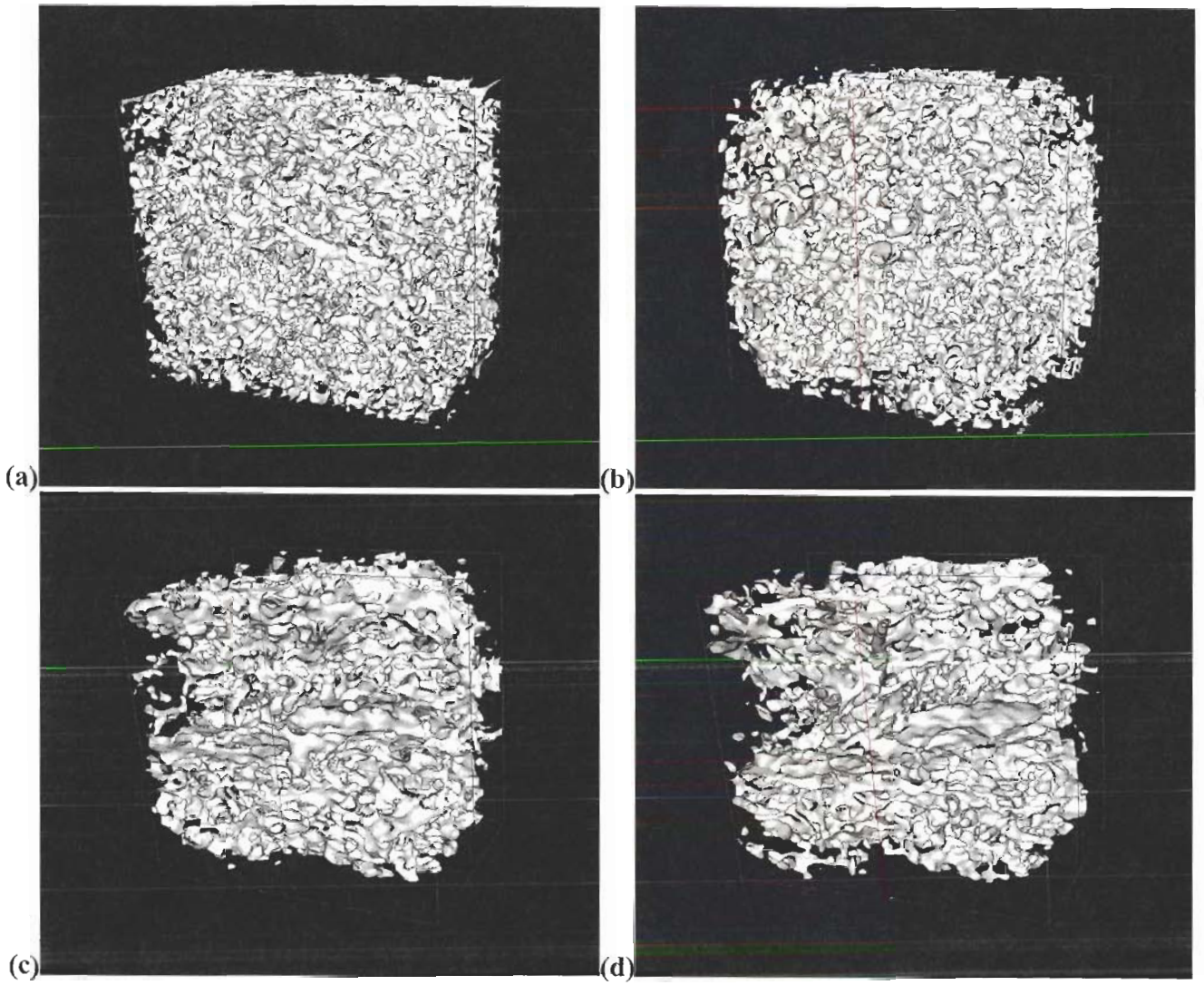

Figure 4-21 Three-dimensional isosurfaces of flat bog soil volumes at 25 cm depth.

4.7 Conclusion

There was a general increase in air-filled porosity, in all the samples, as the soil tension increased for both terrain types. As each peat sub-sample desaturated, some of the pores became air-filled and as a result, the conductive portion of the pore's cross-sectional area diminished (Hillel, 1998). The more decomposed peat, found in deeper soil layers, contained smaller pores where water contents are much higher and air-filled porosity values lower when compared to less decomposed, upper-layer peat. The active porosity or the percentage of pores that actively transmit water through the soil was measured at residual moisture content (5.0 m matric suction); where any water retained at this tension level is the residual water that stays in storage. Results show that three-dimensional imagery derived from CT technology is potentially a valuable tool for measuring active porosity of peat.

By using two-dimensional slices taken from the three-dimensional soil volumes; this permitted direct measurements of pore properties such as pore area, pore diameter and hydraulic radius to be made. Results shows considerable increases in the number of small pores were detectable with increased depth.

The manner in which hydraulic conductivity varies with changes in soil moisture is highly influenced by the pore size distribution of the soil (Ward and Robinson, 2000). The capillary forces exerted by surface tension of soil water, are influenced by the pore size distribution of the soil (Rose, 1966). The pores that have been filled with air are the ones identified in air-filled porosity and pore size distributions. When larger pores have been emptied at higher matric suctions, continuity is disrupted and the water within a

pore space may become immobile (Hillel, 1998). Schwarzel et al. (2002) maintain that deriving pore size distribution from water retention data leads to underestimates of water content due to draining and shrinkage of the peat at higher water tensions. The pore size distribution results show that this method of analysing two-dimensional slices from three-dimensional volumes serves as an improvement to methods that derive pore size distribution from water retention estimates and thin sections of peat cores. The CT scanned images are a fast and non-destructive method of producing raster images of peat samples that can be easily manipulated. Because the slices used for pore size distribution analysis are from three-dimensional blocks, they can be cropped and orientated in any direction. Thin sections are limited to a single orientation.

Three-dimensional isosurface volumes create accurate representations of peat volumes with the ability to manipulate and visualize the internal soil structure qualitatively. Results show that at saturation, the soil and water comprise the majority of the volume but as the tension increases, the soil/water volume decreases and air space increases.

CHAPTER 5:
HYDRAULIC CONDUCTIVITY

5.1 The flow of water in unsaturated peat

The goal of this experiment was to measure the unsaturated hydraulic conductivity of sub-samples taken adjacent to those sub-samples used in the MicroCT scanner, at similar soil tensions. By determining how moisture changes with soil tension, this better approximates hydraulic conductivity (Ward and Robinson, 2000) and provides greater insight into the relationship between soil moisture and hydraulic conductivity. Direct measurements of unsaturated hydraulic conductivity were done to support the three-dimensional active porosity results at a range of matric potentials.

The soil tensions ranged from 0.06 m up to 0.40 m. Figure 5-1 shows the unsaturated hydraulic conductivity measured at 3 cm, 10 cm and 18 cm depth sub-samples from the peat plateau. The figure shows a sharp initial decrease in hydraulic conductivity with increased matric suction and depth. At 3 cm depth, the hydraulic conductivity drops quicker than it does in the deeper depth sub-samplesfrom low matric suction to higher matric suction. In the flat bog, the hydraulic conductivity was greater at deeper depths than at shallower depths for equivalent tensions (Figure 5-2). For example at 0.2 m tension, the hydraulic conductivity ranges from 1.1×10^{-6} m s^{-1} at 3 cm depth, 4.2×10^{-6} m s^{-1} at 10 cm depth, 1.2×10^{-5} m s^{-1} at 20 cm depth, up to 2.5×10^{-5} m s^{-1} at 25 cm depth. Unsaturated flow behaves opposite to saturated flow in that more porous shallower layers conduct water slower than deeper, more decomposed layers since deeper

soil layers contain the most micropores (Hillel, 1998). A higher hydraulic conductivity is found at deeper depths because peat with smaller pores retains more water than peat with larger pores, at the same soil tension. Schwarzel et al. (2002) also reported that for equivalent moisture contents, estimates of unsaturated hydraulic conductivity of peat extracted from a moorland in Germany were found to have similar results where a higher hydraulic conductivity was found at deeper depths than shallower depths. Schwarzel et al. (2002) determined that the highest hydraulic conductivities were found in strongly humified peat and lower conductivities in peat containing apparent plant species.

The results from the peat plateau are unexpected; however, previous studies have concluded that "the use of hydraulic conductivity, as a parameter to define the transmission characteristics of peat, is by no means straightforward" (Rycroft et al., 1975 p. 553). Hydraulic conductivity varies widely in different peats with this variation related to botanical composition, physical characteristics and humification (Rycroft et al., 1975). The deepest peat plateau sub-samples available for analysis were 18 cm in depth compared to 25 cm for the flat bog. If soil blocks were taken from deeper depths in the peat plateau, it is plausible that there would be a similar increase in hydraulic conductivity.

a. 3 cm depth

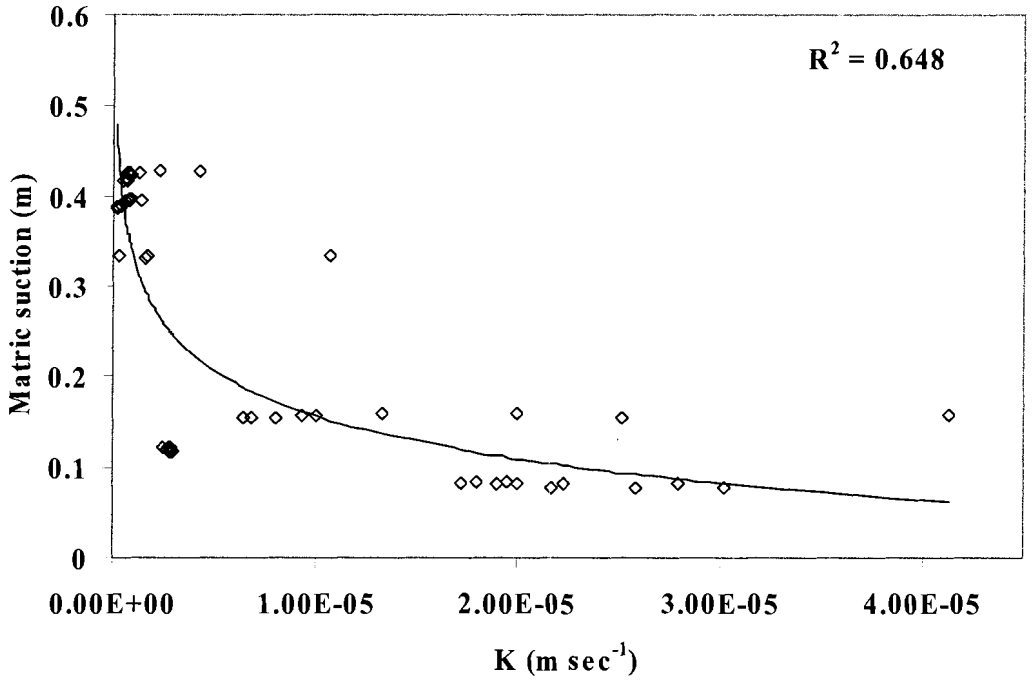

b. 10 cm depth

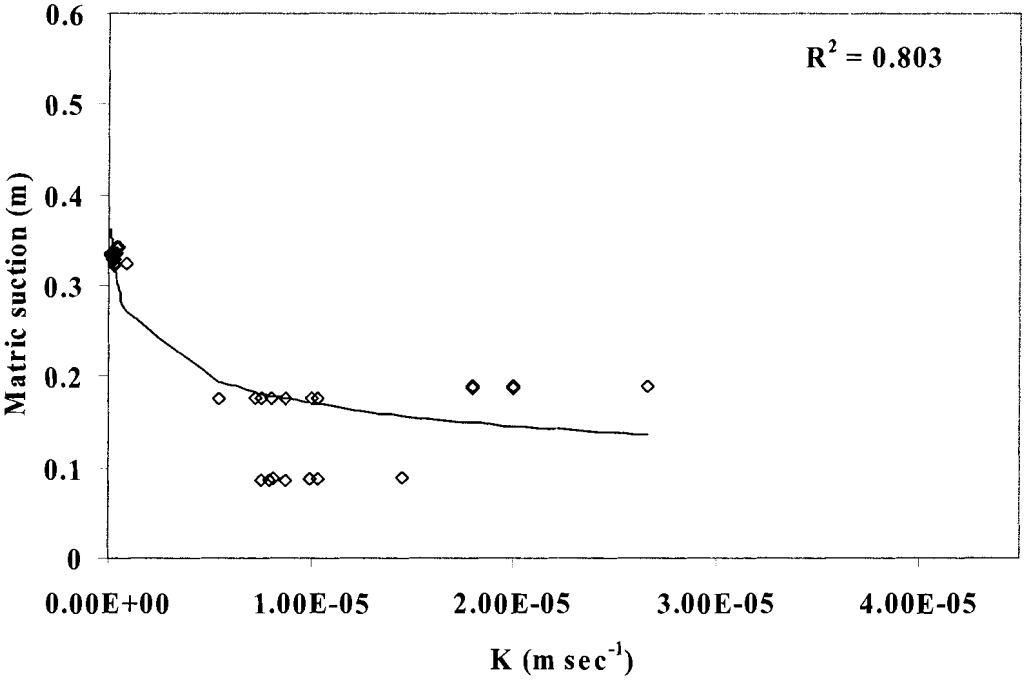

c. 18 cm depth

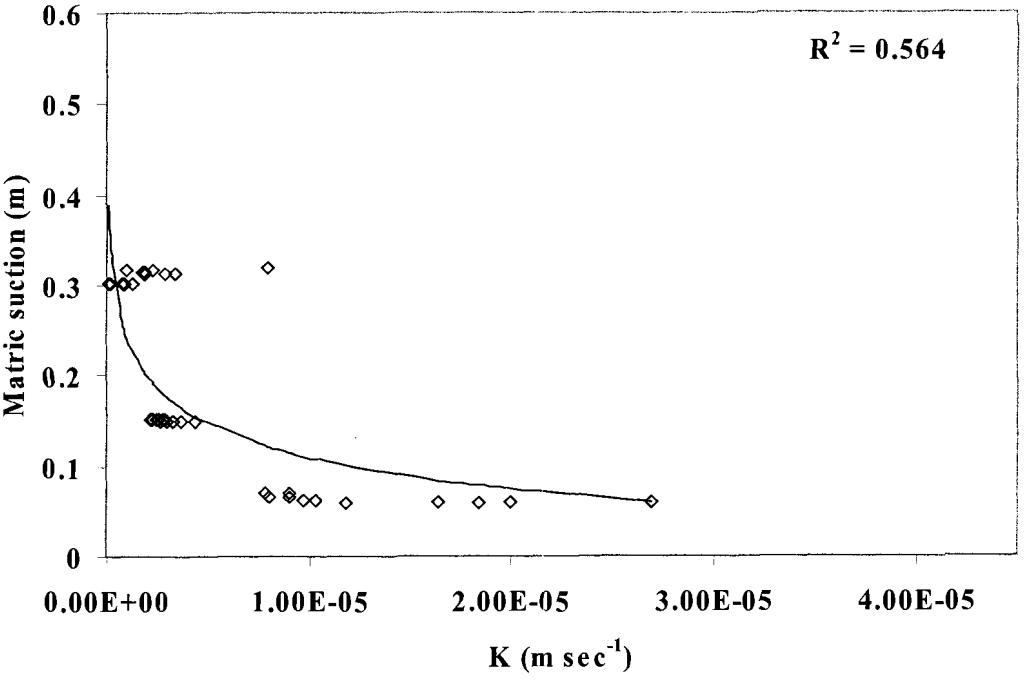

Figure 5-1 Unsaturated hydraulic conductivity using peat plateau sub-samples (a) 3 cm depth (b) 10 cm depth (c) 18 cm depth.

a. 3 cm depth

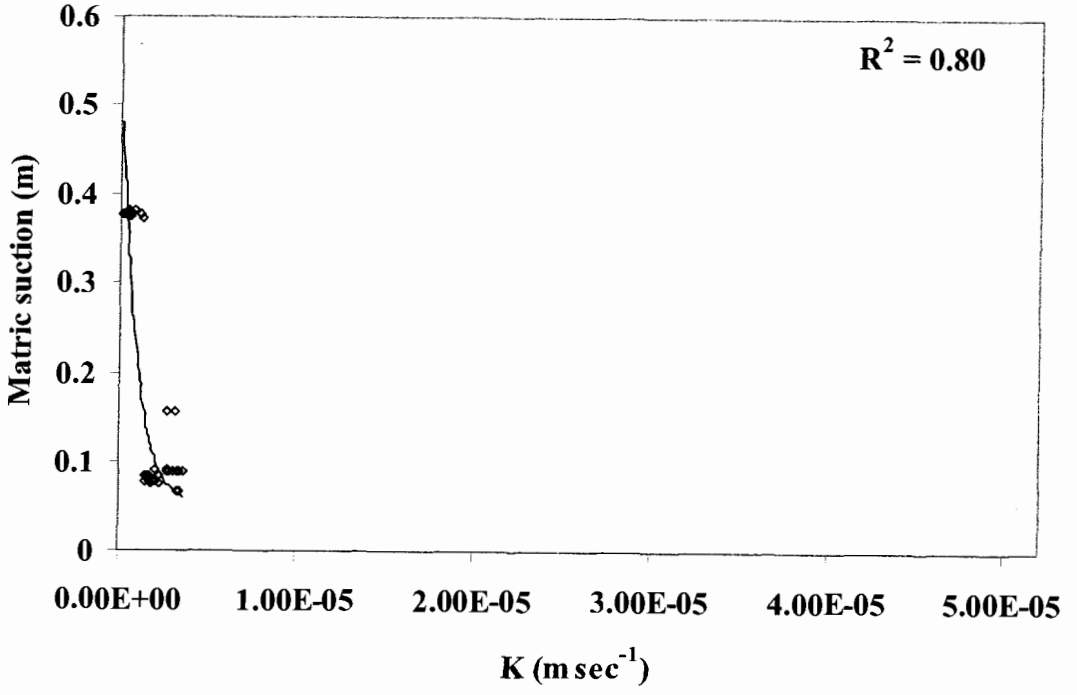

b. 10 cm depth

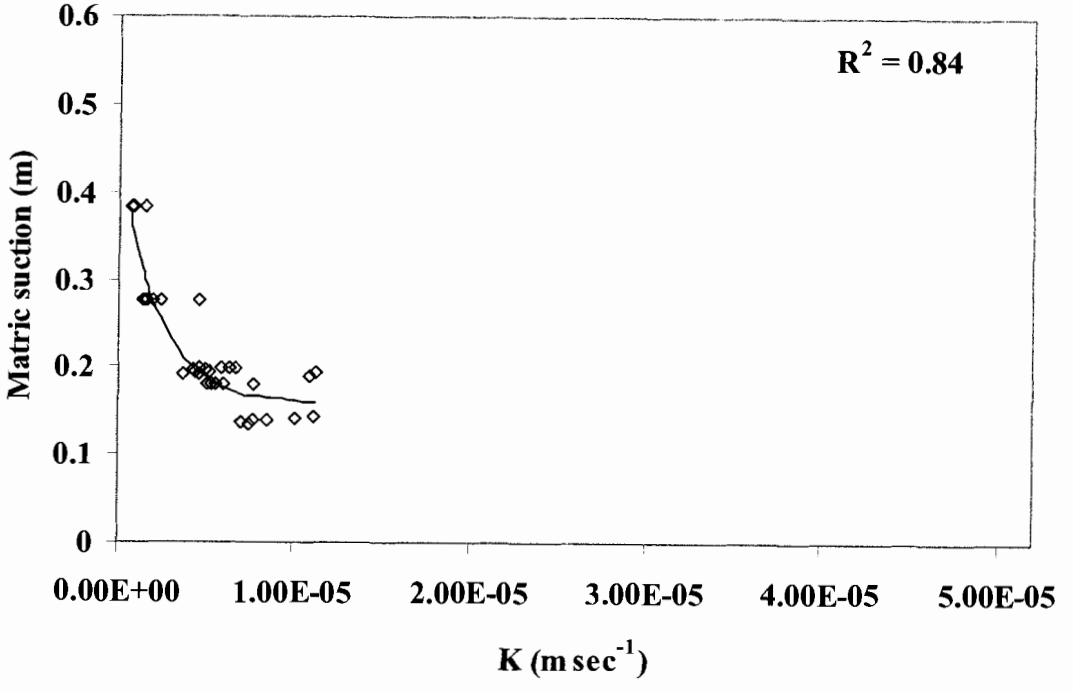

c. 20 cm depth

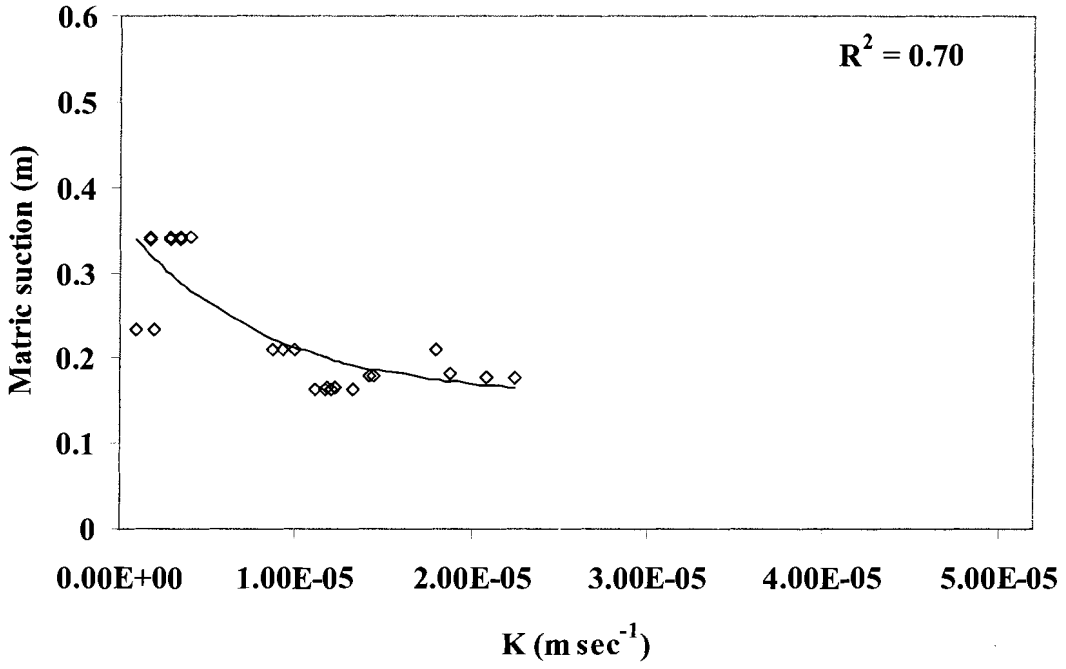

d. 25 cm depth

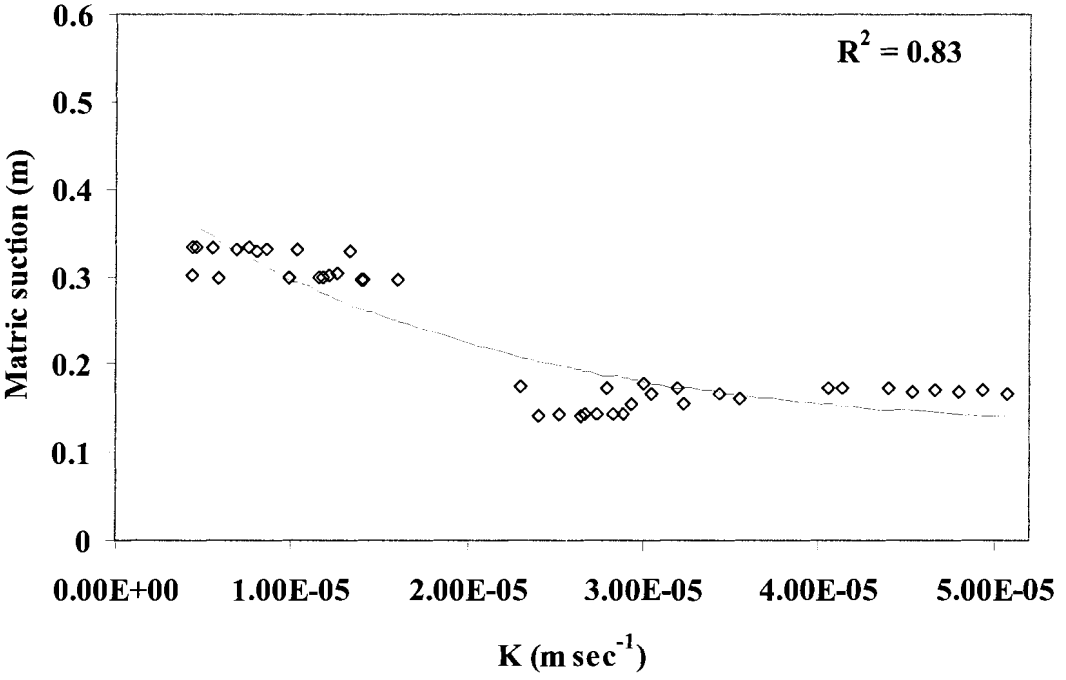

Figure 5-2 Unsaturated hydraulic conductivity using flat bog sub-samples (a) 3 cm depth (b) 10 cm depth (c) 20 cm depth (d) 25 cm depth.

The soil moisture and hydraulic conductivity curves (Figure 5-3 and 5-4) are similar in shape. The expectation is that as the moisture content changes, the hydraulic conductivity should follow a similar pattern, since hydraulic conductivity is dependent on soil moisture content. In some instances the hydraulic conductivity data fit the volumetric moisture curve better than the hydraulic conductivity curve (Figure 5-4 (b) and (d)). The transition from saturation to unsaturation in a soil creates a steep decline in hydraulic conductivity, which may decrease by several orders of magnitude (Hillel, 1998). Figure 5-3 and Figure 5-4 show a sharp decline in hydraulic conductivity with de-saturation. There was also a decrease in the range of hydraulic conductivity with increasing matric suction. This was seen in all cases but most significantly in Figure 5-3 (c).

The unsaturated hydraulic conductivity results agree with the data presented in Chapter 4, which demonstrates that with increased tension, water is removed from the soil as more pores become filled with air. Since large pores readily lose water, the peat rapidly becomes less conductive and the flow path among pores, more tortuous (Hillel, 1998). Water must then flow through smaller pores, along hydration films and over particle surfaces (Hillel, 1998). At high suctions, there is an overall decrease in the size and number of conducting pores. Since the sub-samples taken from lower depths have a low air-filled porosity (Figure 4-2 (c) and Figure 4-3 (c) and (d)), they have smaller pores and therefore a higher water content, maintaining hydraulic conductivities near that of saturation. These factors contribute to the flow of water through an unsaturated sample, which explains why the hydraulic conductivity is higher in the deeper depth sub-samples than in the shallower depth sub-samples at the same matric suctions. The soil moisture characteristic and hydraulic conductivity curves only demonstrate desorption of the sub-

samples since they were measured from a wet state to a drier state.

a. Peat plateau 3 cm depth

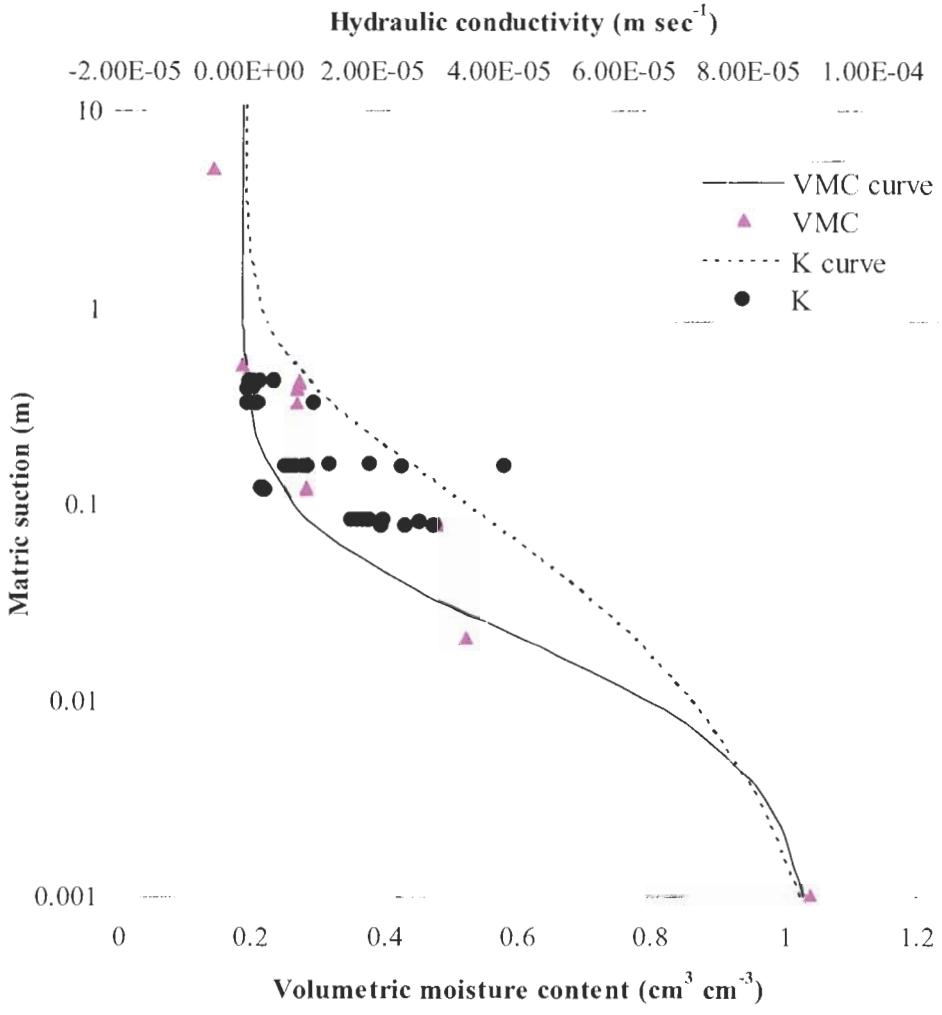

b. Peat plateau 10 cm depth

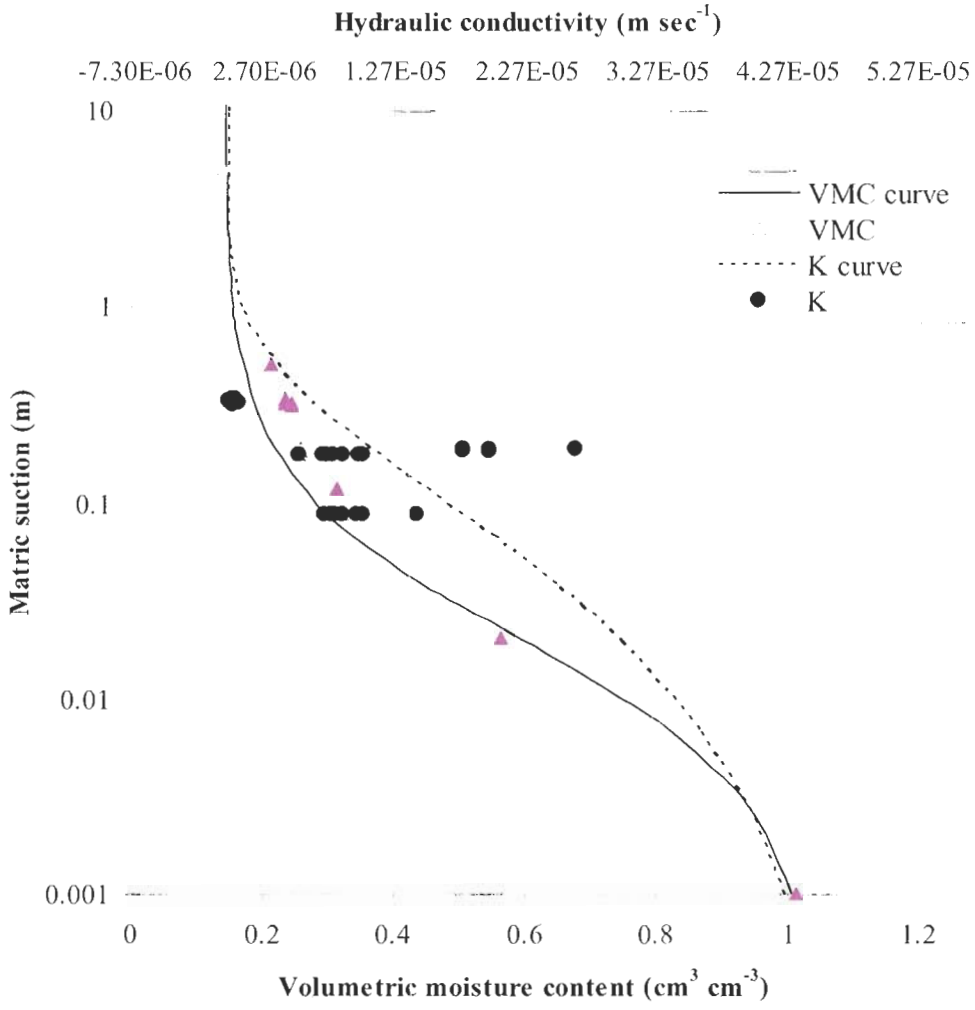

c. Peat plateau 18 cm depth

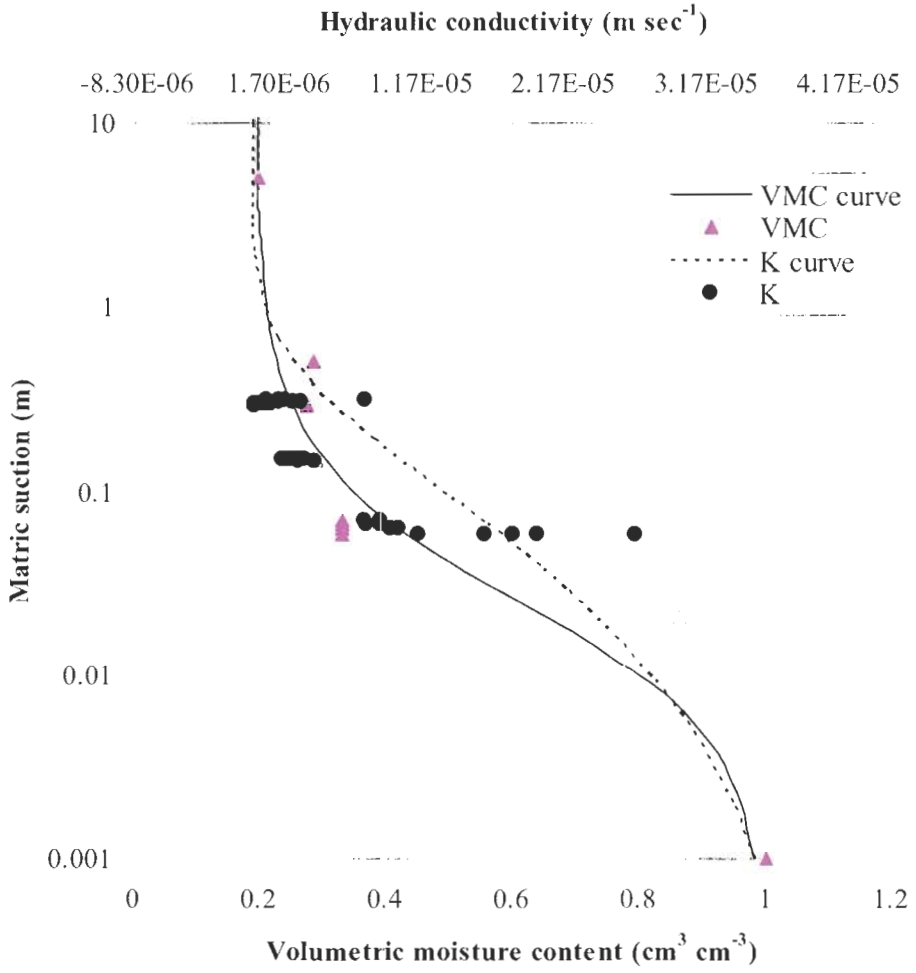

Figure 5-3 Volumetric moisture content (VMC) versus matric suction and unsaturated hydraulic conductivity (K) versus matric suction in the peat plateau.
(a) 3 cm depth (b) 10 cm depth (c) 18 cm depth.

a. Flat bog 3 cm depth

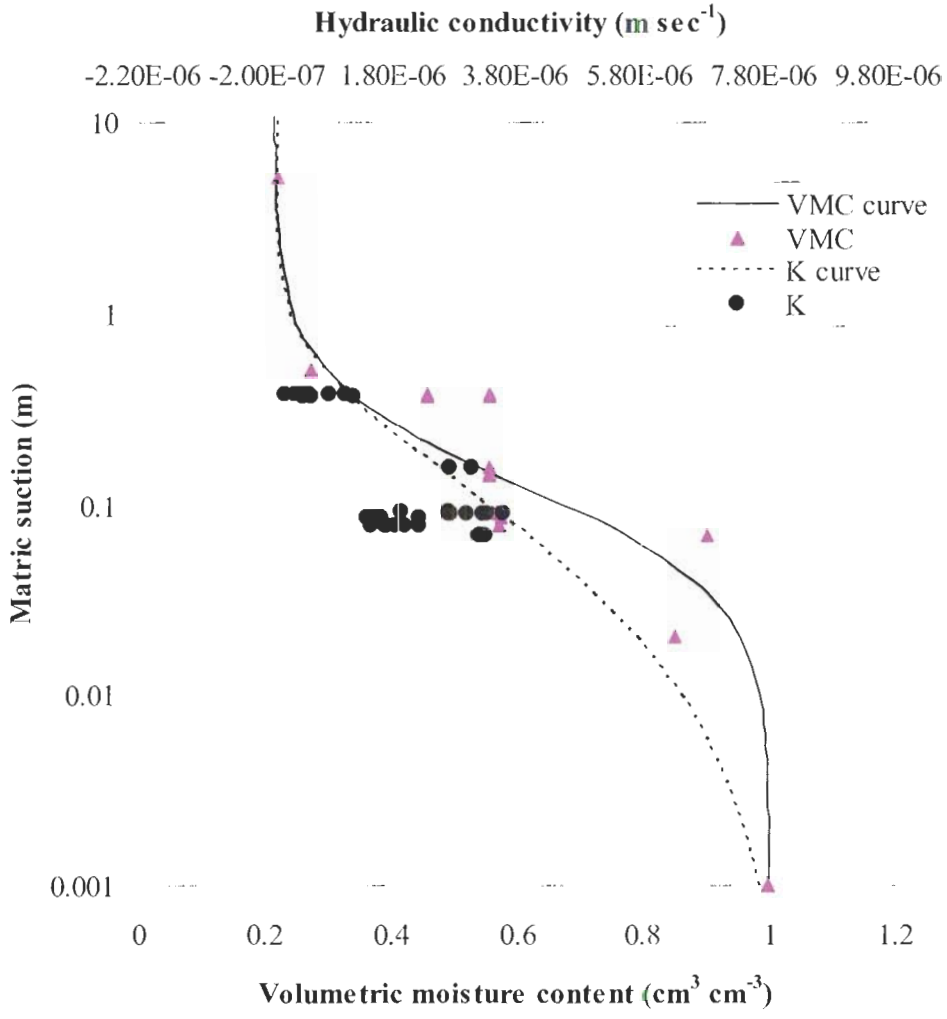

b. Flat bog 10 cm depth

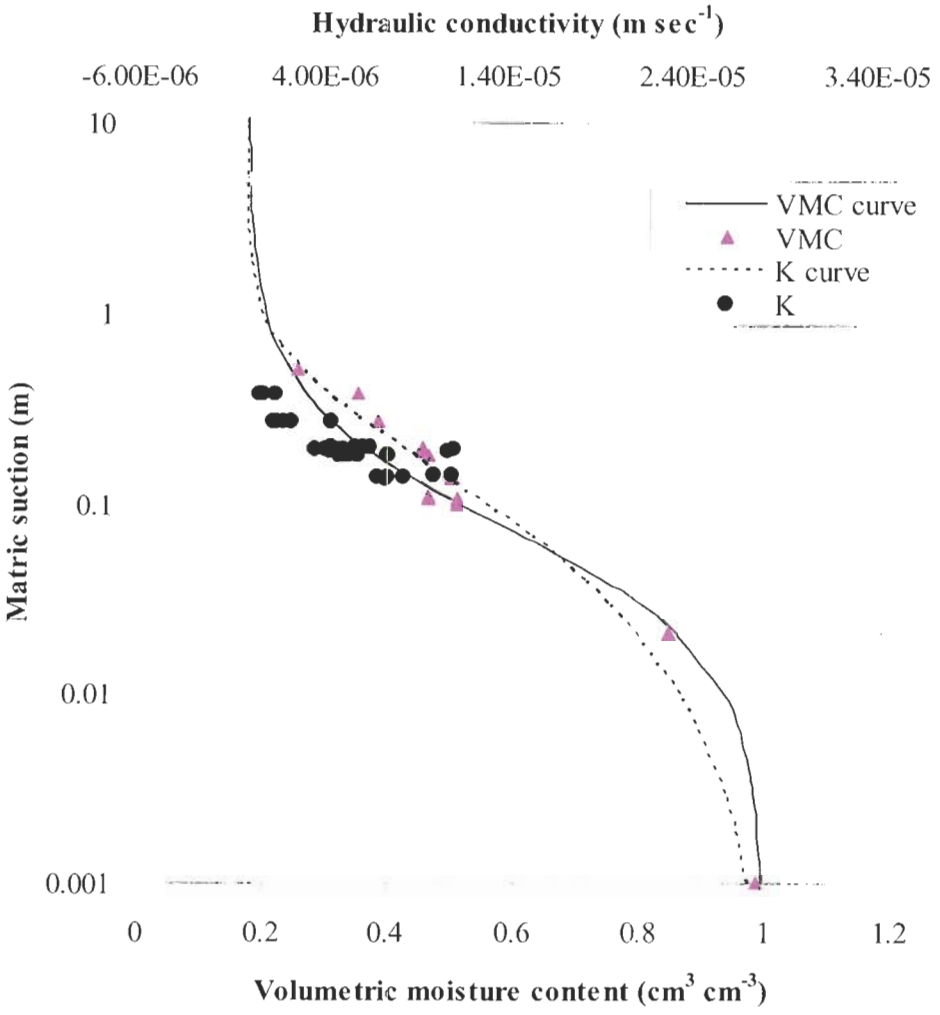

c. Flat bog 20 cm depth

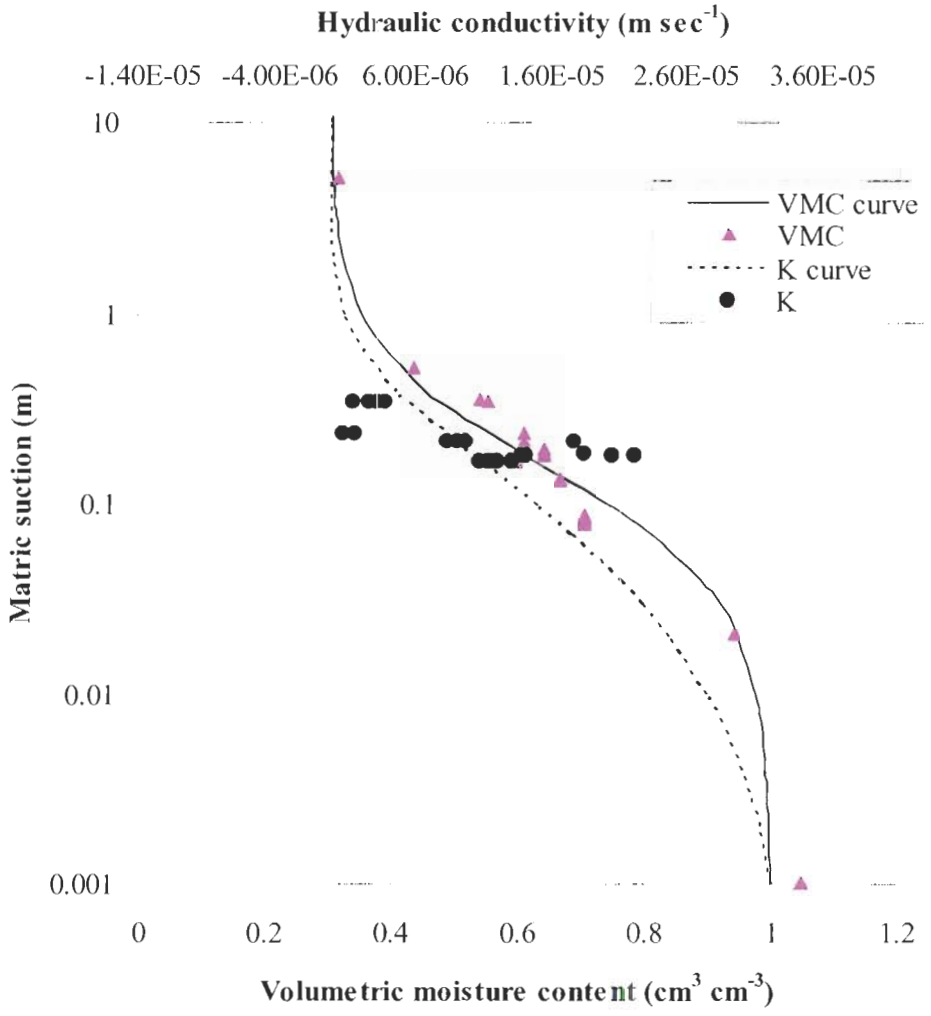

d. Flat bog 25 cm depth

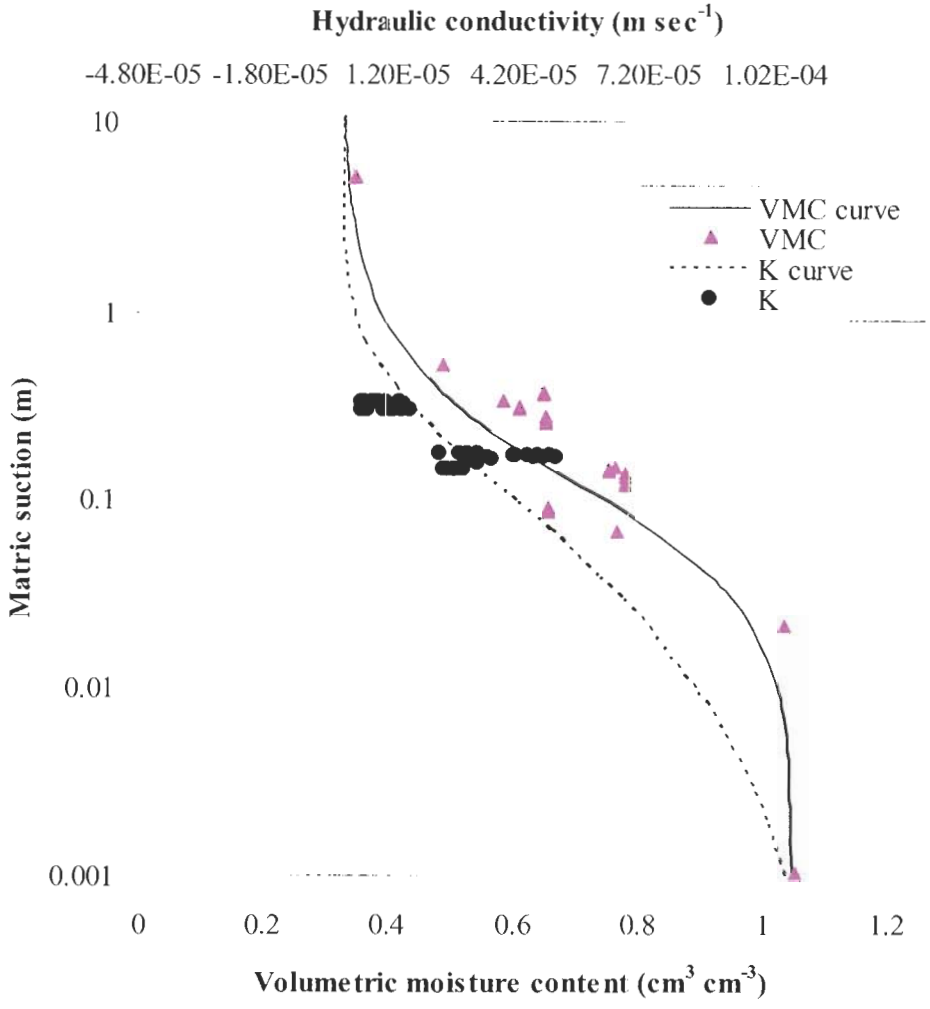

Figure 5-4 Volumetric moisture content (VMC) versus matric suction and unsaturated hydraulic conductivity (K) versus matric suction in the flat bog.
(a) 3 cm depth (b) 10 cm depth (c) 20 cm depth (d) 25 cm depth.

5.2 Conclusion

Unsaturated hydraulic conductivity was measured from a lateral perspective for a range of soil depths for two terrain types. The small range of soil tensions achieved with this experiment was constrained by the soil itself. At high soil tensions it was difficult to measure the slow rate at which the water moved through the sub-samples especially in

the shallow depth sub-samples. At low soil tensions, it was also difficult to retain water in the highly porous peat sub-samples.

The results show that there is a sharp initial decrease in hydraulic conductivity as matric suction increases and volumetric soil moisture decreases in all the sub-samples. At the same moisture contents, the hydraulic conductivity is greater at deeper depths than at shallower depths in the flat bog sub-samples. The hydraulic conductivity data agrees with the data presented in Chapter 4, which demonstrates that when water is removed, more pores become filled with air reducing the storage of water in the peat. In wet mineral soils, hydraulic conductivity is largely related to the texture of the soil, in that when the soil becomes coarser, water is transmitted more easily through larger water-filled pores than smaller pores (Ward and Robinson, 2000). As matric suction increases and the soil dries, the larger pores drain first (Ward and Robinson, 2000). As the largest pores are drained, the hydraulic conductivity is rapidly reduced (Baird, 1997). In unsaturated peat sub-samples the deeper peat layers are more conductive than the shallower less decomposed layers due to their greater number of micropores, which make more connections to permit the flow of water (Hillel, 1998). As a result, changes in pore size with depth, is related to the flux of water in the peat sub-samples.

CHAPTER 6:
PORE STRUCTURE

6.1 Pore size (two-dimensional) measured at two levels of soil moisture

A comparison of the two-dimensional slices or raster images (Figure 3-20, 3-21 and Figure 3-22, 3-23) of peat show a range of air-filled pore sizes. Because of this, the pores give the impression of being larger and more defined with increased soil tension (0.5 m to 5.0 m). Only air-filled pores were visible in the peat plateau and flat bog images. 60 and 135 pores were detectable at the 0.5 m and 5.0 m tensions respectively, in the peat plateau images, indicating a more than two-fold increase in air-filled porosity. 246 and 381 pores were detectable in the flat bog images, at the 0.5 m and 5.0 m tensions respectively, indicating a 65% increase in air-filled porosity. The figures not only display a change in air-filled pore size and number but also a change in soil appearance with drying. This produced variation in the content of both soil and air in the images (Figure 3-20, 3-21 and Figure 3-22, 3-23).

6.1.1 Pore area at two levels of soil moisture

In the peat plateau images, the total air-filled pore area increased with increased matric suction since the wetter sub-sample had a smaller total air-filled pore area (Figure 6-1). At 0.5 m matric suction, all the air-filled pores in the sub-sample were 0.3 mm^2 or less in area. At 5.0 m matric suction, this changes considerably as pores were as large as 4 mm^2 in area. When the sub-sample was in a drier state (5.0 m tension), 25% of the total pore area consisted of pores that were 0.3 mm^2 or less in area indicating that small pores

represented a significant proportion of the total pore area. Additionally, the range of pores sizes (both smaller and larger pores) increased with increased from 0.5 m to 5.0 m tension (Figure 6-2).

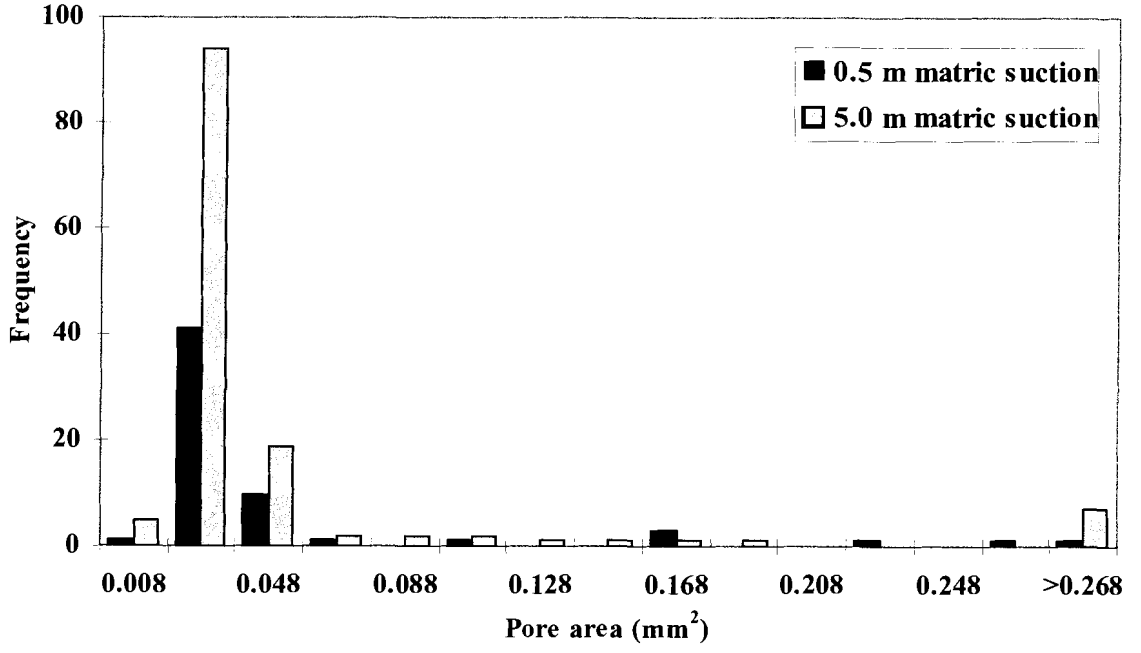

Figure 6-1 Frequency of pores of the peat plateau two-dimensional slices (18 cm depth) at 0.5 m and 5.0 m matric suctions.

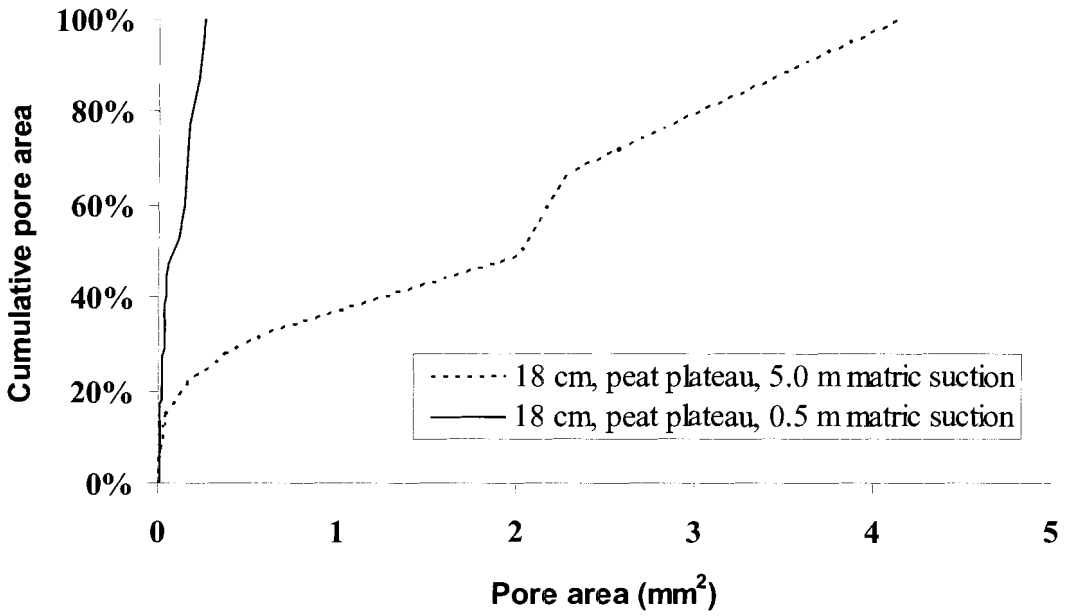

Figure 6-2 Cumulative frequency distribution of air-filled pore area measured from the binary images of the peat plateau slices (18 cm depth) for pores visible at 0.5 m and 5.0 m matric suctions.

Similar to the peat plateau sub-sample, the flat bog images showed that the total air-filled pore area increased with increased matric suction. Because the wetter sub-sample had a smaller total air-filled pore area, there was a considerable increase in the number of small pores with increased matric suction – from 0.5 m to 5.0 m (Figure 6-3). At 0.5 m matric suction, pores that were 2 mm^2 or less represented 79% of the total pore area. Alternatively, at 5.0 m matric suction, pores of the same size range represented 84% of the total pore area, however there was also an increase in the number of pores greater than 2 mm^2 (Figure 6-4).

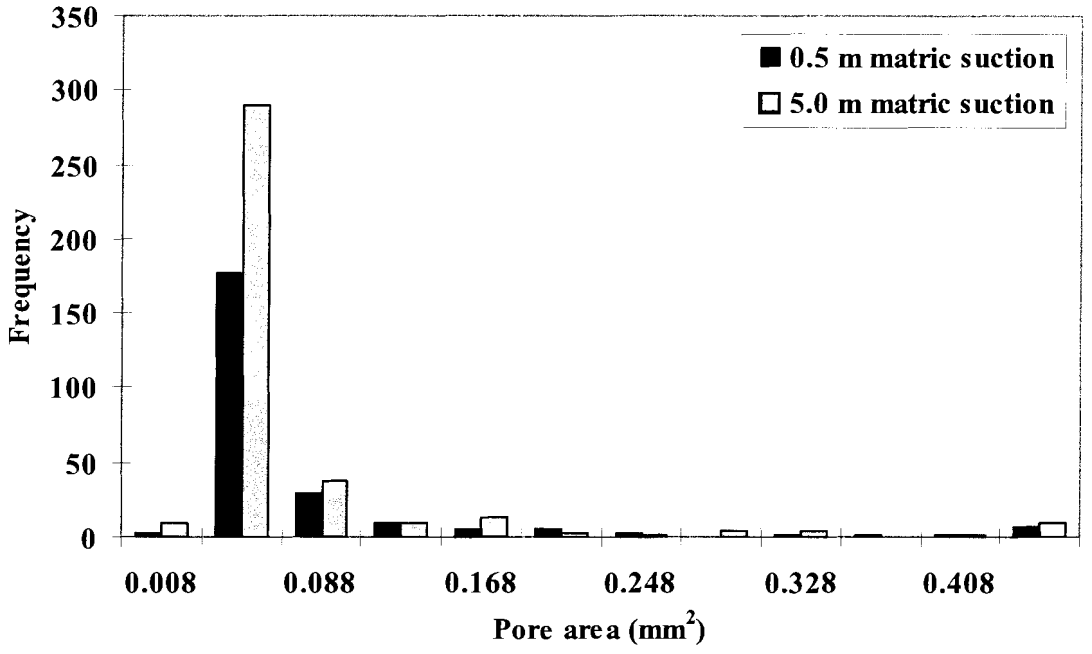

Figure 6-3 Frequency of pores of the flat bog two-dimensional slices (25 cm depth) at 0.5 m and 5.0 m matric suctions.

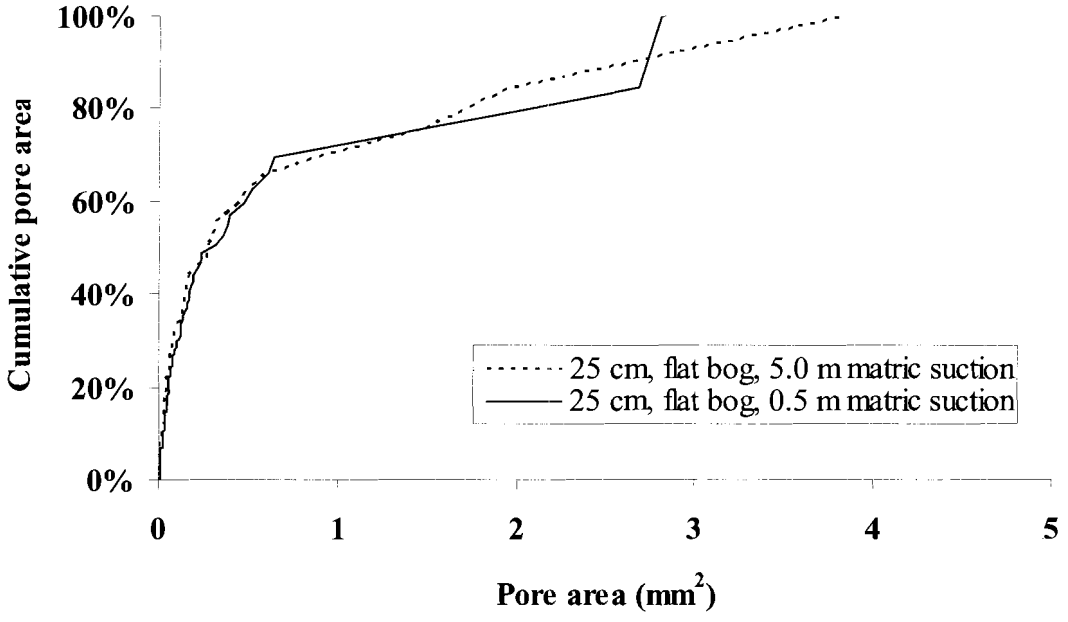

Figure 6-4 Cumulative frequency distribution pore area measured from the binary images of the flat bog slices (25 cm depth) for pores visible at 0.5 m and 5.0 m matric suctions.

6.1.2 Pore diameter at two levels of soil moisture

In the peat plateau images, the air-filled diameter of pores increased with increased matric suction as did the number of small pores that had drained and filled with air. Figure 6-5 shows a comparison of the two moisture contents where with increased matric suction not only had the pores increased in size but also more small pores had become air-filled. At 0.5 m matric suction, 100% pores were classified as 0.5 mm or less in air-filled diameter whereas, at 5.0 m matric suction, pores were much larger where 100% were 3.3 mm or less in diameter (Figure 6-6).

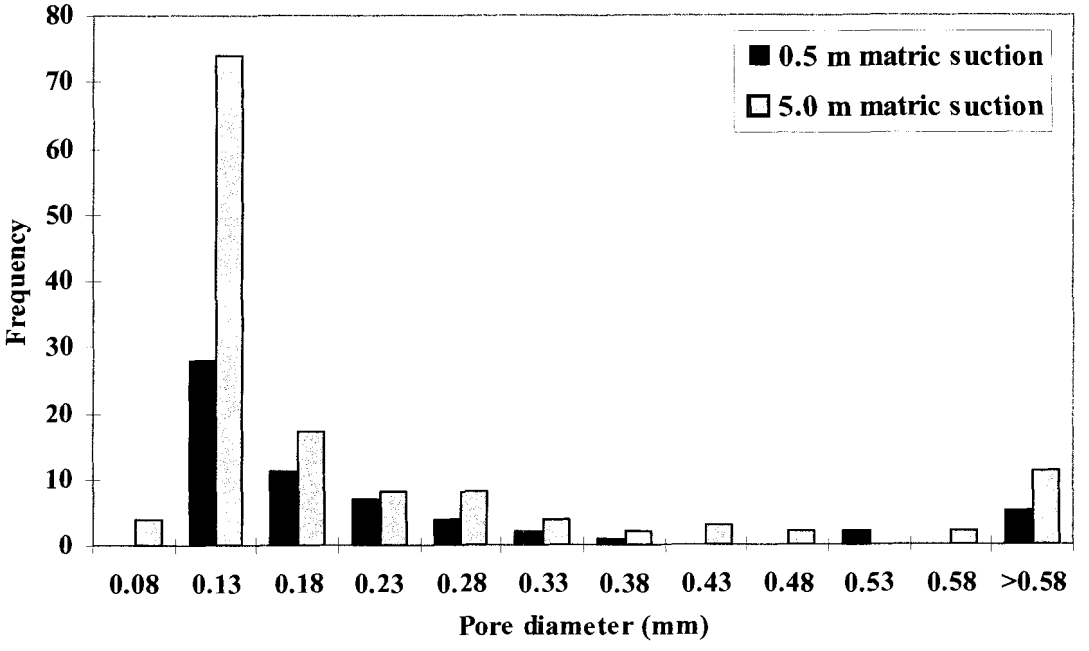

Figure 6-5 Frequency of pores of the peat plateau two-dimensional slices (18 cm depth) at 0.5 m and 5.0 m matric suctions.

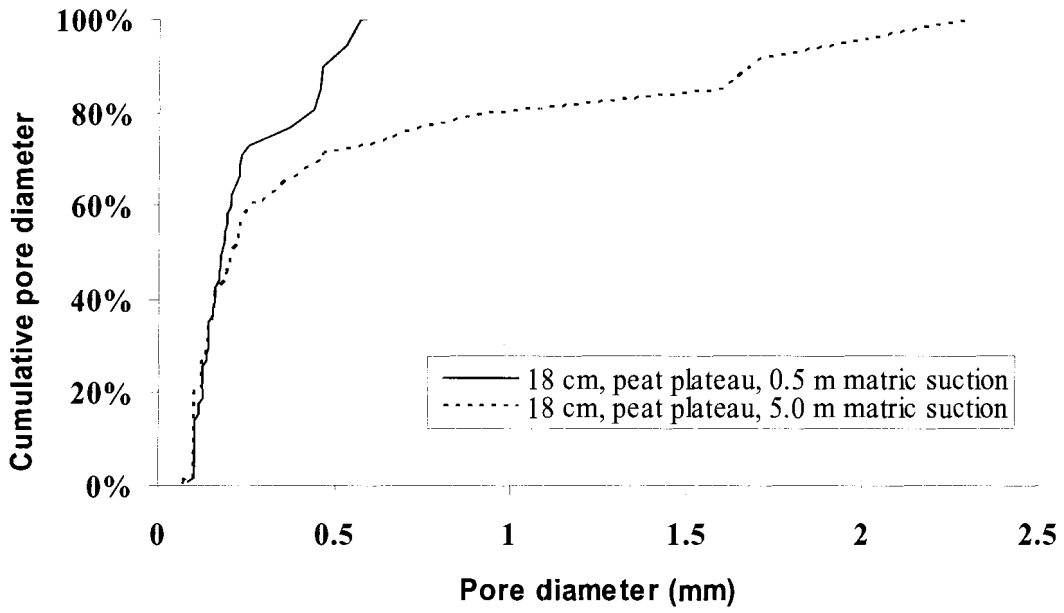

Figure 6-6 Cumulative frequency distribution of pore diameter measured from the binary images of the peat plateau slices (18 cm depth) for pores visible at 0.5 m and 5.0 m matric suctions.

In the flat bog images, the air-filled diameter of pores increased with increased matric suction. Similar to the peat plateau images, the number of small pores that were once saturated in the wetter sub-sample had now drained and filled with air at increased matric suctions (Figure 6-7). At 0.5 m matric suction, 74% of pores are classified as 0.5 mm or less in air-filled diameter and at 5.0 m matric suction, 80% of pores were 0.5 mm or less in diameter (Figure 6-8).

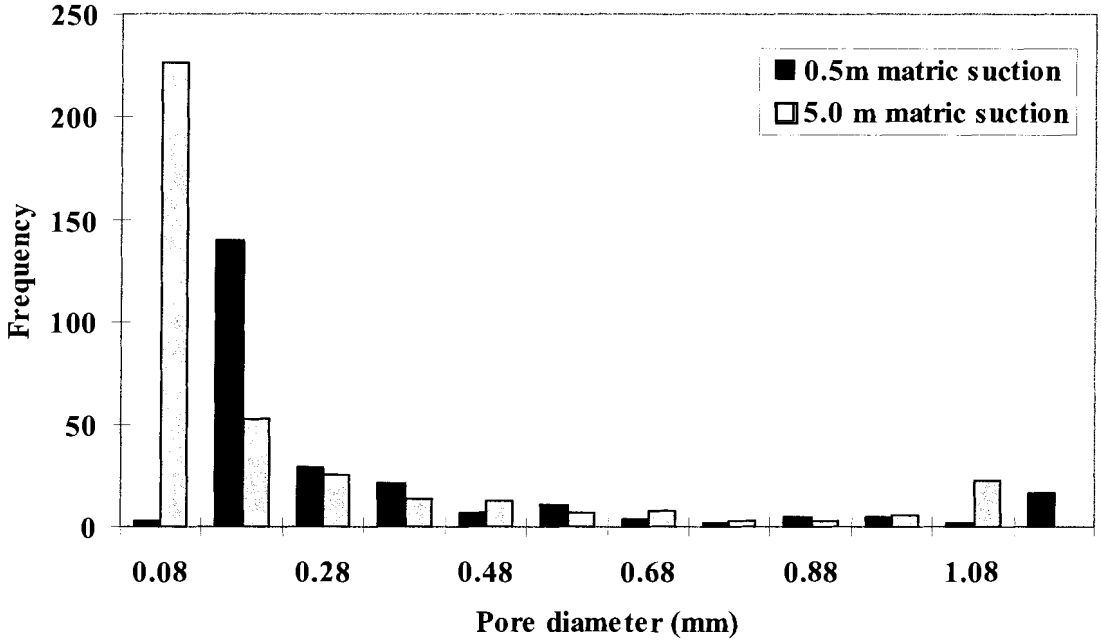

Figure 6-7 Frequency of pores of the flat bog two-dimensional slices (25 cm depth) at 0.5 m and 5.0 m matric suctions.

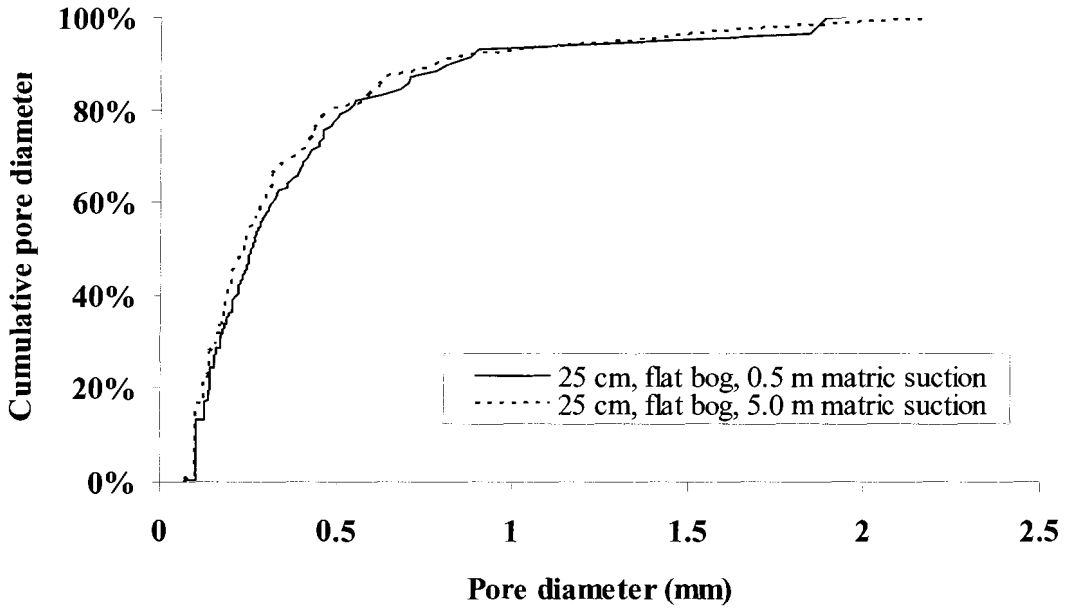

Figure 6-8 Cumulative frequency distribution pore diameter measured from the binary images of the flat bog slices (25 cm depth) for pores visible at 0.5 m and 5.0 m matric suctions.

6.1.3 Hydraulic radius at two levels of soil moisture

In the peat plateau, the results of the pore hydraulic radii measurements showed that as the pores became filled with air (which is evident in both measurements of pore area and diameter discussed previously) that pore hydraulic radii also increased with increased matric suction (Figure 6-9). For example Figure 6-10 shows that pores that were 0.07 mm or less in hydraulic radius constituted 51% of all pores in the wetter sub-sample but only 38% of all pores in the drier sub-sample. As well, pores that were 0.19 mm or less in hydraulic radius constituted 93% of pores in the drier sub-sample but 100% of pores in the wetter sub-samples. This was further confirmed by Figure 6-9 which showed that a larger number of smaller hydraulic radii existed in the 5.0 m sub-sample than the 0.5 m sub-sample.

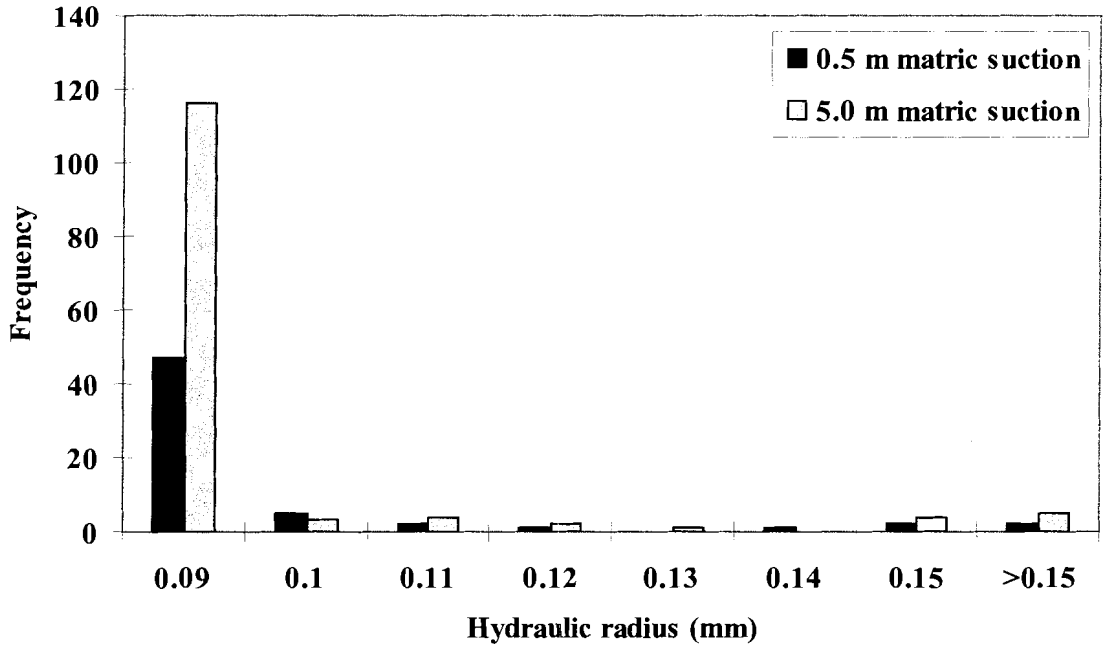

Figure 6-9 Frequency of pores of the peat plateau two-dimensional slices (18 cm depth) at 0.5 m and 5.0 m matric suctions.

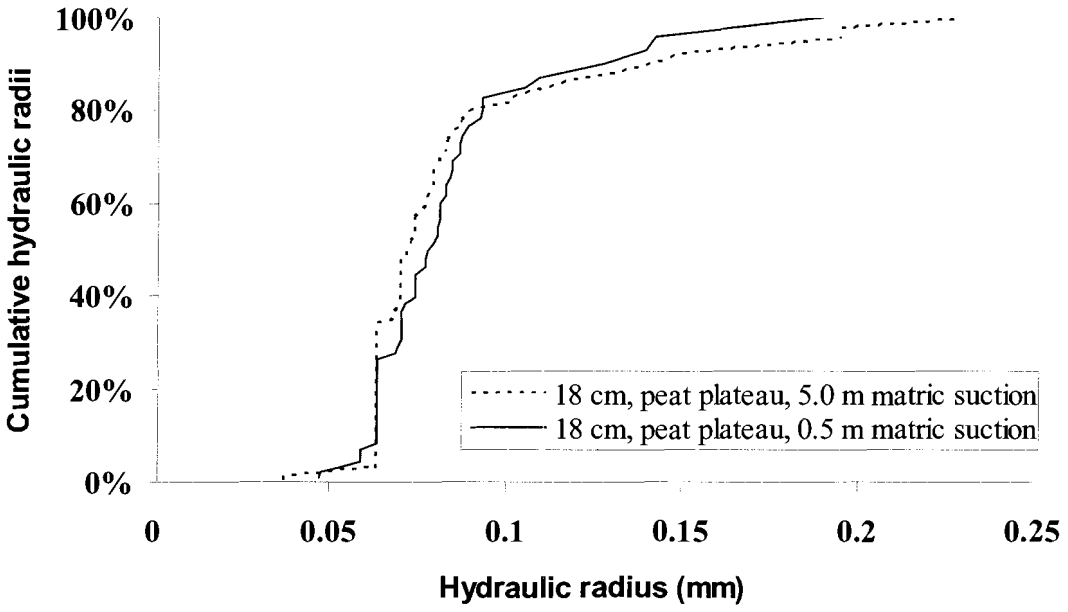

Figure 6-10 Cumulative frequency distribution pore hydraulic radii measured from the binary images of the peat plateau slices (18 cm depth) for pores visible at 0.5 m and 5.0 m matric suctions.

In the flat bog, there was a general increase in pore hydraulic radii with increasing soil tension for most pore sizes (Figure 6-11). For example at 0.5 m matric suction, pores with hydraulic radii that were 0.1 mm in size or less constitute 84% of all pores, whereas at 5.0 m matric suction, pores in that radii range, constitute 93% of all pores at that tension (Figure 6-12).

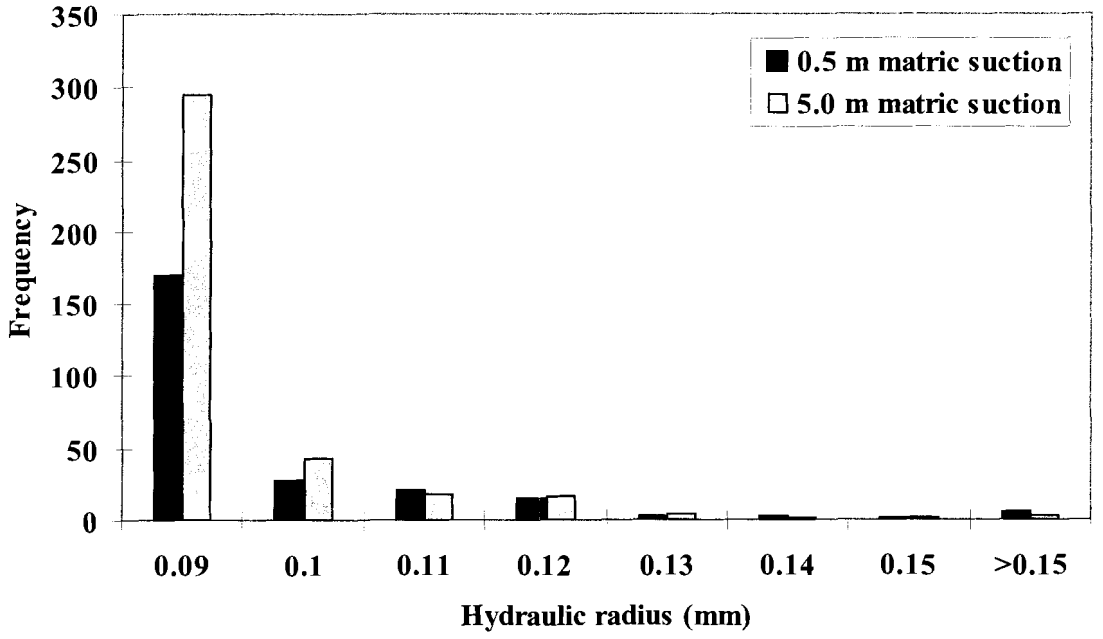

Figure 6-11 Frequency of pores of the flat bog two-dimensional slices (25 cm depth) at 0.5 m and 5.0 m matric suctions.

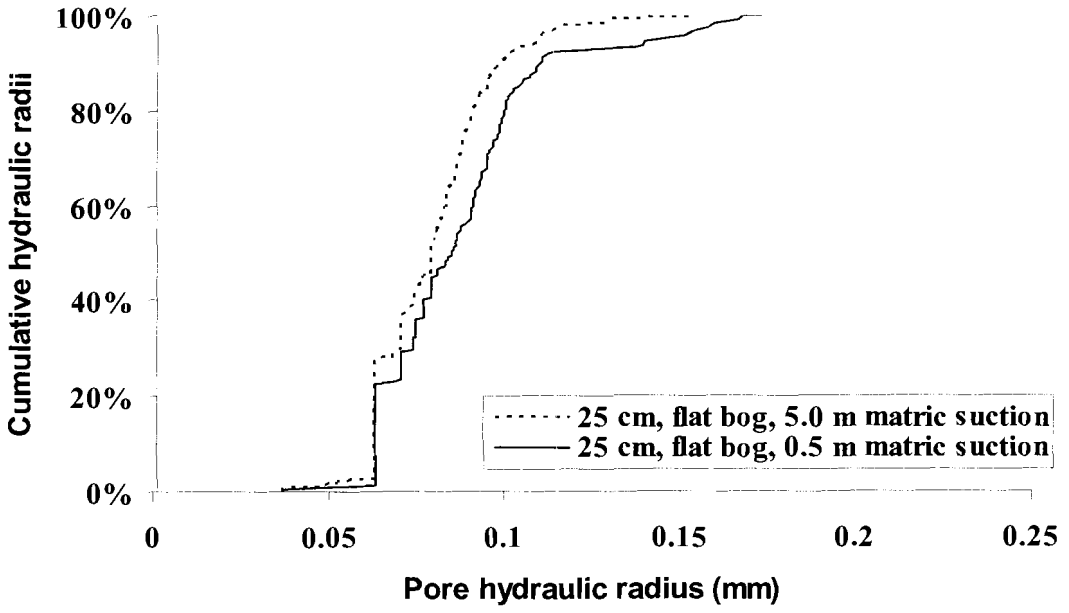

Figure 6-12 Cumulative frequency distribution hydraulic radii measured from the binary images of the flat bog slices (25 cm depth) for pores visible at 0.5 m and 5.0 m matric suction.

6.2 Microscopic spaces of porous *Sphagnum* cells with variations in pore structure and moisture content

6.2.1 Hyaline cell structure and decomposition

Twenty micron resolution images were used to compare variations in cell structure with depth and decomposition between four flat bog sub-samples. Examination of the MicroCT images shows that the hyaline cell wall thickenings or fibrils are dense and define the cell's shape. The leaves of *Sphagnum* are only one cell thick and are attached to stems that consist of thin-walled cells and a periphery of narrower cells with thicker walls (Ligron and Duckett, 1998). The hyaline cell walls, in particular, have a secondary wall framework which prevents these cells from bursting when they are full of water, or from collapsing and losing their shape when they are dry (Kremer et al. 2004). At 3 cm depth, (Figure 6-13(a) and Figure 6-14(a)) the narrow, ovate branches and cells are distinct but have already started to decompose, as it is evident that the cells have started to lose their structural integrity. At this depth, the cells are in the early stages of decomposition and the cell walls have in some cases, broken away from the rest of the cell. At deeper depths, the soil has lost most of its structural integrity due to more advanced decomposition (Figures 6-13 and 6-14 (b), (c) and (d)).

Hoag and Price (1997) found that at upper soil depths, the hyaline cells and their open structure were more apparent than at lower soil depths and that below 0.40 m, the peat was darker, more compact and relatively decomposed with few preserved roots and grasses present. The occurrence of an acrotelm and catotelm in the flat bog, discussed in Chapter 4, confirms that the former is composed of living and poorly decomposed plant

debris, while the latter contains more decomposed plant debris because of a slow exchange of water (Ivanov, 1981).

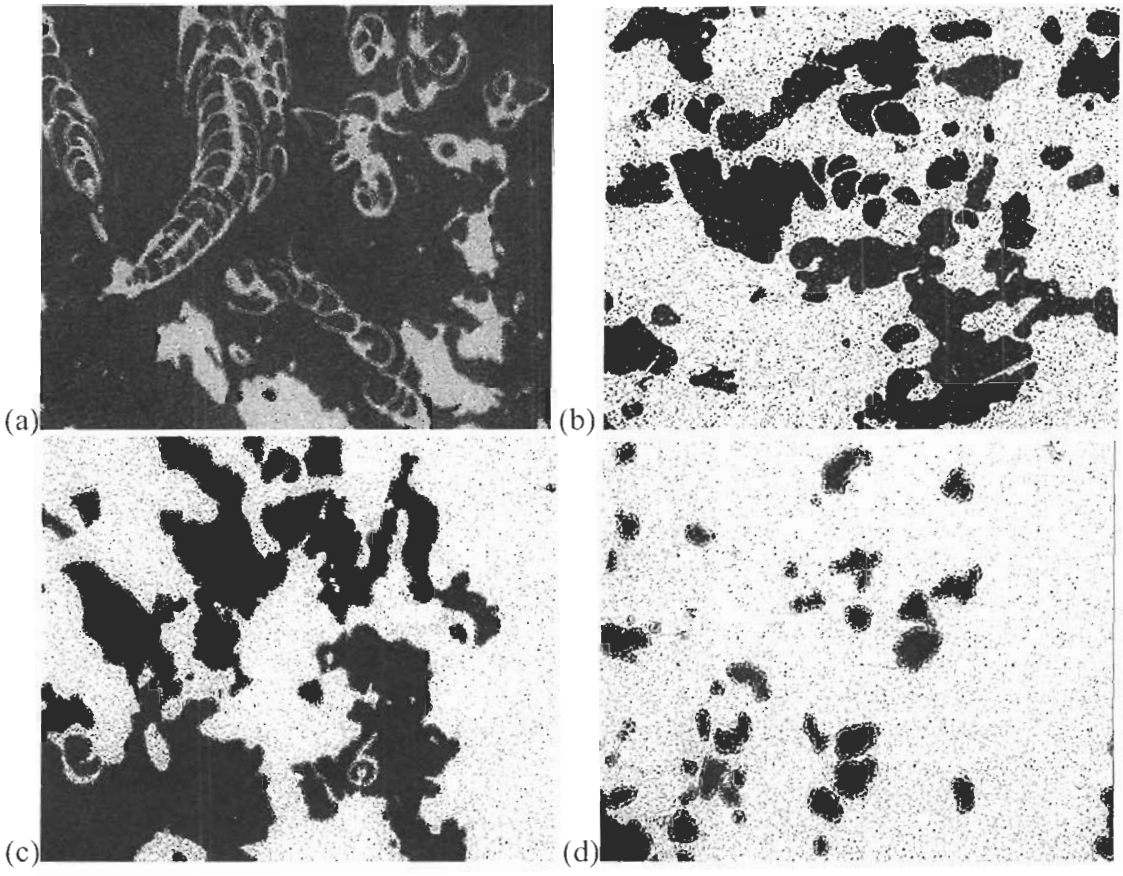

Figure 6-13 Two-dimensional slices (20 µm thickness and resolution) of flat bog soil. Black represents air and grey represents soil and water content, analysed at an unknown moisture content. (a) 3 cm depth (b) 15 cm depth (c) 25 cm depth (d) 35 cm depth. Scale: (x,y) 15.50 x 19.96 mm.

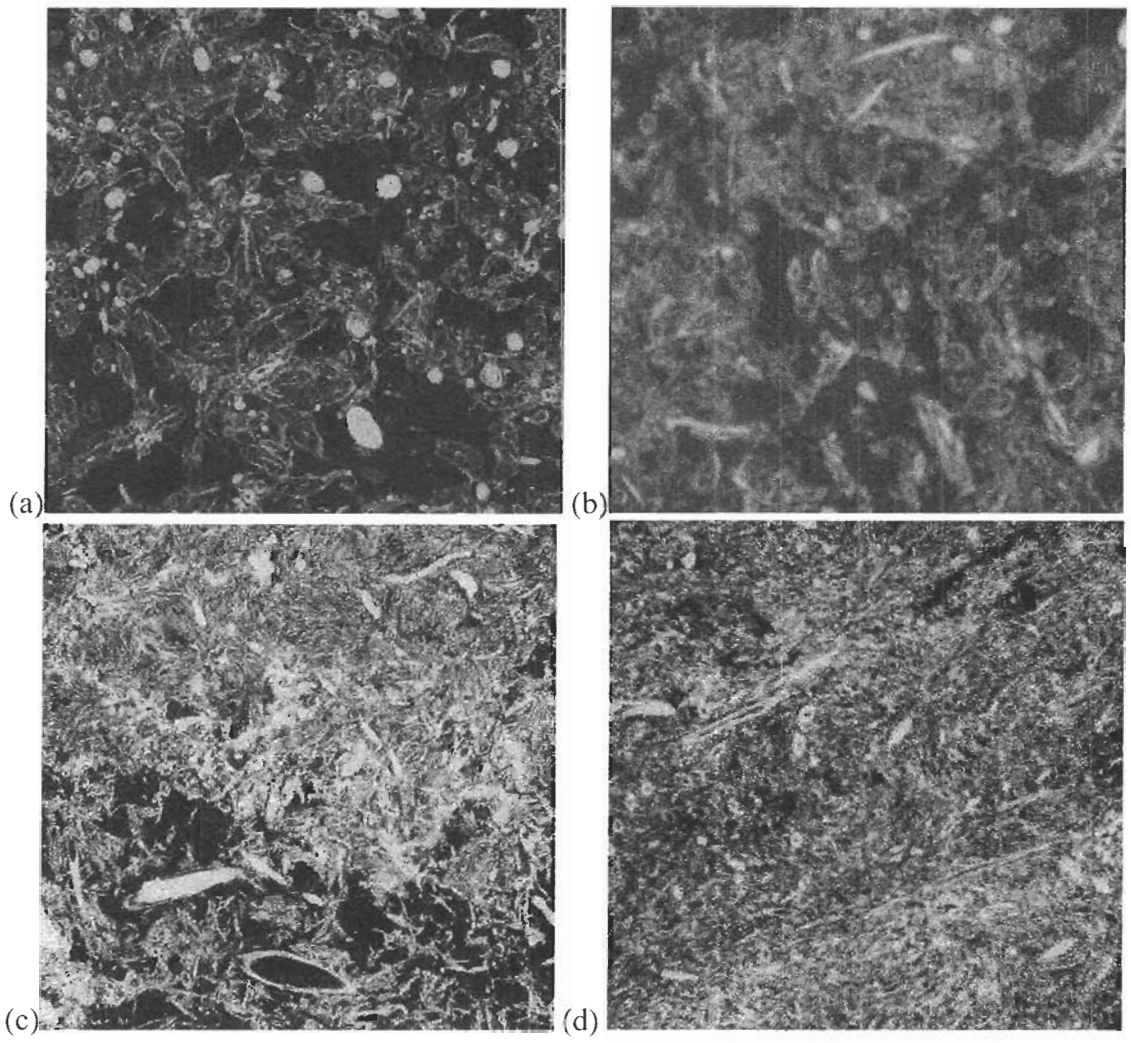

Figure 6-14 Two-dimensional slices (20 µm thickness and resolution) of flat bog soil. Black represents air and grey represents soil and water content, at 5.0 m matric suction. (a) 3 cm depth (b) 10 cm depth (c) 20 cm depth (d) 25 cm depth. Scale: (x,y) 30.61, 30.50 mm.

6.2.2 Hyaline cell structure and moisture content

The adsorptive ability of *Sphagnum* is due to the behaviour of the porous *Sphagnum* cells. The water holding capacity of *Sphagnum* is twenty times its dry weight (Richardson, 1981). *Sphagnum* has little control over the rate at which water moves through it and has low tolerance for desiccation (Hayward and Clymo, 1982). At negative matric potentials, the cytoplasm within the cells becomes viscous and gel-like

(Richardson, 1981). Water is drawn through the cells using capillary films to avoid desiccation. Capillary pressure allows water to be retained by the moss through the use of a network of capillary spaces. Capillarity results from the water's surface tension and its contact angle with the organic matter (Hillel, 1998). When soil is unsaturated, capillarity produces curved menisci (Hillel, 1998). Additionally, the soil also forms hydration envelopes over the particle surfaces as a means of adsorption (Hillel, 1998). Capillarity and adsorption are the combined result of applying a matric potential or matric suction on soil. *Sphagnum* also has intracellular adsorption, which intensifies the amount of water retained at each level of matric suction. Romanov (1968) acknowledged three types of water retention in peat: adsorbed, intracellular and capillary water (Hayward and Clymo, 1982).

Results of this study show that with changes in moisture, a capillary film is present around the *Sphagnum* leaves at 0.5 m tension, but when the tension increases to 5.0 m, the film becomes broken and discontinuous and the hyaline cells become more visibly defined (Figure 6-15 (c) and (d)). When lacking a continuous capillary film, *Sphagnum* stops conducting water (Hayward and Clymo, 1982). At 3 cm, 10 cm and 20 cm depth, the images (Figure 6-15, 6-16, 6-17) show a gradual desiccation of the hyaline and chlorophyllose cells with increased soil tension. In all the aforementioned figures image (a) is saturated; (b) is 0.02 m matric suction; (c) is 0.5 m matric suction; and (d) is 5.0 m matric suction. Images (a) and (b) have high water content so the peat is not easily distinguished. Image (c) shows a capillary fringe around the hyaline and chlorophyllose cells. When the highest soil tension is applied, (d) the fibrous cell walls are visibly evident. Adsorbed, intracellular and capillary water was retained in the peat until enough

matric suction was applied to lessen or even remove the water from around the cell edges. This creates a discontinuous capillary film that increases air-filled pore size and decreases hydraulic conductivity. The upper depth sub-samples show this transition best but at 25 cm depth (Figure 6-18); the peat is too advanced in decomposition to show evidence of a capillary film at all tension levels.

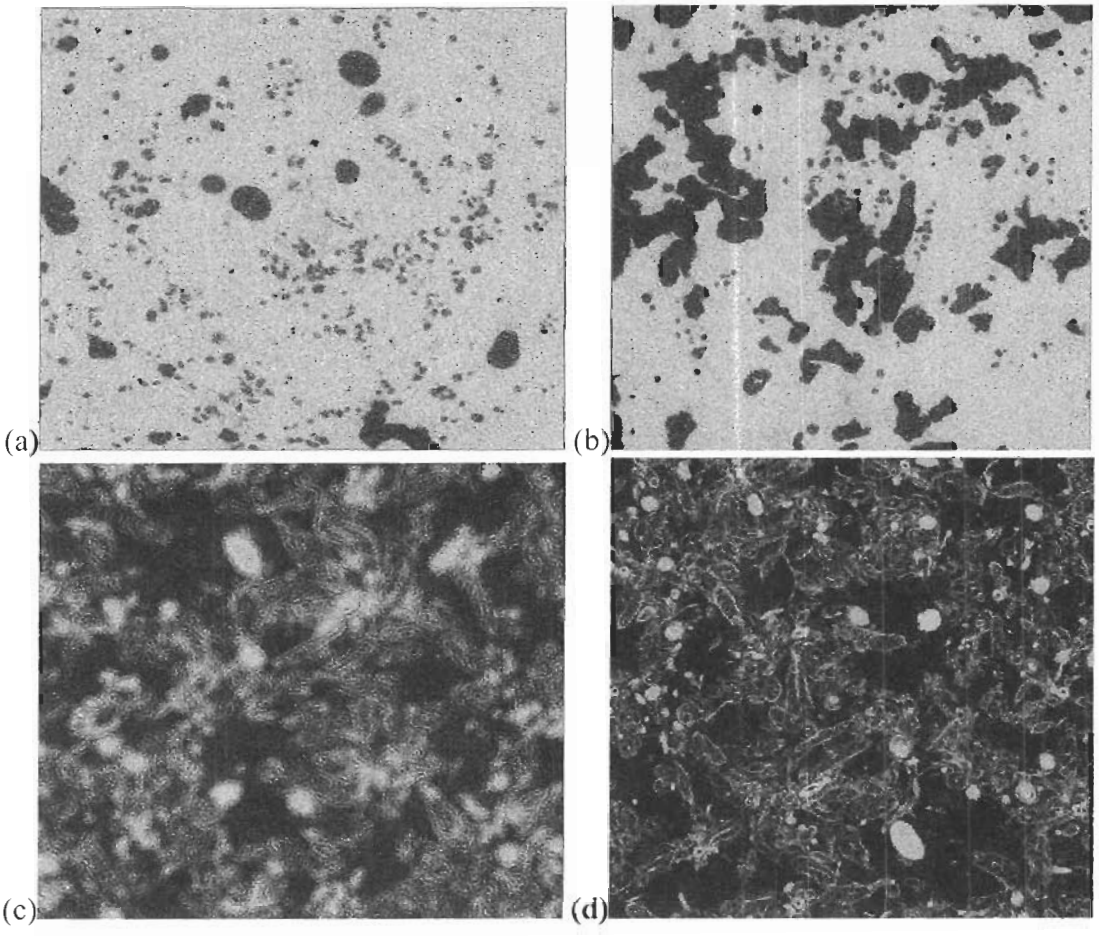

Figure 6-15 Two-dimensional slices (20 μm thickness and resolution) at 3 cm depth of flat bog soil. Black represents air and grey represents soil and water content. (a) Saturated (b) 0.02 m matric suction (c) 0.5 m matric suction (d) 5.0 m matric suction. Scale: (x,y) 30.61, 30.50 mm.

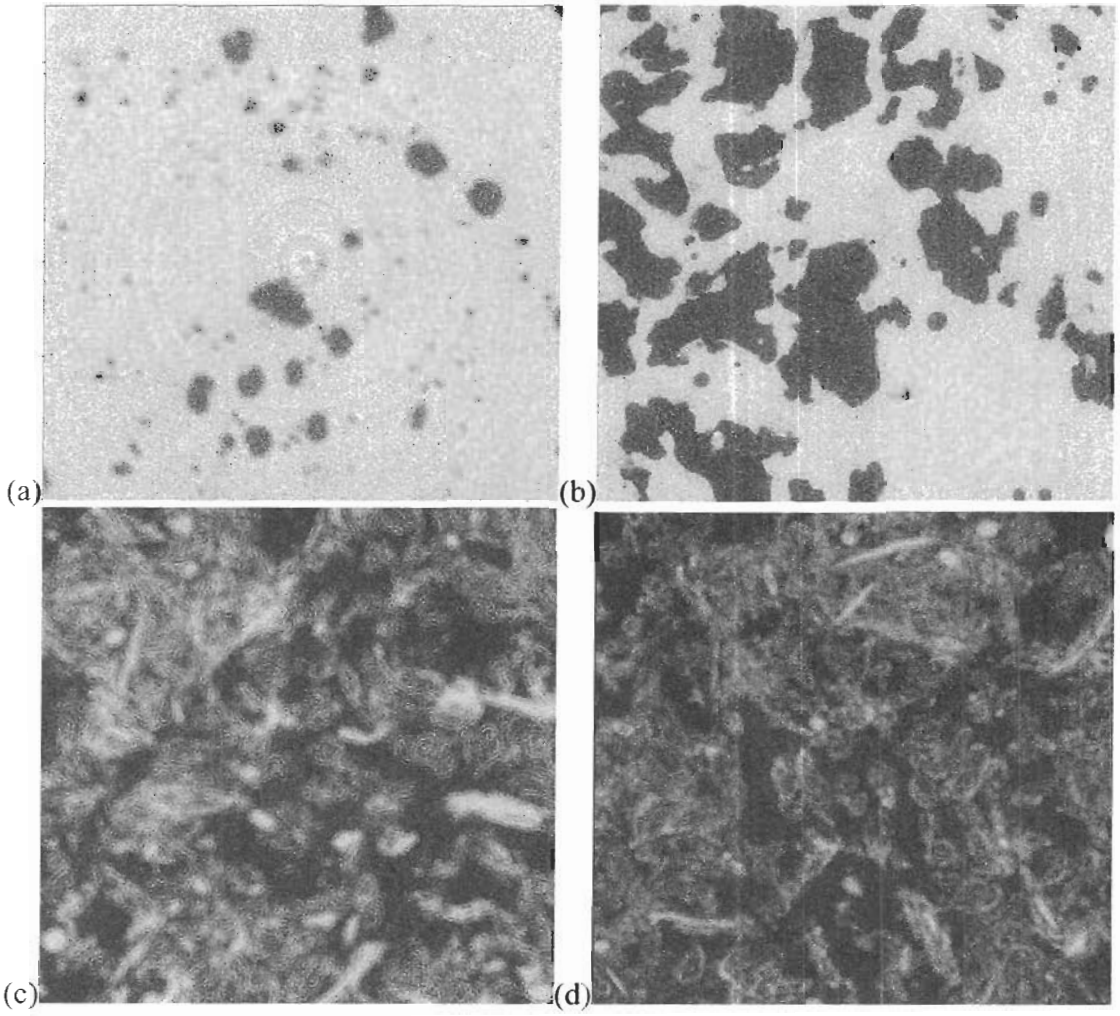

Figure 6-16 Two-dimensional slices (20 μm thickness and resolution) at 10 cm depth of flat bog soil Black represents air and grey represents soil and water content. (a) Saturated (b) 0.02 m matric suction (c) 0.5 m matric suction (d) 5.0 m matric suction. Scale: (x,y) 30.61, 30.50 mm.

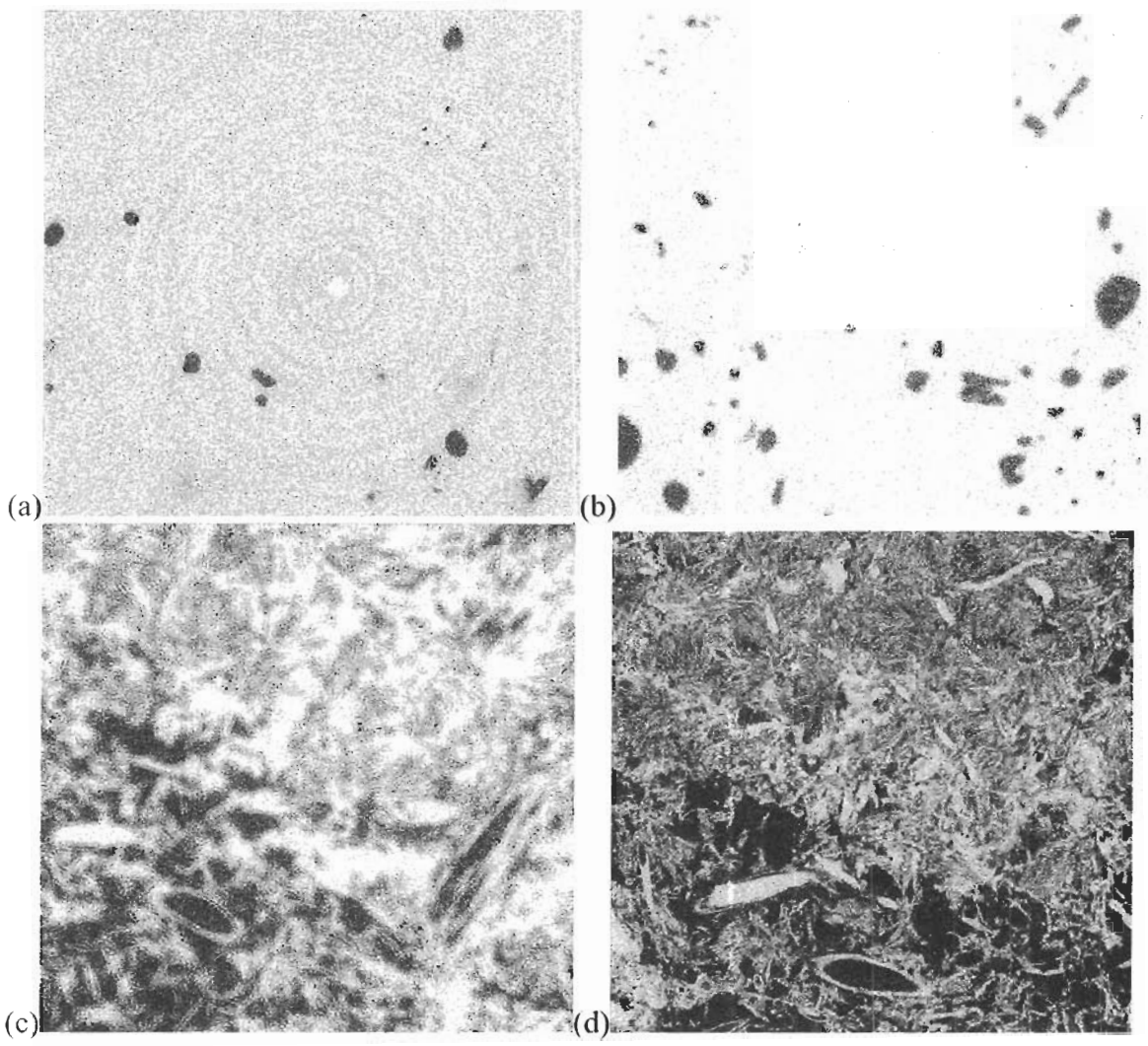

Figure 6-17 Two-dimensional slices (20 µm thickness and resolution) at 20 cm depth of flat bog soil. Black represents air and grey represents soil and water content. (a) Saturated (b) 0.02 m matric suction (c) 0.5 m matric suction (d) 5.0 m matric suction. Scale: (x,y) 30.61, 30.50 mm.

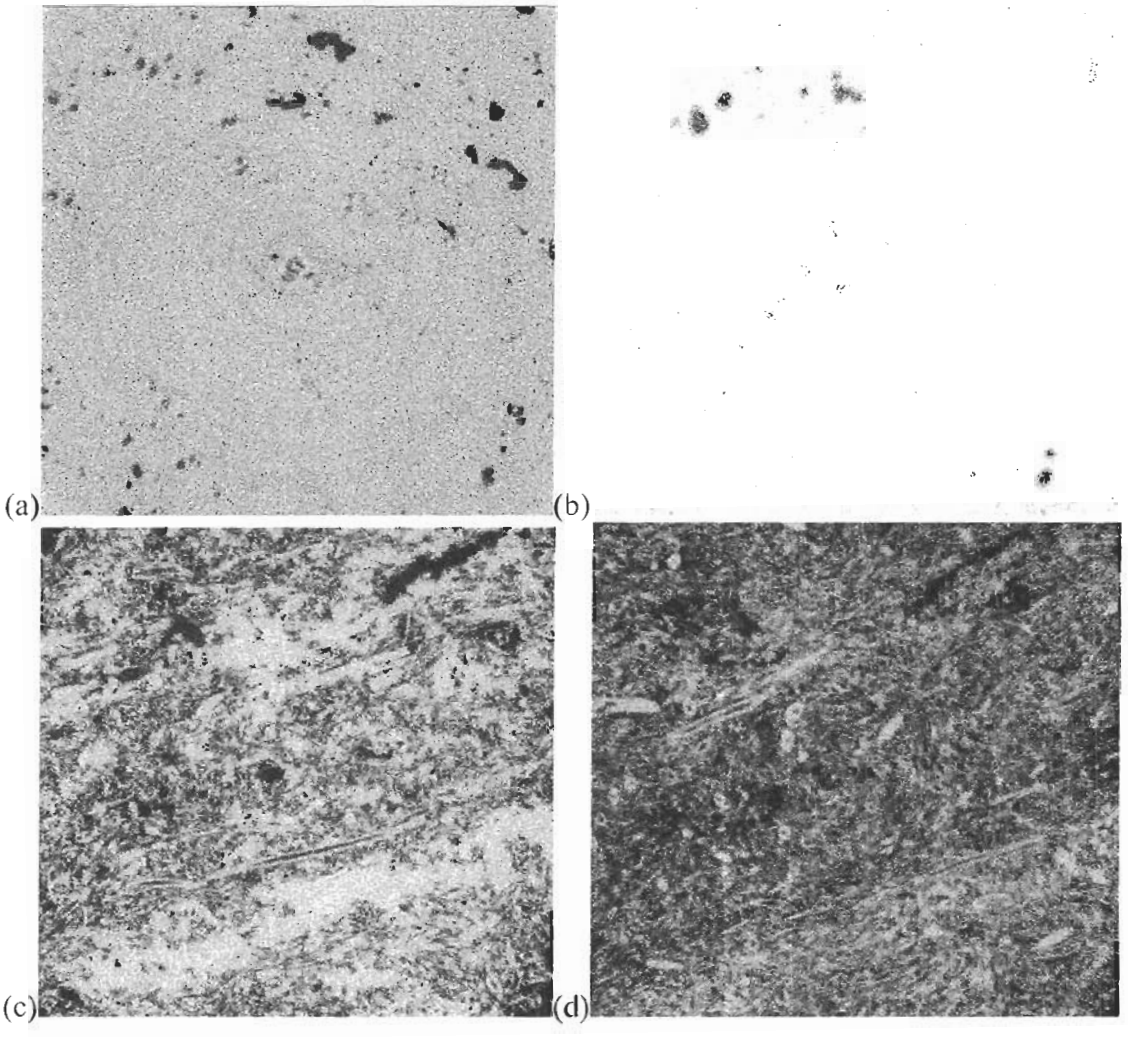

Figure 6-18 Two-dimensional slices (20 µm thickness and resolution) at 25 cm depth of flat bog soil. Black represents air and grey represents soil and water content. (a) Saturated (b) 0.02 m matric suction (c) 0.5 m matric suction (d) 5.0 m matric suction. Scale: (x,y) 30.61, 30.50 mm.

6.2.3 Changes in matric suction and its relationship to density variations in MicroCT scanned images

When peat sub-samples were scanned, challenges emerged with interpreting the images. *Sphagnum* contains adsorbed, intracellular and capillary water which made image interpretation difficult for distinguishing soil particles from water in the images. This is largely because the water retained by the *Sphagnum* leaves changed the density of

the peat. In order to test this finding, a peat sample was oven-dried to remove most of the water in the soil. A unimodal distribution was created from the scanned image to approximate the density (Figure 6-19). The figure shows that peat has an average greyscale of -637, which is close to that of air (-1000). Conversely, Figure 6-20 shows a 10 cm flat bog sub-sample at 0.02 m matric suction where the density of peat has now increased, so it is close to that of water (0). This difference indicates strong attenuation differences in peat that is dry versus peat that is wet.

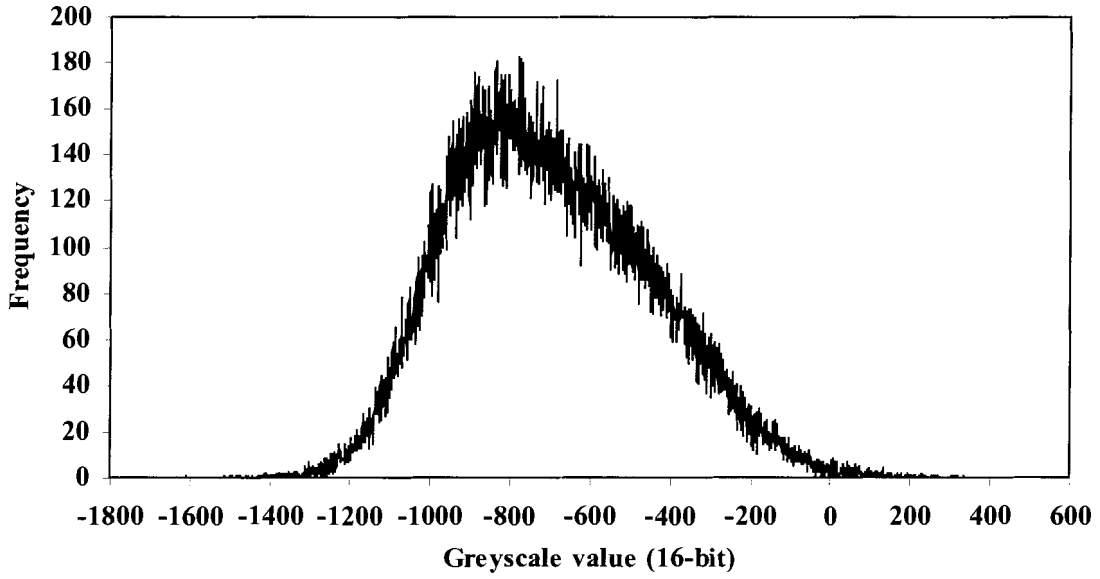

Figure 6-19 A peat sample that has been oven-dried to remove most of the water in the soil. The average greyscale value for peat shown here is -637.

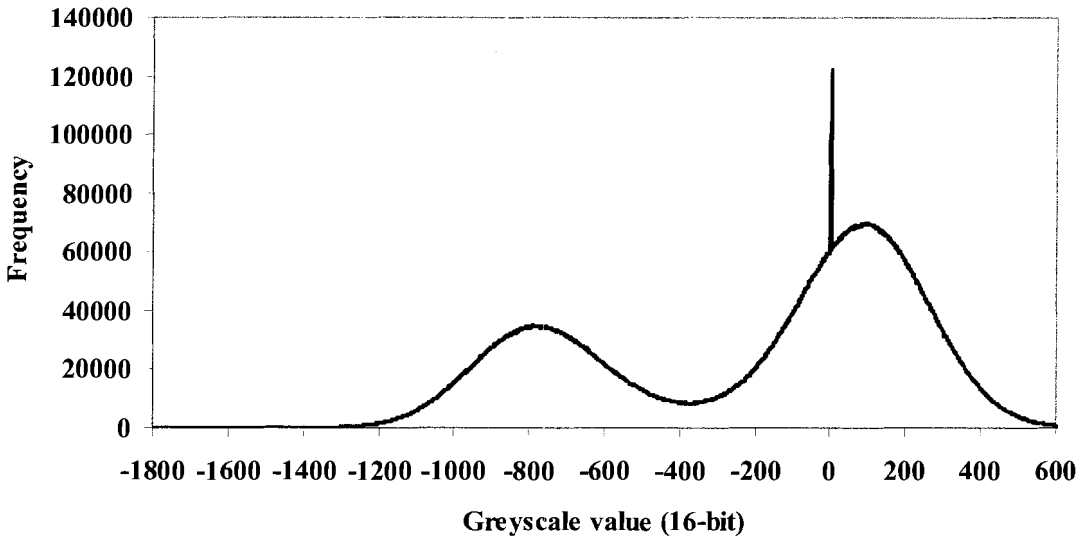

Figure 6-20 A 10 cm flat bog sub-sample analysed at 0.02 m matric suction. The high portion of the bimodal distribution represents the soil and water content and the small portion represents the air content.

6.3 Conclusion

Specific pores were measured for air-filled pore area, diameter and hydraulic radius at two levels of soil tension. Results of this study show that with increased soil tension, the air-filled pores increased in size and number in both the peat plateau and flat bog sub-samples. The pores became filled with air as the water remaining in the soil became disconnected due to the degradation of capillary films around the pore edges.

Peat at shallow depths is composed of living and poorly decomposed plant debris. At shallow depths, the hyaline cell walls have, in some cases, broken away from the rest of the cell but at deeper depths, the cells are more advanced in decomposition and the cells are not as visible. The water holding capacity of *Sphagnum* is twenty times its dry weight as water is stored in its cell structure in order to avoid desiccation. Water is also

easily extracted from the *Sphagnum* cells. At high soil tensions, the capillary films become disconnected and the *Sphagnum* cells are more visible in the CT images.

CT technology was evaluated to determine its utility in the analysis of soil physical properties and to make a credible and beneficial contribution to wetland hydrology. Initial stages of analysis proved to be promising in regards to visualizing images on a computer screen. When the peat was scanned initially at an unknown moisture content, the frequency distribution showed a deviation between soil/water and air, which was displayed clearly as a bimodal distribution. Despite numerous attempts, the soil and water became difficult to separate as individual entities. Air was the easiest entity to distinguish in the images. The main problem in distinguishing these entities was that peat has a low density, close to that of air, which changed in relation to its moisture content. The absorptive behaviour of the *Sphagnum* cells themselves assisted in varying the density of the peat. A consistent density value for peat was therefore not attainable. Because peat takes up water into its hyaline cells, the peat took on densities close to that of water.

CHAPTER 7:
DISCUSSION

7.1 Overview

The previous chapters summarized the results derived from images created with a MicroCT scanner and results obtained from a permeameter. The results of the previous chapters confirm that capillary pressure is a function of physical and hydrological properties of peat. In Chapter 4, the moisture-tension association indicated that the majority of moisture had drained from the soil at 0.05 m tension. This varied with depth and terrain type. At residual moisture content (5.0 m matric suction), capillary pressure contributed to the retention of water.

By determining air-filled porosity for both the peat plateau and flat bog sub-samples, it was confirmed that the largest pores drained first. Since the shallower samples have the largest number of large pore sizes, the air-filled porosity was higher than in the deeper samples. The number of large pores decreased with increased depth and decomposition, particularly in the flat bog where results indicate a large change in air-filled porosity between 10 cm and 20 cm depths. The results of the air-filled porosity, along with bulk density and water level data, indicated that an acrotelm and catotelm existed in the flat bog between those depths and also suggests that MicroCT technology is a viable method for analyzing and estimating air-filled porosity of peat.

Since the largest pores drain first, they are the most connective and are more conducive to flow at saturation. At 5.0 m tension, the pores that retain water at this

tension are likely closed and dead-end pores that do not contribute to flow whereas, the pores that have filled with air are pores that actively conduct water at saturation. The air-filled porosity determined at residual moisture content (5.0 m tension) is therefore the active porosity, since it is the volume of pores that actively transmits the flow of water in saturated peat.

Pore size distribution of air-filled pores was measured at residual moisture for three soil properties: pore area, pore diameter and pore hydraulic radius. The number of pores detected at lower depths is significantly larger likely because the sub-samples are in later stages of decomposition and more compacted than at upper depths. Overall, there was an increase in the number of small pore areas, diameters and hydraulic radii with depth. This result is related to the viscosity of the water in the peat sub-samples. Reynolds number is inversely related to viscosity. As pore diameter decreases with depth, Reynolds number decreases and resistance to flow and likelihood of laminar flow both increase. The flow and storage of water in soil increases with increasing pore diameter, d. C, is a constant of proportionality and refers to the shape, orientation and connectivity of the pores as discussed in Chapter 6. Cd^2 is the permeability of the soil which is directly proportional to the magnitude of hydraulic conductivity (Freeze and Cherry, 1979).

In Chapter 4, direct measurements of unsaturated hydraulic conductivity supported the air-filled porosity and active porosity results. Comparing the two measured results facilitates a greater understanding of the percentages of pores that are active and the lateral flow rate at which water moves through the peat at various depths. From saturation to unsaturation, there was a sharp decline in the hydraulic conductivity, particularly with increased matric suction. Overall, the unsaturated hydraulic conductivity

was quite low. It is therefore assumed that soil layers containing more micropores have higher rates of unsaturated flow. The moisture-tension and hydraulic conductivity-tension curves are similar in shape. This shows that hydraulic conductivity in unsaturated soil decreases in a similar manner as both matric suction increases and volumetric soil moisture decreases. Unsaturated hydraulic conductivity is dependent on the conductance of pores within the sub-samples which is in turn based on the interconnectivity of the pores. Since smaller pores contribute greatly to connectivity in unsaturated soil, they are largely responsible for hydraulic conductivity in the sub-samples. When larger pores have been emptied at higher matric suctions, continuity is disrupted and the water within a pore space may become immobile.

Changes in pore saturated area were evident when specific pores were magnified. There was an increase in pore area, pore diameter and pore hydraulic radius with increased matric suction from 0.5 m to 5.0 m as more pores were detectable as the soil dried. It is evident that the connectivity and capillarity had been reduced substantially at 5.0 m tension.

Examination of the porous *Sphagnum* hyaline cells showed that the hyaline cell wall thickenings or fibrils are relatively dense and define the cell's shape. Three types of water retentions exist in peat: adsorbed, intracellular and capillary water. *Sphagnum* has intracellular absorption, which intensifies with increased matric suction. A capillary fringe or a network of capillary spaces, allows for water to be retained by the peat. Capillarity results from the water's surface tension and its contact angle with the organic matter. A capillary film is evident around the *Sphagnum* leaves at 0.5 m tension, but

when the tension increases to 5.0 m, the film has broken and the hyaline cells then become more visibly defined.

Measurements of air filled porosity, active porosity, pore size distribution and unsaturated hydraulic conductivity of peat indicated that the flow of water was constrained by the lack of capillary films in the largest *Sphagnum* pores. Lacking capillary films, *Sphagnum* stops conducting water causing hydraulic conductivity to slow drastically. It is assumed that adsorbed, intracellular and capillary water had been retained in the soil until enough matric suction was applied to reduce the water from the hyaline cells and from around the cell edges. Because the hyaline cells adsorb water, the images generated by the CT scanner do not distinguish between organic soil and water due to their similar densities. As a result, only air-filled pores were measurable. Since most of the larger air–filled pores are the ones responsible for contributing to conductivity, results suggest that air-filled porosity at 5.0 m tension, provides a reasonable estimate of active porosity.

CHAPTER 8:
CONCLUSION

The goal of this research was to explore computed tomographic imagery for use in soil analysis while addressing challenges in the acquisition, manipulation and interpretation of the three-dimensional images. Using a MicroCT scanner to analyze the peat sub-samples, allowed for characterization of the internal dynamics of peat in a short amount of time through the use of imagery. The images provided a view of the soil from all dimensions and provided information on soil pores and soil structure, in each soil sub-sample. In particular, this research focused on the measurement of physical and hydrological properties of organic soil in two and three-dimensions. The measured soil properties consisted of air-filled porosity with variations in soil tension; active porosity at residual moisture content; pore size distribution including pore area, pore diameter and pore hydraulic radius - at the highest tension level; unsaturated hydraulic conductivity with variations in soil tension; pore saturated area at two levels of soil tension; and an examination of porous *Sphagnum* cells and capillarity with changes in tension. Results suggest that the use of MicroCT imagery is suitable for use in this type of soil analysis.

Some of the drawbacks of this methodology have been described throughout the thesis. Specifically, the images were constrained to small sizes due to computer processing limitations and because soil and water were not distinguishable from each other in the images this restricted quantitative estimates only to air content. One additional drawback is the availability and expense of a MicroCT scanner. Because a CT

scanner is an expensive piece of equipment (approximately $400,000.00) it is not feasible for purchase and use in every laboratory. Overtime, as technology improves, costs may decrease and MicroCT scanners may be more accessible to researchers.

The methods developed in this thesis research have considerable potential for application towards additional in-depth hydrological analysis of organic soil. Software advances explicitly developed for thresholding and interpretation could significantly improve quantitative image analysis. Advancements in computer processing power could also improve the manipulation of larger file sized images so that larger soil samples could be analysed. Future considerations for this technology might consist of measuring three-dimensional tortuosity by determining any and all flow paths throughout soil samples. This would include measuring the interconnectivity and shape of the pores; accomplished using images at the highest possible resolution (~ 5 microns) with many more soil samples. Larger samples at a greater number of soil tensions, including a hysteretic curve, could be implemented.

APPENDICES

Appendix A: Vegetation at Scotty Creek

Table A- 1 Dominant tree species at Scotty Creek

Picea mariana	Black Spruce
Larix laricina	Tamarack
Pinus contorta var. latifolia	Lodgepole Pine
Betula papyrifera var. papyrifera	Paper Birch

Table A- 2 Dominant shrub species at Scotty Creek

Betula pumila var. glandulifera	Dwarf Birch
Kalmia polifolia	Northern Bog-Laurel
Chamaedaphne calyculata	Leatherleaf Shrub
Oxycoccus microcarpus	Small Bog Cranberry
Vacinium vitis-idaea	Lingonberry
Alnus crispa	Green Alder
Ledum groenlandicum	Common Labrador Tea
Betula glandulosa	Bog Birch
Salix arbusculoides	Little-Tree Willow
Salix discolor	Pussy Willow
Andromeda polifolia	Dwarf Bog-Rosemary

Table A- 3 Dominant lichen species at Scotty Creek

Cladina mitis	Green reindeer lichen
Cladina rangiferina	Grey reindeer lichen
Flavocetraria nivalis	Flattened snow lichen
Clandonia Amaurocraea	
Cladonia chlorophaea	False pixie-cup lichen
Cladina stellaris	Northern reindeer lichen
Icmadophila ericetorum	Spray paint lichen/Fairy puke
Parmelia sulcata	Waxpaper lichen
Tuckermannopsis americana	Leafy brown bark lichen
Xanthoria fallax	Powdered orange lichen
Clandonia Borealis	Red pixie-cup lichen
Bryoria fuscescens	Speckled horsehair lichen
Evernia mesomorpha	Spruce moss lichen
Brachythecium rivulare	Waterside feather moss
Cladonia crispata	Shrub funnel lichen

Table A- 4 Dominant moss species at Scotty Creek

Bryum pseudotriquetrum	Tall clustered thread moss
Campylium stellatum	Yellow star moss
Helodium blandowii	Blandow's feather moss
Sphagnum capillifolium	Acute-leaved peat moss
Sphagnum magellanicum	Midway peat moss
Sphagnum angustifolium	Poor fen moss
Sphagnum fuscum	Rusty peat moss
Sphagnum squarrosum	Square rose peat moss
Sphagnum riparium	Shore-growing peat moss
Bryum Capillare	Capillary thread moss
Sphagnum girgensohnii	Girgensohn's peat moss

Table A- 5 Other common vegetation at Scotty Creek

Type	*Latin*	Common
Club-Moss	*Lycopodium annotinum*	Stiff Club-Moss
Liverwort	*Marchantia polymorpha*	Green-Tongue
Aquatic plants	*Typha latifolia*	Common Cattail
	Menyanthes trifoliata	Buck-bean
Horsetails	*Equisetum fluviatile*	Swamp Horsetail
Insect-eating plants	*Sarracenia purpurea*	Pitcher-plant
	Drosera rotunifolia	Round-leaved Sundew
Wild flowers	*Rubus chamaemorus*	Cloudberry
	Smilacina trifolia	Three-leaved False Solomon's-seal

Appendix B: Frequency distribution histograms of greyscale values

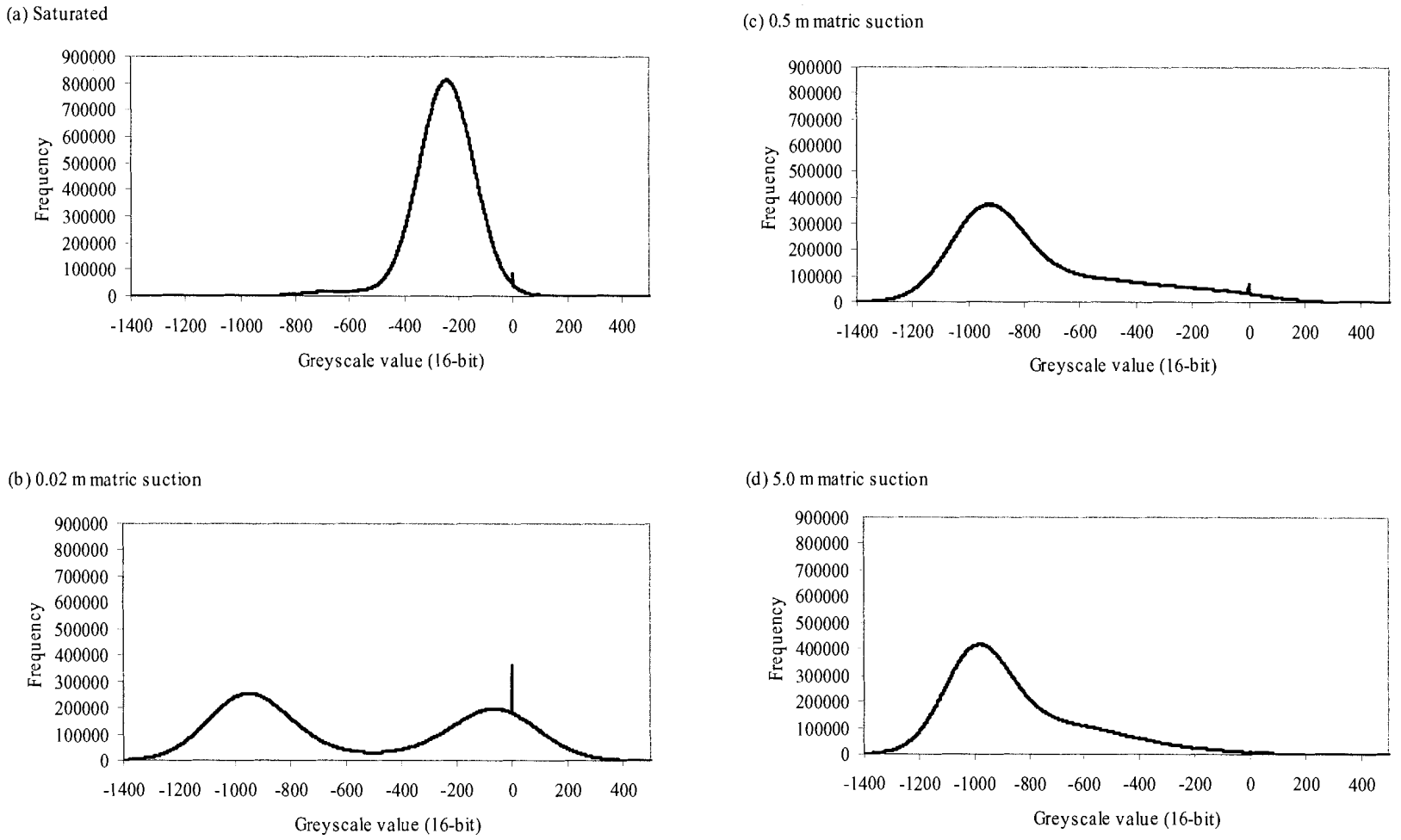

Figure B- 1 Histograms of voxel values, peat plateau sub-samples, 3 cm depth. (a) saturated (b) 0.02 m matric suction (c) 0.5 m matric suction (d) 5.0 m matric suction.

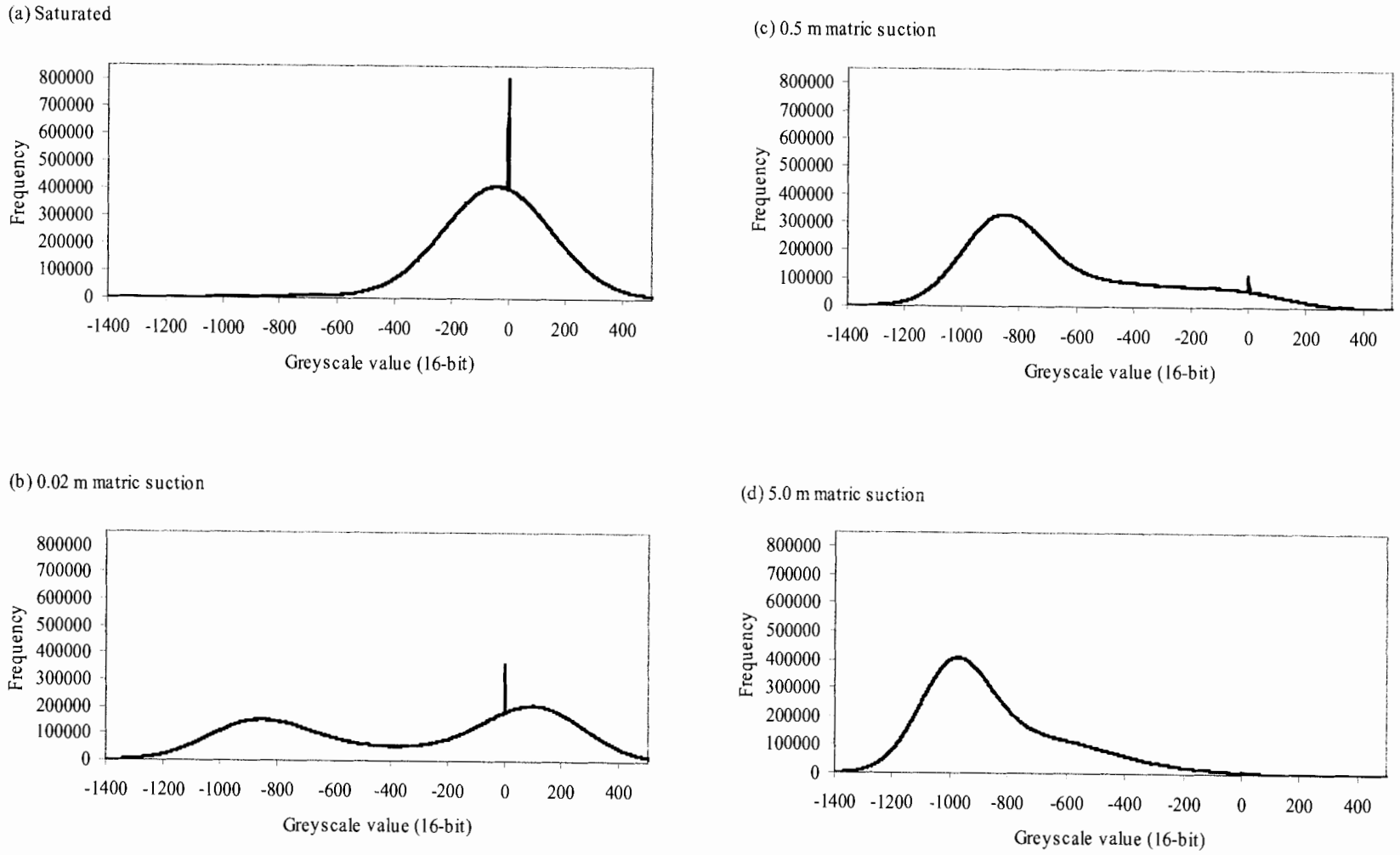

Figure B- 2 Histograms of voxel values, peat plateau sub-samples, 10 cm depth. (a) saturated (b) 0.02 m matric suction (c) 0.5 m matric suction (d) 5.0 m matric suction.

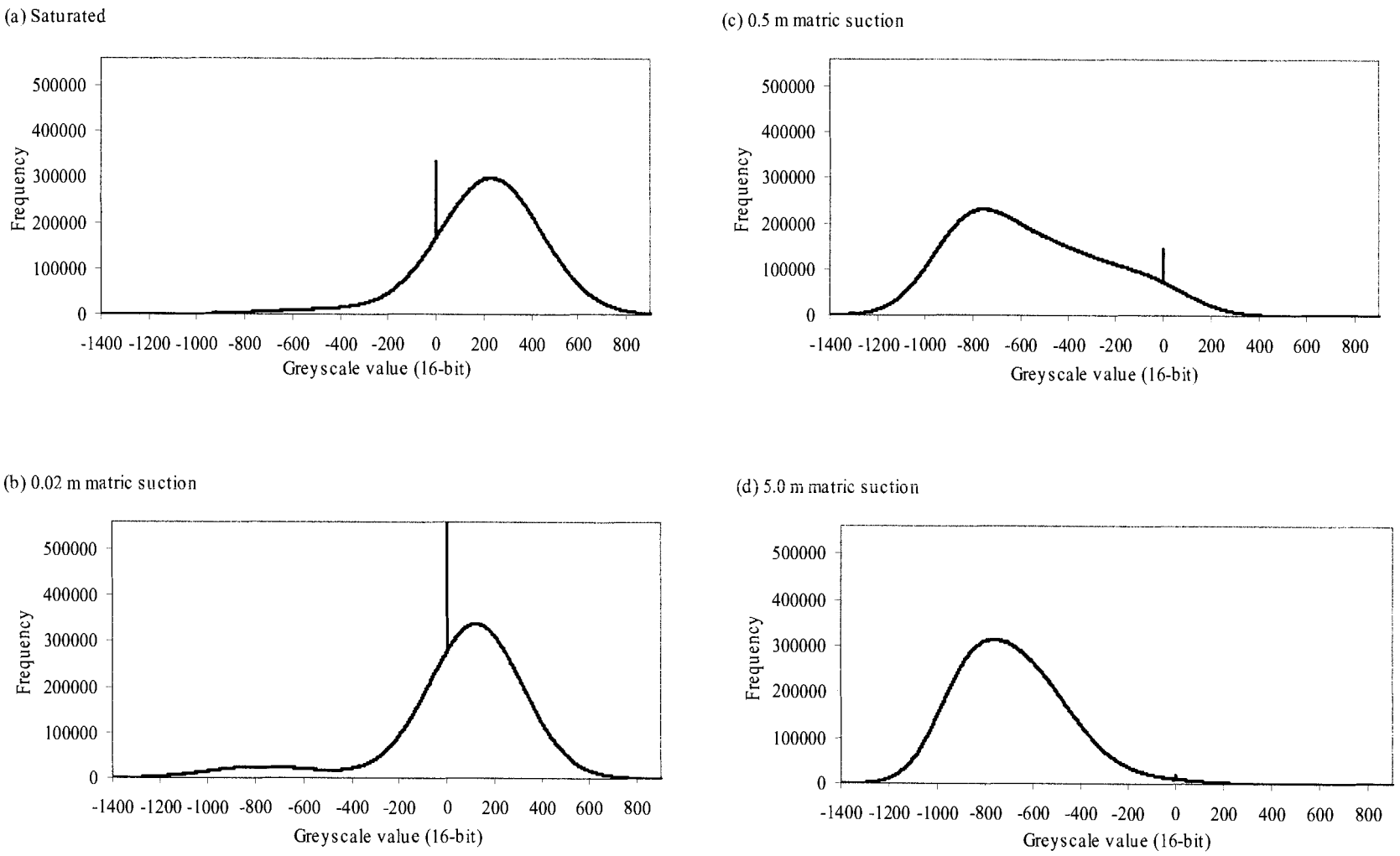

Figure B- 3 Histograms of voxel values, peat plateau sub-samples, 18 cm depth. (a) saturated (b) 0.02 m matric suction (c) 0.5 m matric suction (d) 5.0 m matric suction.

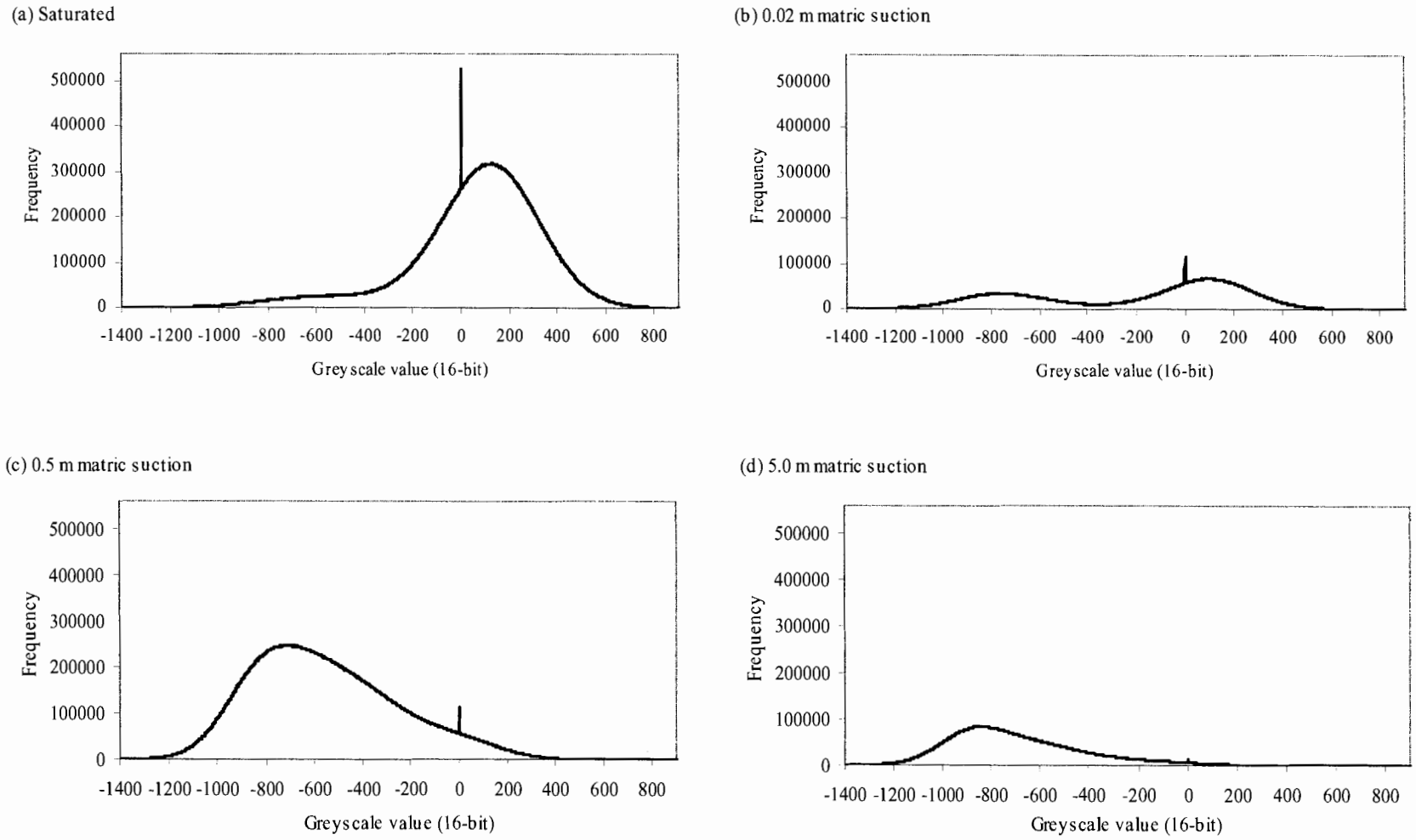

Figure B- 4 Histograms of voxel values, flat bog sub-samples, 3 cm depth. (a) saturated (b) 0.02 m matric suction (c) 0.5 m matric suction (d) 5.0 m matric suction.

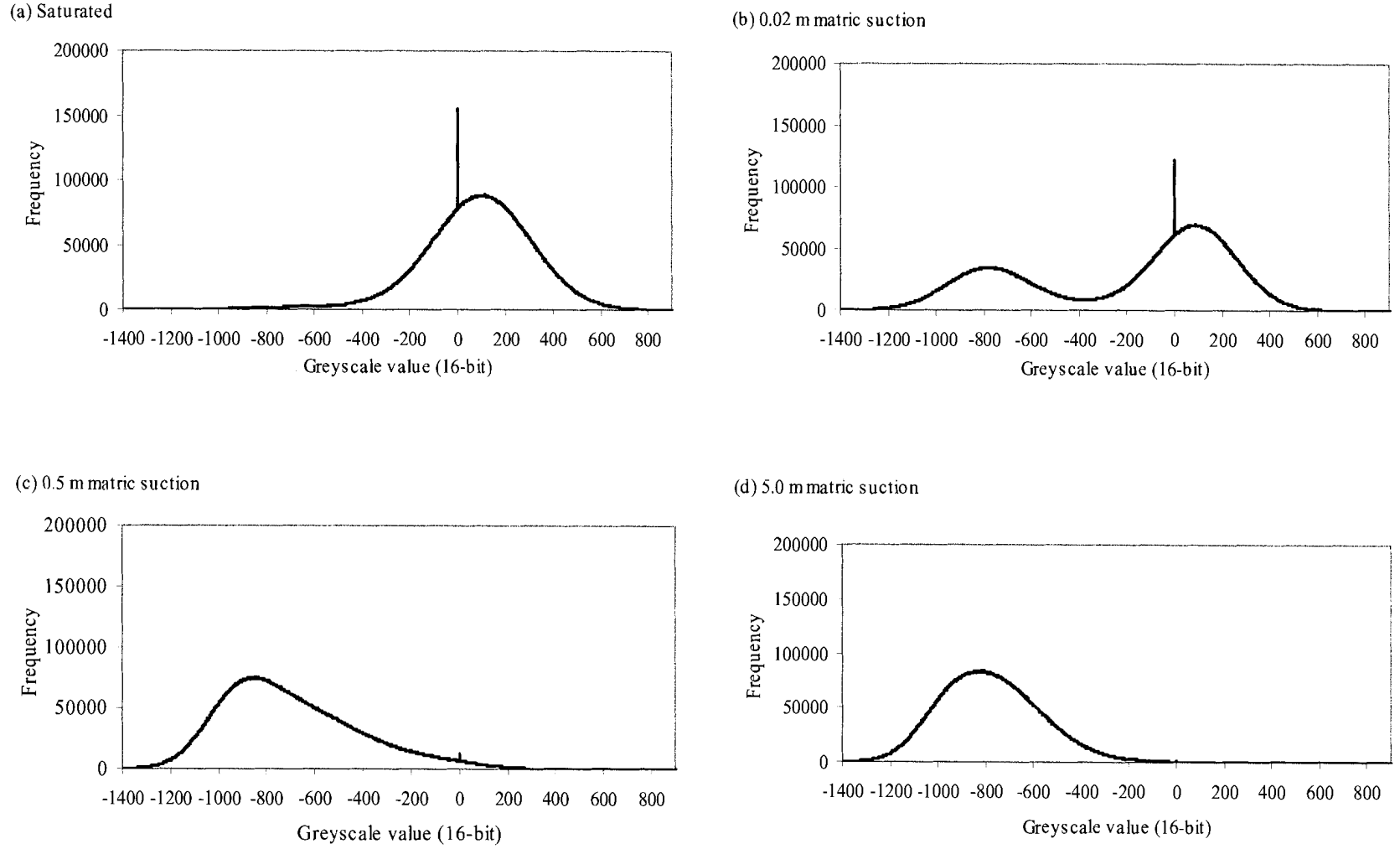

Figure B- 5 Histograms of voxel values, flat bog sub-samples, 10 cm depth. (a) saturated (b) 0.02 m matric suction (c) 0.5 m matric suction (d) 5.0 m matric suction.

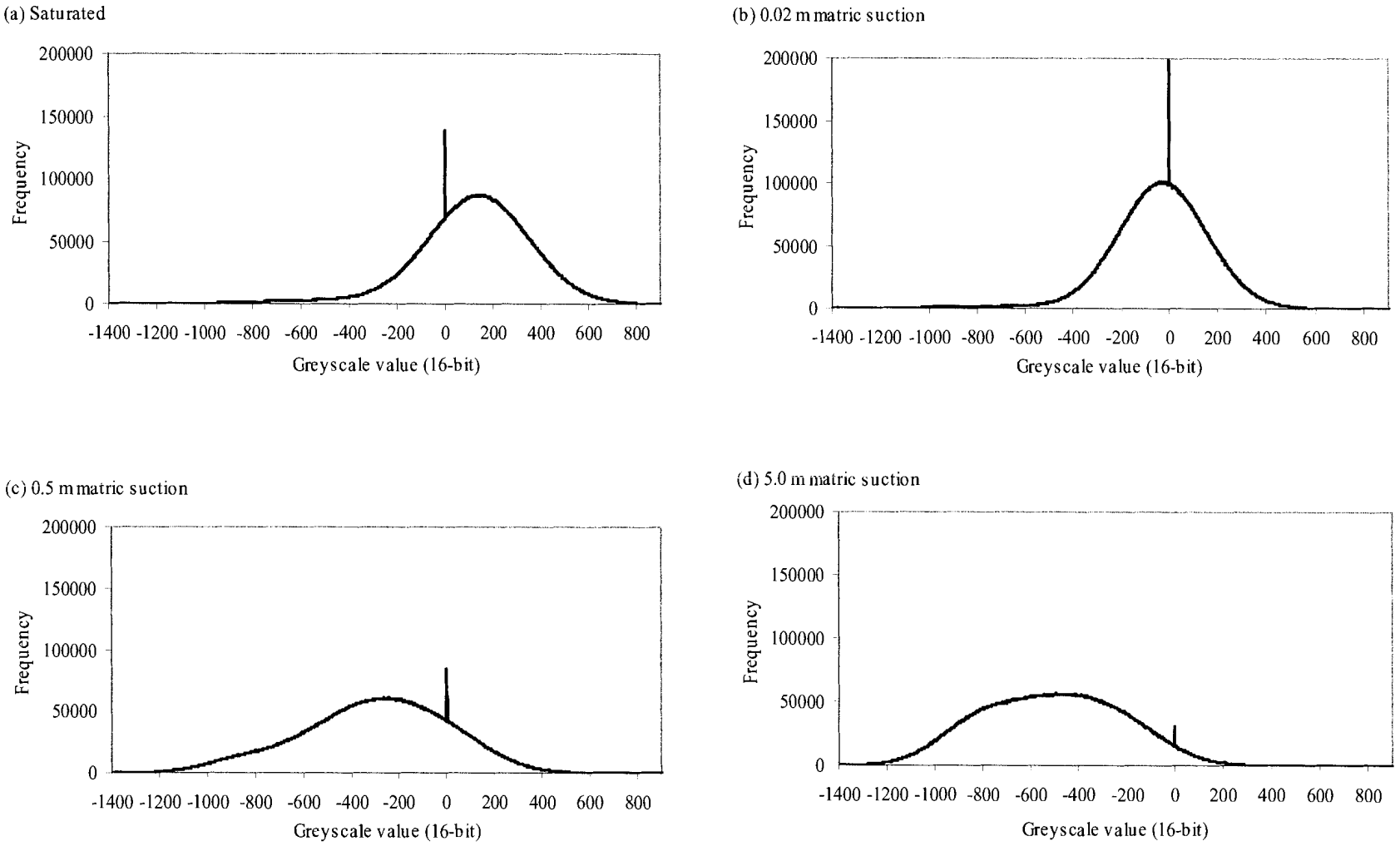

Figure B- 6 Histograms of voxel values, flat bog sub-samples, 20 cm depth. (a) saturated (b) 0.02 m matric suction (c) 0.5 m matric suction (d) 5.0 m matric suction.

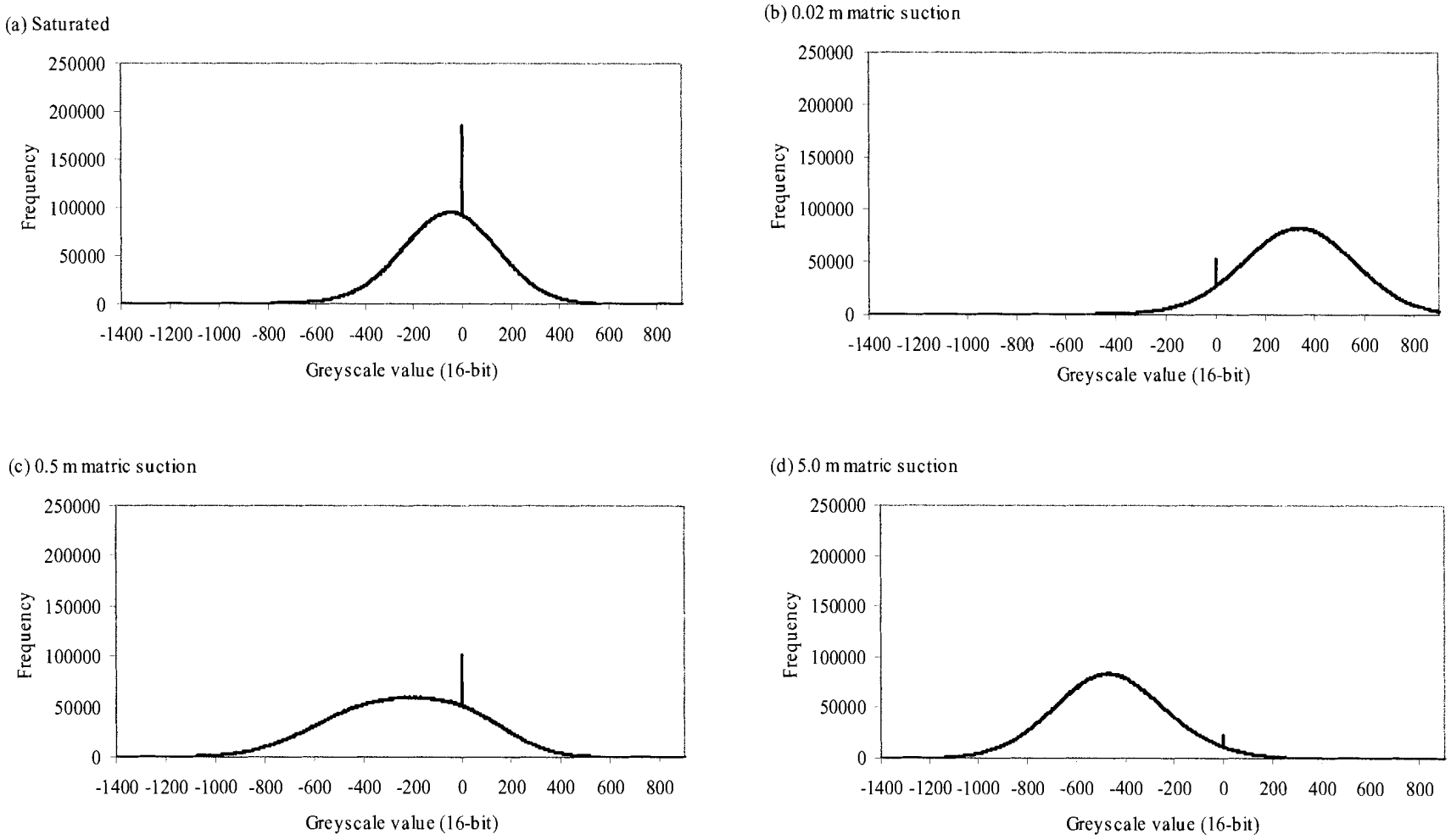

Figure B- 7 Histograms of voxel values, flat bog sub-samples, 25 cm depth. (a) saturated (b) 0.02 m matric suction (c) 0.5 m matric suction (d) 5.0 m matric suction.

Appendix C: Air-filled porosity

Table C- 1 Peat plateau 3 cm depth

Matric suction head (m)	Volumetric moisture content (cm^3 cm^{-3})	Air-filled porosity (%)	Soil/water content (%)
0.001	1.04	4.21	95.79
0.020	0.52	59.08	40.92
0.510	0.18	77.84	22.16
5.100	0.14	86.45	13.55

Table C- 2 Peat plateau 10 cm depth

Matric suction head (m)	Volumetric moisture content (cm^3 cm^{-3})	Air-filled porosity (%)	Soil/water content (%)
0.001	1.01	7.08	92.92
0.020	0.56	42.68	57.32
0.510	0.21	70.50	29.50
5.100	0.14	79.29	20.71

Table C- 3 Peat plateau 18 cm depth

Matric suction head (m)	Volumetric moisture content (cm^3 cm^{-3})	Air-filled porosity (%)	Soil/water content (%)
0.001	1.00	5.00	95.00
0.020	0.86	8.93	91.07
0.510	0.28	64.26	35.74
5.100	0.19	77.92	22.09

Table C- 4 Flat bog 3 cm depth

Matric suction head (m)	Volumetric moisture content (cm^3 cm^{-3})	Air-filled porosity (%)	Soil/water content (%)
0.001	1.00	8.16	91.84
0.020	0.85	22.77	77.23
0.510	0.27	79.62	20.38
5.100	0.22	89.45	10.55

Table C- 5 Flat bog 10 cm depth

Matric suction head (m)	Volumetric moisture content (cm^3 cm^{-3})	Air-filled porosity (%)	Soil/water content (%)
0.001	0.99	7.76	92.24
0.020	0.85	19.20	80.80
0.510	0.26	71.54	28.49
5.100	0.18	86.64	13.36

Table C- 6 Flat bog 20 cm depth

Matric suction head (m)	Volumetric moisture content (cm^3 cm^{-3})	Air-filled porosity (%)	Soil/water content (%)
0.001	1.05	5.35	94.65
0.020	0.94	10.05	89.95
0.510	0.43	41.82	58.18
5.100	0.31	54.87	45.13

Table C- 7 Flat bog 25 cm depth

Matric suction head (m)	Volumetric moisture content (cm^3 cm^{-3})	Air-filled porosity (%)	Soil/water content (%)
0.001	1.05	2.09	97.91
0.020	1.03	3.10	96.90
0.510	0.48	38.69	61.31
5.100	0.34	51.66	48.34

REFERENCE LIST

Aylesworth, J.M. and Kettles, I.M., 2000. Distribution of peatlands. In: Dyke, L.D. and Brooks, G.R., Editors, 2000. The Physical Environment of the Mackenzie Valley, Northwest Territories: A Base Line for the Assessment of Environmental Change. Geological Survey of Canada Bulletin 547, pp. 49–55.

Baird, A.J., 1997. Field estimation of macropore functioning and surface hydraulic conductivity in a fen peat. Hydrological Processes, 11: 287-295.

Beven, K. and Germann, P., 1982. Macropores and water flow in soils. Water Resources Research, 18(5): 1311-1325.

Boelter, D.H., 1968. Important physical properties of peat materials, Proceedings of the 3rd International Peat Congress, Quebec, pp. 150-156.

Boelter, D.H., 1976. Methods for analysing the hydrological characteristics of organic soils in marsh-ridden areas, Forest Service, US Department of Agriculture, Grand Rapids, Minnesota.

Booltink, H.W.G., Bouma, J. and Gimenez, D., 1991. Suction crust infiltrometer for measuring hydraulic conductivity of unsaturated soil near saturation. Soil Science Society of America Journal, 55: 566-568.

Brady, N.C. and Weil, R.R., 2002. The Nature and Properties of Soils. Pearson Education, Inc., Upper Saddle River, New Jersey, USA, 960 pp.

Brooks, R.H. and Corey, A.T., 1964. Hydraulic properties of porous media, University Hydrology Paper no. 3, Fort Collins, Colorado State.

Brown, D., Lopes, R.T. and Motta, L.M.G., 2000. Dual energy computerized tomography in compacted soil. Geotechnical and Geological Engineering, 18: 221-238.

Brown, R.J.E. and Williams, G.P., 1972. The freezing of peatland, Ottawa.

Burrough, P.A. and McDonnell, R.A., 1998. Principles of geographic information systems. Oxford University Press, Oxford, N.Y., 333 pp.

Cady, J.G., Wilding, L.P. and Drees, L.R., 1986. Petrographic Microsopic Techniques. In: A. Klute (Editor), Methods of Soil Analysis. Part 1 - Physical and Mineralogical Methods. American Society of Agronomy, Inc. Soil Science Society of America, Inc., Madison, Wisconsin USA, pp. 185-218.

The Canadian System of Soil Classification, 1998. Soil Classification Working Group. 3rd ed. Agriculture and Agri-Food Canada Publication 1646, 187 pp.

Carmack, E.C., 2000. The Arctic Ocean's freshwater budget: sources, storage and export. In: Lewis, E.L., Jones, E.P., Lemke, P., Prowse, T.D. and Wadhams, P., Editors, 2000. *The Freshwater Budget of the Arctic Ocean*, Kluwer, Dordrecht, Netherlands, pp. 91–126.

Chandler, D.G., Seyfried, M., Murdock, M. and McNamara, J.P., 2004. Field calibration of water content reflectometers. Soil Science Society of America Journal, 68: 1501-1507.

Charman, D., 2002. Peatlands and Environmental Change. Wiley, New York.

Couclelis, H. 1985. Cellular worlds: a framework for modeling micro-macro dynamics. Environment and Planning, 17: 585-596.

Curry, T.S.I., Dowdey, J.E. and Murry, R.C.J., 1990. Christensen's Physics of Diagnostic Radiology. Lippincott Williams & Wilkins, Philadelphia, Pennsylvania, 521 pp.

Dinel, H. and Levesque, M., 1976. Physical properties of organic soils. In: M.R. Carter (Editor)., Soil Sampling and Methods of Analysis, pp. 441-471.

Dingman, S.L., 2002. Physical hydrology. Prentice Hall, Upper Saddle River, N.J., 639 pp.

Ellis, S., 2001. Image: *Sphagnum rubellum*, Biology Department at the University of British Columbia. http://www.botany.ubc.ca/bryophyte/sem/hyaline_cells.html, accessed 04/30/2005

Fox, C.A. and Parent, L.E., 1993. Micromorphological methodology for organic soils. In: M.R. Carter (Editor), Soil sampling and methods of analysis. Lewis Publishers, pp. 473-485.

Freeze, R.A. and Cherry, J.A., 1979. Groundwater. Prentice-Hall, Enlgewood Cliffs, N.J., 614 pp.

Glaser, P.H. and Janssens, J.A., 1986. Raised bogs in eastern North America: transitions in landforms and gross stratigraphy. Canadian Journal of Botany, 64: 395-415.

Halsey, L.A., Vitt, D.H. and Gignac, L.D., 2000. Sphagnum-dominated peatlands in North America since the last glacial maximum: their occurrence and extent. The Bryologist, 103(2): 334-352.

Hayashi, M. and Quinton, W.L., 2004. Constant-head well permeameter tests for soils underlain by impermeable layers. Canadian Journal of Soil Science, 84(255-264).

Hayashi, M., Quinton, W.L., Pietroniro, A. and Gibson, J.J., 2004. Hydrological functions of wetlands in a discontinuous permafrost basin indicated by isotopic and chemical signatures. Journal of Hydrology, 296: 81-97.

Hayashi, M. and Rosenberry, D.O., 2002. Effects of groundwater exchange on the hydrology and ecology of surface waters. Ground water, 40: 309-316.

Hayward, P.M. and Clymo, R.S., 1982. Profiles of water content and pore size in *Sphagnum* and peat, and their relation to peat bog ecology, The Royal Society of London. Series B., Biological Sciences. The Royal Society, London, pp. 299-325.

Heginbottom, J.A., Radburn, L.K., 1992. Permafrost and ground ice conditions of Northwestern Canada. Geological Survey of Canada, Map 1691A.

Hillel, D., 1998. Environmental soil physics: fundamentals, applications, and environmental considerations. Academic Press, 771 pp.

Hoag, R.S. and Price, J.S., 1997. The effects of matrix diffusion on solute transport and retardation in undisturbed peat in laboratory columns. Journal of Contaminant Hydrology (28): 193-205.

Hobbie, J.E., 1984. The ecology of tundra ponds of the Arctic Coastal Plain: A community profile. U.S. Fish and Wildlife Service FWS/OBS-83/25.

Ingram, H.A.P., 1978. Soil layers in mires: function and terminology. Journal of Soil Science (29): 224-227.

Ingram, H.A.P., 1983. Mires: swamp, bog, and moor, general studies. Hydrology. In: A.J.P. Gore (Editor), Ecosystems of the World, Volume 4A. Elsevier: New York; 67-158.

Itami, R.M., 1994. Simulating spatial dynamics: cellular automata. Landscape and Urban Planning (30): 27-47.

Ivanov, G., 1981. Water movement in mirelands. Academic Press, London.

Joyal, P., Blain, J. and Parent, L.E., 1989. Utilization of tempe cells in determination of physical properties of peat based substrates. Acta Hortic, 238: 63-66.

Ketcham, R.A. and Carlson, W.D., 2001. Acquisition, optimization and interpretation of X-ray computed tomographic imagery: applications to the geosciences. Computers & Geosciences, 27(4): 381-400.

Ketcham, R.A. and Iturrino, G.J., 2005. Nondestructive high-resolution visualization and measurement of anisotropic effective porosity in complex lithologies using high-resolution X-ray computed tomography. Journal of Hydrology (30): 92–106

Klute, A. and Dirksen, C., 1986. Hydraulic conductivity and diffusivity: laboratory methods. In: A. Klute (Editor), Methods of soil analysis Part 1 - Physical and mineralogical methods. American Society of Agronomy, Inc. Soil Science Society of America, Inc., Madison, Wisconsin, USA, pp. 1188.

Kremer, C., Pettolino, F., Bacic, A. and Drinnan, A., 2004. Distribution of cell wall components in *Sphagnum* hyaline cells and in liverwort and hornwort elators. Planta, 212: 1023-1035.

Ligrone, R. and Duckett, J.G., 1998. The leafy stems of the *Sphagnum* (Bryophyta) contain highly differentiated polarized cells with axial arrays of endoplasmic microtubules. New Phytology(140): 567-579.

Lu, N. and Likos, W.J., 2004. Unsaturated soil mechanics. Wiley & Sons, Inc., Hoboken, New Jersey, 556 pp.

Mori, Y., Maruyama, T. and Mitsuno, T., 1999. Soft X-ray radiography of drainage patterns of structured soils. Soil Science Society of America Journal, 63(4): 733-740.

Mualem, Y., 1976. A new model for prediction the hydraulic conductivity of unsaturated porous media. Water Resources Research, 12: 513-522.

National Research Council, 1995. Wetlands: Characteristics and Boundaries. National Academy Press, Washington, D.C.

National Wetlands Working Group, 1988. Wetlands of Canada. Polyscience publications Inc., Ottawa, Ontario, 451 pp.

Parent, L.E. and Caron, J., 1993. Physical properties of organic soils. In: M.R. Carter (Editor), Soil Sampling and Methods of Analysis. Lewis Publishers, pp. 441-471.

Price, J.S., 2003. The role and character of seasonal peat soil deformation on the hydrology of undisturbed and cutover peatlands. Water Resources Research.

Price, J.S. and Schlotzhauer, M., 1999. Importance of shrinkage and compression in determining water storage changes in peat: the case of a mined peatland. Hydrological Processes, 13: 2591-2601.

Price, J.S. and Waddington, J.M., 2000. Advances in Canadian wetland hydrology and biogeochemistry. Hydrological Processes, 14: 1579 -1589.

Price, J.S. and Whitehead, G.S., 2004. The influence of past and present hydrological conditions on Sphagnum recolonization and succession in a block-cut bog, Quebec. Hydrological Processes, 18: 315-328.

Quinton, W.L. and Gray, D.M., 2003. Subsurface drainage from organic soils in permafrost terrain: the major factors to be represented in a runoff model, 8th International Conference on Permafrost, Davos, Switzerland., pp. 6.

Quinton, W.L., Gray, D.M. and Marsh, P., 2000. Subsurface drainage from hummock-covered hillslopes in the Arctic tundra. Journal of Hydrology, 237: 113-125.

Quinton, W.L., Hayashi, M., Blais, K.E., Wright, N. and Peitroniro, A., 2004. The water balance of wetland-dominated permafrost basins. In: D.L. Kane and D. Yang (Editors), Northern Research Basins Water Balance. (Proceedings of a workshop held at Victoria, Canada, March 2004) IAHS Publication, Wallingford, Oxfordshire, pp. 186-194.

Quinton, W.L., Hayashi, M. and Pietroniro, A., 2003. Connectivity and storage functions of channel fens and flat bogs in northern basins. Hydrological processes, 17(18): 3665-3684.

Reynolds, W. D., Elrick, D. E. and Topp, G. C. 1983. A re-examination of the constant head well permeameter method for measuring saturated hydraulic conductivity above the water table. Soil Science. 136: 250–268.

Richards, J.A. and Jia, X., 1999. Remote Sensing Digital Image Analysis: An Introduction, Springer-Verlag, Berlin, Germany.

Richardson, D.H.S., 1981. The Biology of Mosses. Blackwell Scientific Publications, Oxford, 220 pp.

Robinson, S.D. and Moore, T.R., 1999. Carbon and peat accumulation over the past 1200 years in a landscape with discontinuous permafrost, Northwestern Canada. Global Biogeochemical Cycles, 13(2): 591-601.

Robinson, S.D. and Moore, T.R., 2000. The influence of permafrost and fire upon carbon accumulation in high boreal peatlands, Northwest Territories, Canada. Arctic, Antarctic and Alpine Research, 32(2): 155 -166.

Robinson, V.B., 2003. A perspective on the fundamentals of fuzzy sets and their use in geographic information systems. Transactions in GIS, 7(1): 3-30.

Romanov, V.V., 1968. Hydrophysics of bogs, National Science Foundation, Israel Program for Scientific Translations, Washington, D.C. 299 pp.

Rose, C.W., 1966. Agricultural Physics. Pergamon, Oxford.

Royer, J.M. and Vachaud, G., 1975. Field determination of hysteresis in soil-water characteristics. Soil Science Society of America Journal, 39: 221-223.

Rycroft, D.W., Williams, D.J.A. and Ingram, H.A.P., 1975. The transmission of water through peat: I. Review. Journal of Ecology, 63(2): 535-556.

Siegel, D.I., Reeve, A.S., Glaser, P.H. and Romanowicz, E.A., 1995. Climate-driven flushing of pore water in peatlands. Nature. (374): 531-533.

Schwarzel, K., Manfred, R., Sauerbrey, R. and Wessolek, G., 2002. Soil physical characteristics of peat soils. J. Plant Nutr. Soil Sci.(165): 479-486.

Shi, B., Murakami, Y., Wu, Z., Chen, J. and Inyang, H., 1999. Monitoring of internal failure evolution in soils using computerization X-ray tomography. Engineering Geology, 54: 321-328.

Silinis, U. and Rothwell, R.L., 1998. Forest peatland drainage and subsidence affect soil water retention and transport properties in an Alberta peatland. Soil Science Society of America Journal, 62: 1048-1056.

Soil Classification Working Group. 1998. The Canadian System of Soil Classification, 3rd ed. Agriculture and Agri-Food Canada Publication 1646, 187 pp.

van Breemen, N. 1995. How *Sphagnum* bogs down other plants. Trends in Ecology & Evolution, 10(7): 270-275.

van Genuchten, M.T., 1980. A closed-form equation for predicting the hydraulic conductivity of unsaturated soils. Soil Science Society of America Journal, 44: 892-898.

Verry, E.S. and Boelter, D.H., 1978. Peatland hydrology. Wetland functions and values: the state of our understanding. American Water Resources Association: 389-402.

Walker, J.P., Willgoose, G.R. and Kalma, J.D., 2004. In situ measurement of soil moisture: a comparison of techniques. Journal of Hydrology, 293: 85-99.

Ward, R.C. and Robinson, M., 2000. Principles of hydrology. McGraw-Hill Publishing Company, London, 450 pp.

Whittow, J. 1984. Dictionary of Physical Geography. Harmondsworth, Middlesex, England, Penguin Books.

Wolfram, S. 1984. Universality and complexity in cellular automata. Physica, D 10(1-2), 1-35.

Wright, N., 2004. Unpublished water level data from Scotty Creek, NT. Simon Fraser University.